

POLITECNICO DI TORINO



Dipartimento di Ingegneria Meccanica e Aerospaziale

Corso di Laurea Magistrale: Ingegneria Meccanica

“Niobium micro-alloyed steels for automotive applications”

Relatore: Prof. Paolo Matteis

Laureando: Alberto Tina

Anno Accademico: 2019/2020

CONTENT

INTRODUCTION.....	3
1. NIOBIUM	5
1.1 Discovery and history	5
1.2 Properties	6
1.3 Mining and production	8
1.4 Ferroniobium addition during steelmaking	12
1.5 Economical evaluations.....	15
2. STEELS: PROCESSING AND PROPERTIES	18
2.1 Steelmaking.....	18
2.2 Hot rolling	20
2.3 Inclusions effect	24
2.4 Properties and relation with applications	26
3. MICROSCOPY METHOD.....	33
3.1 Light microscopy.....	33
3.2 Transmission Electron Microscopy.....	34
3.3 Scanning Electron Microscope.....	35
3.4 Electron Backscattered Diffraction	36
3.5 Atom Probe Tomography.....	36
4. NIOBIUM EFFECTS ON STEEL	38
4.1 Delay of recrystallization and grain refinement	38
4.2 Precipitation	43
4.2.1 Precipitation strengthening.....	53
4.2.2 Investigation method for precipitation	56
4.2.3 An example of a case study	58
4.3 Comparison with other elements.....	61
4.4 Weldability.....	66
4.5 Hydrogen embrittlement	70
4.6 Corrosion resistance	77
5. NIOBIUM IN AUTOMOTIVE STEELS	82
5.1 Dual phase	82
5.2 Transformation induced plasticity.....	88
5.3 Martensitic and press hardening.....	91
5.4 Interstitial free	96
5.5 Bake hardening.....	101

CONCLUSION	105
REFERENCES.....	107
ACKNOWLEDGEMENT	111

INTRODUCTION

The automotive world in the last decades focuses its attention in developing new complex shapes, provided with higher strength but especially with reduced weight. The regulations of the last years, in fact, require more and more stringent targets for the CO₂ emissions of automobiles: in 2015, for example, the request was 130 g CO₂/km, while in 2020 this value changes to 95 g CO₂/km in the EU. Further cut for emission target will result in 80 g CO₂/km in 2025 and 65 g CO₂/km in 2030. Manufacturers have interest in keeping the emission under the goal because otherwise they have to pay a penalty for excess in emissions: in EU this amounts to 95€ for each g/km in exceedance [1].

In order to reach these objectives, there are some options: engine evolution (smaller and more efficient), introduction and improvement of electrical or hybrid system (that will replace totally or partially the internal combustion engine), introduction of energy recovery system (for example regarding brake, wheel or aerodynamic) and weight reduction. This last aspect is “simple” but effective, because it has been noted that a weight reduction of about 50 kg result in saving 4 g CO₂/km that may represent a valid contribution in some critical cases near to the critical requested margin.

Steels represent a preeminent fraction of an automobile’s weight, so their lightening is interesting for car manufacturers: in fact, it could represents, in relation, cost saving and more competitiveness on the market, CO₂ emission contained and reduction in fuel consumption (which is an advantage also in the lifetime of the vehicle). Beside weight reduction, modern steels for passengers cars have to accommodate other targets such as adequate levels of strength, formability, endurance, energy absorption, stability, welding, resistance to fracture,...

Niobium is an element that enhances most of the mentioned characteristics and it is the main subject of this thesis. It has several applications in an automobile (for example in batteries, brakes and electronic components), but this work will focus on its use in steel. In this field niobium is mainly deployed as a microalloying element, which means that it is added to steel in very reduced quantity, usually in the order of 0,01 - 0,1%. Its primary property (as well as the other principal microalloying elements titanium and vanadium) is to form small carbides that exert a control of grain size in the steel components production.

Strengthening mechanisms attributed to niobium are mainly grain refinement, precipitation hardening and, partially, solid solution. The first is the most important since it bring a strong contribute in strength and toughness, and it is the only mechanism to improve both. It is related to precipitation and, in fact, a relevant part of the discussion will be dedicated at these aspects.

Deposits of this element are dislocated in some parts of the world, but the largest is in Brazil. Here there is the leading company in the production and commercialization of niobium products: CBMM. A great deal of researches and information is owned to it, thanks to which it is possible a continuous development.

The main objective of this investigation is to provide an overview of niobium usage in automotive steels, and it is structured as follows: first of all it is presented a chapter regarding general information about niobium, such as discovery, characteristics and extraction. Then, there is a section concerning steels, starting from steelmaking to their properties in relation to the applications; production process of the usual method (hot rolling) used to obtain pre-product is described here. In addition, there is an initial presentation of the various type that could be encountered in a vehicle.

In this work there are a lot of figures that are intended to clarify the concepts explained, and also provide a graphical feedback: therefore a lot of diagrams will be exposed, but also a several microscopic images; in fact some metallurgical notions will be given, and the relative pictures are useful. For these reason a brief part about microscopic methods is integrated, in order to explain the source of the figures and their acquisition methods.

Subsequently it begins the central part of the thesis, composed by two large chapters: the first exhibits the above-mentioned effects of niobium on steel. Since these mechanisms and consequences are similar in most steel type, in this part not just refers to the automotive ones, but also in other industry sectors, such as, for example, linepipe for oil transportation. Applications field of niobium, in fact, is fairly wide.

The second and last important chapter is focused on the typologies of steels used in automobile construction: depending on the function, in a vehicle there are several kinds of steel. Obviously, correlation with niobium and eventual peculiarities will be treated.

Along the entire work, interrelations with practical experiments will be exposed: although it has not been made new additional experiment, a literature review has been carried out and several works of some authors are presented. Comparison with practice, in fact, is an essential point of view, in order to understand the theoretical arguments.

1. NIOBIUM

1.1 Discovery and history

[2-4] Niobium (Nb) is a metallic element, ductile, and its appearance is grey color and shiny, as it can be seen in figure 1.1. It was discovered in 1801 by Charles Hatchett, a scientist that found it in a sample of ore, sent to England by John Winthrop some decades earlier. This sample was taken in a river bed in Connecticut, so, for a geographical and historical question (in memory of Cristoforo Colombo discoverer of the sample's origin continent), Hatchett gave the name of columbium at this element. Still today in USA this name is used.

Shortly after, in 1802, it was discovered tantalum, another element with similar features that occurs together with niobium, so it was thought that it was the same element. Despite the difference between the densities of these ones, the confusion remain until 1844, when professor Heinrich Rose noticed that they were two different materials; since Rose didn't know the Hatchett's work, he named the new element niobium, taking inspiration from the Greek mythology: in fact, being the latter similar to tantalum, he gave the name niobium from Niobe, the daughter of Tantalus.

Later, in 1864, Christian Blomstrand was the first to obtain niobium by a reduction of niobium chloride, with hydrogen and heat, and two years later a Swiss chemist, J.C. Galissard de Marignac, developed an industrial process of separation. These were further confirmation of the "independence" of the element, but it's only in 1950 that the official name it was adopted by IUPAC.

With the development of an industrial process and the related greater availability there was an increase in interest and the firsts attempts for application, initially as alloying element for stabilisation in special steels (for example Cr-Ni steels). In the early twentieth century, then, there were some test in incandescent filaments and the association with tungsten in cutting tools. Nevertheless in this period the availability and the use of niobium still remain restricted, and the commercial use was stuck, despite the discovery of the strengthening effect on steels, in 1939, by Becket and Frank.

At the end of World War II, in the fifties, there was the rebuilding of industry, and steels with better features (strength, toughness, formability) were required in a lot of sectors, like energy, transport and civil engineering: in this situation niobium took importance in metallurgy as a potential alloying element (main topic of this thesis). For example it can be mentioned the



Figure 1.1 Sample of niobium

utilization in pipeline for oil and gas transportation.

In those years also space exploration, and the interest about niobium in aerospace applications increased; in addition there were also produced the first alloys in nuclear field.

The discovery of new deposit in Brazil (it will be discussed in the next section) gave a further impulse: metallurgical plants were developed and from the sixties niobium quantities were unrestricted for industrial steel purpose. Knowledge of physical metallurgical basis, in relationship with niobium effect, was fundamental to obtain optimum utilization and optimised features, so numerous working groups (in university and laboratory) made a substantial contribution to understanding how niobium works as microalloying of steel. These studies were carried out at an international level by engineers and researchers, who worked with common interest in scientific progress; experiences exchange produced a productive environment, and numerous conferences took place in the following years. A milestone in these events was the symposium “Niobium” in 1981 in San Francisco, where a lot of aspect regarding mining and applications were illustrated.

The researches didn't stop in that period but has continued and still continue today, with an increased number of application (not only in steel industry), that will be mentioned in the discussion.

1.2 Properties

[2,5,6] The presence of niobium in earth's crust is about 19 ppm, but from an industrial point of view it is rare because the total number of mines in relation at the actual extraction rate, leads to a supply of hundreds of years. Its frequency is similar to tin or molybdenum, but in comparison, it occurs in a form that it cannot be extracted directly (its combination with other elements in some mineral will be treated in the next section).

Niobium is a transition metal and it is located in the middle of the periodic table of elements, in particular in group V, period 5, and it's nearby other alloying elements, such vanadium, molybdenum, manganese, ...

In air it is very stable, and it has a bluish tinge, if the exposure to air at room temperature is protracted; its low affinity for oxygen lasts until 200 °C, above which it begins to oxidize. On the contrary niobium has good affinity to carbon and nitrogen, and it is an important aspect for his application in steel, as will be described subsequently. Also the corrosion resistance is high, in fact only, for example, hydrofluoric acid and concentrated sulfuric acid can corrode it, while most acids don't attack it at room temperature; hot alkalis can also make it instable, due to the dissolution of the protective layer.

Niobium has some oxidation states, but the most stable is the +5, in fact niobium oxide Nb_2O_5 , after mining, is the “starting point material” from which a lot of product are obtained. In the pure form niobium has a high melting point, so it's preferable to have special alloys, like FeNb or NiNb, to melt the material at an eutectic composition.

Concerning the electromagnetic properties, it has a relatively high critical temperature of 9,25 K, below which it becomes superconductive: being the pure material with the highest critical temperature, his importance in this field is remarkable. In the pure state or in alloying with others materials (some example are noteworthy, having even higher temperature), it has various applications such as equipment for magnetic resonance or even at CERN, where it has been used for over forty years in particle accelerators.

In nuclear field, instead, it has been employed in claddings for nuclear reactors, due to its corrosion resistance and its compatibility with uranium. In addition niobium has some isotopes, with different half-life (for example ^{93}Nb is found in nature).

From a medical point of view it is considered non-toxic, non-allergenic and biocompatible (in fact there are jewelry application), although niobium dust can irritate eyes and skin; about its dust, lastly, it's remarkable to say that it is highly flammable.

Table 1 summarizes the main features of niobium in the pure state.

Atomic number	41
Atomic radius	2,08 Å
Atomic weight	92,906
Main oxidation state	+1, +2, +3, +5
Crystal structure	Body centered cubic
Density	8,57 g/cm ³
Hardness	145 HB (Brinell)
	151 HV (Vickers)
	6 (Mohs)
Melting point	2741 K
Electric conductivity	$6,58 \cdot 10^6$ A/Vm
Thermal conductivity	53,7 W/mK
Magnetism (natural state)	paramagnetic
Young's modulus	105000 MPa
Poisson ratio	0,38

Table 1 Main properties

1.3 Mining and production

[5-7] Niobium's occurrence in the world is localized in some sites, where its concentration (it's found always into other minerals and never in pure form) is higher; the main deposits are located in Brazil, Canada, Australia, South Africa, Russia and China, but the most important is Brazil. Here, in particular near Araxá (Minas Gerais) arises the largest niobium reserve in the world; it's in this place that a Brazilian geologist, Djama Guimarães, discovered the presence of pyrochlore (from which is obtained niobium) in 1954. This is considered the origin of CBMM, Companhia Brasileira de Metalurgia e Mineração.

CBMM was founded in 1955 and nowadays it supplies more than 80% of the world niobium product. In 1961 it begins mining and operation product, and with more than 50 years of investment in development of technologies and application, it has become the world leader; to confirm this, it's useful to say that the production capability of ferroniobium FeNb (the element used in niobium steelmaking) has grown up constantly from 1800 tonnes in 1965, to 150000 tonnes in 2020. Considering that the world consumption will be around 100000 tonnes this year (the global health emergency has slightly reduced demand and consumption), it's obvious that CBMM is at the forefront of its sector.

As said before, the first finding in Araxá was in 1954: after preliminary studies, geological mapping and samples evaluations (1958), the activity started with the construction of the first plant in 1960.

In figure 1.2 the extraction site is shown: it is an open-pit mine and over time its dimensions have grown up to several square kilometres. Very closed to the mine there is the plant where the finals products are obtained.



Figure 1.2 Aerial image of a portion of the mine

Niobium in nature doesn't appear in pure state but always in combination some minerals, which are primarily three:

- Pyrochlore $(\text{Na,Ca})\text{Nb}_2\text{O}_6(\text{OH,F})$
- Columbite $(\text{Fe,Mn})(\text{Nb,Ta})_2\text{O}_6$
- Euxenite $(\text{Y,Ca,Ce,U,Th})(\text{Nb,Ta,Ti})_2\text{O}_6$

In particular the most important is pyrochlore (figure 1.3a), present, in turn, into carbonatite. The site of Araxá is rich of this mineral. The ore is composed by a series of element in addition at pyrochlore: some of these are quartz, limonite, magnetite, barite, monazite, phosphorus, rare earths and also traces of tantalum, which sometimes is found together with niobium due their similarity.

Niobium, in pyrochlore, is in oxidized form, precisely Nb_2O_5 ; its average content is about 2,3%, but there are isolated zone with 5%. The Araxá complex has an approximately circular shape of about 4,5 km in diameter, and the depth reaches also 200 meters before fresh rocks are encountered, in particular in a circumscribed area of 1,8 kilometres in diameter. High niobium concentration occurs in weathering zone, which extends from the surface to the fresh rocks; it is stands out for its light brown colouring.

Studies based on a deep hole drilling program, revealed that there is a large niobium reserve in deepness: fresh carbonatite with a slightly lower concentration (about 1,5%) were found even at 800 meters depth. An estimation assumes a Nb_2O_5 quantity of more than 1 billion tonnes; this would assure CBMM a large production for a very long time.



Figure 1.3 (a) on the left a crystal of pyrochlore and (b) on the right the final product: ferroniobium

The process, which leads to ferroniobium (figure 1.3b), begins with the ore extraction through bulldozer, and it's characterised by mechanical dismantlement, loading and material transportation. Then heavy trucks carry the material, from different areas of the mine (for a first mixing), into the homogenizer. The term derives from the operation of homogenization, necessary due to the different concentrations of the ore in various part of the mine.

Subsequently the process moves to the production plant, where it takes place the concentration: this is a physical separation conducted with water, in which the heavy parts sink. The main steps are: crushing, magnetic separation and flotation; in figure 1.4 are visible a large crusher (a) and the flotation circuit (b), where it takes place the separation and the concentration of niobium mineral (through selective froth flotation of pyrochlore). The flotation concentrates are filtered and thickened in a disk filter and transferred to the next process.

All concentrator tailings go to a large tailing pond for sedimentation of the solids waste. Here there is a recycle of the water used in the process.

With this operation there is an enrichment of Nb_2O_5 from 2.3% to over 50%.



Figure 1.4 (a) the crushing plant and (b) a flotation cell

The subsequent step is the refine, which is done in a leaching plant. It consists of two parts:

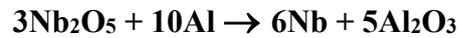
- I. **Desulphurization:** the material goes through a series of filter that remove water and palletize the mixture (figure 1.5). Then, into some container, it's added calcium chloride, which, through chemical reaction, removes sulfur. The percentage of Nb_2O_5 now reaches about 56%.
- II. **Dephosphorization:** in this step the aim is the removal of phosphorus and lead, which are undesirable. In a vessel, having electrodes to activate the reactions, it's added the previous desulphurized concentrate, coal and iron scrap: lead chloride are formed, volatilized and picked up by a cooling tower. Simultaneously phosphorus binds to iron forming FeP, that is removed through a separate casting. The refined concentrate is cast, granulated and again filtered and dried. After these operations the content of Nb_2O_5 is around 60%.

All the slags and filtered are treated before going to the tailings disposal system, in order to not create environmental problems (being the system totally enclosed).



Figure 1.5 Transportation of palletized concentrate

At this point it starts the last operation for the ferroniobium production: the aluminothermic reaction; this is a metallurgy process, which reaches also 2400°C. In a large vessel are mixed the refined pyrochlore concentrate, aluminium, iron powder and calcium oxide CaO. These elements combined together lead to the aluminothermic reaction:



During the reaction the slags and products gradually separate into two layer, with the latter sinking and the slags on top of the metal. These are mainly composed by alumina Al_2O_3 and other impurities. Furthermore in the product it remain a little quantity of phosphorus and sulfur, which can be controlled; their removal depends on the degree of purity to be obtained, so an higher level of purity involves a longer process time and more costs.

After the end of the reaction, the slag is removed and finally ferroniobium (deposited on the bottom) is obtained, with a percentage of niobium around 65%; it is kept in a sand bed until it solidifies, and lastly it is crushed to lumps smaller than 100 mm (it's possible to get also 1 mm lumps, it depends on the future use). After that ferroniobium is packed in different possible quantities and granulometries, and it's ready for shipping.

In figure 1.6 is represented a summary scheme of the processes. For completeness there are present also other products of CBMM.

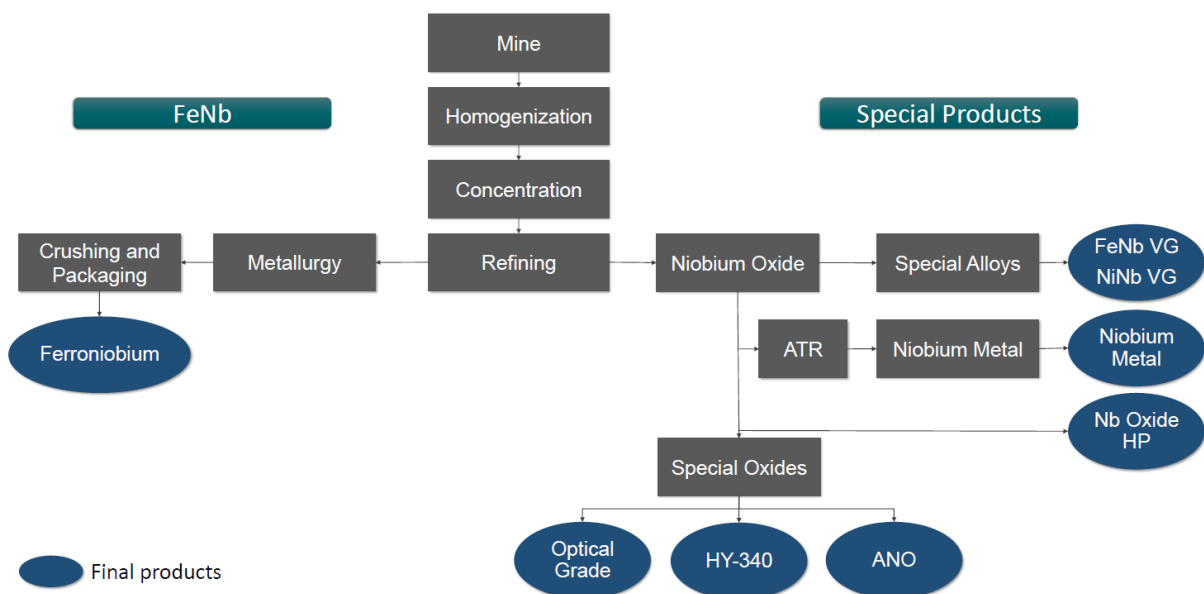


Figure 1.6 Products and processes at CBMM

Beside ferroniobium described above (whose production is however the largest at CBMM), other special product are made: for example special oxides, (in which the initial process is similar), with higher pureness (about 99,8 %), due to the specifications for applications. In fact these oxides are employed in lenses (optical grade) and as a catalyst promoter (Ammonium Niobium Oxalate ANO, and niobium oxide hydrate HY-340), so they need high purity.

ATR represent the process that leads to niobium metal: it consist in multiple re-fusions at high temperature and high vacuum (respectively 3000°C and 10^{-4} mbar) using an electron beam furnace. His applications are superconductive wires and magnetic resonance machine. Acronym VG, instead, means vacuum grade; the difference between these special alloys is the application: VG alloys is used by steelmakers with vacuum furnaces, and it has less impurities having the aim to have less volatile elements.

1.4 Ferroniobium addition during steelmaking

Most of niobium produced is used in the steel industry because its beneficial effect on the steel properties, as it will be explained exhaustively in this thesis.

Niobium can't be added as a pure metal in the liquid steel, because its high melting temperature would make the process unnecessarily long and expensive, so the addition element is ferroniobium: to understand better this "choice" it's important to insert immediately, in figure 1.7, the phase diagram.

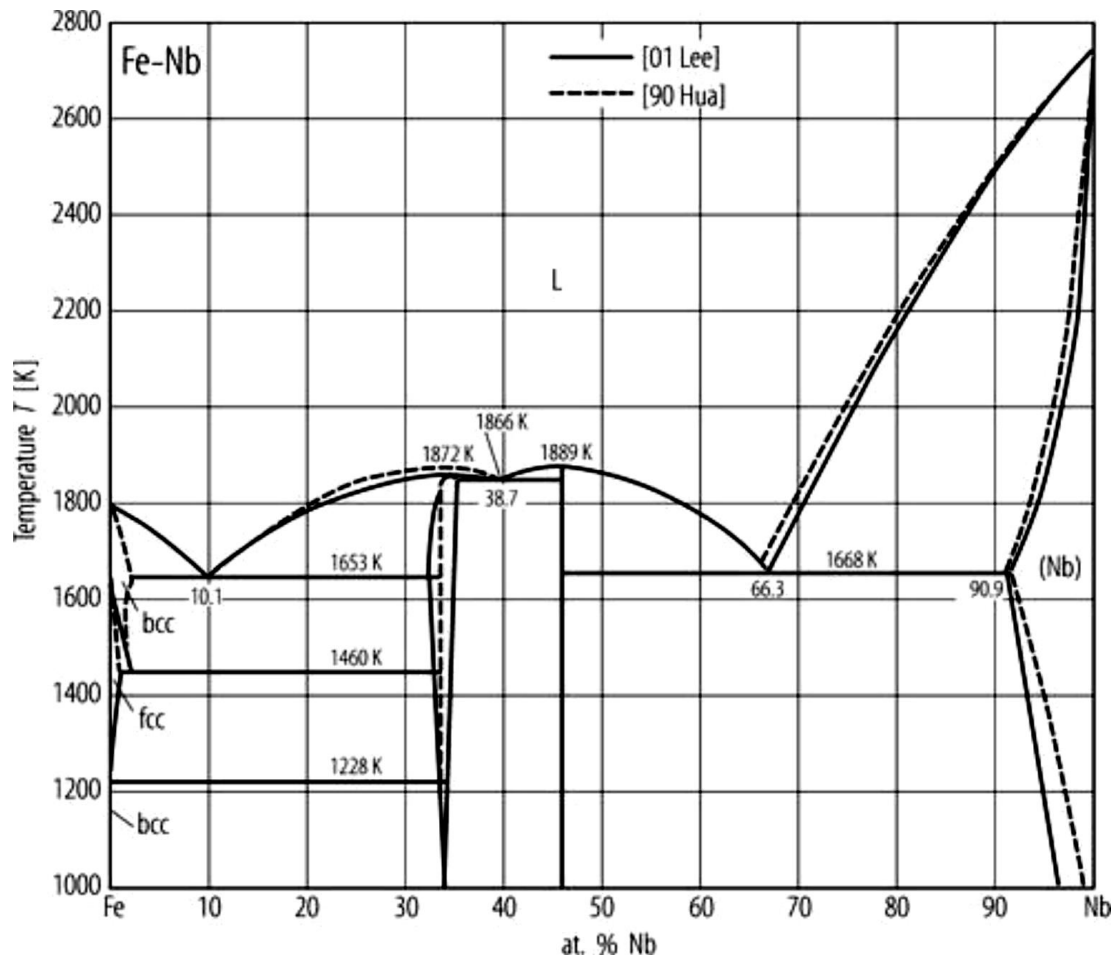


Figure 1.7 FeNb phase diagram

The lower temperature useful for dissolution is the eutectic point, which is located at 66,3 % Nb, that is approximately the composition of FeNb produced at CBMM. There is another eutectic point, at 10 % Nb, that could be used, but it has a small quantity of niobium, therefore it would be needed a larger amount of material. On the other hand the use of pure niobium, as already mentioned, would increase excessively the temperature.

The addition of ferroniobium in liquid steel happens at about 1600°C, but it depends on some factors such as time, size and shape of the particles; therefore for this reason it will be reported the study of E.B. Cruz et al. [8], who investigated the effect of the particles shape and different temperature on the dissolution. First, however, it's convenient to explain the dissolution in general.

Although niobium's affinity for oxygen is relatively low (in comparison to others microalloying element such as vanadium and titanium), it will form oxides that could render it

ineffective during subsequent steel processing, so niobium should be added after the steel was killed.

Also the oxidation with the slag is to be controlled because the interaction could oxidizes niobium and remove it from the steel, so this interaction and the relative loss should be minimized. For this reason it's appropriate to open a sort of eye in the slag layer, to allow the particles to enter directly in the liquid by a chute.

The density of ferroniobium is higher than that of liquid steel (8,1 vs 7,1 g/cm³) and FeNb sink in the melt (with the risk of incomplete dissolution), so an adequate stirring with argon gas or electromagnetic stirrers can promotes an efficient mixing. The dimension of the particles it's also remarkable, in fact bigger pieces dissolve slower and less efficiently than the finer (as it can be seen in the diagrams in figure 1.8); normally the particles doesn't exceed 50 mm.

The dissolution consists of three stages:

- I. Addition to the steel bath at around 1600°C: FeNb (at room temperature) locally freezes the liquid forming a solidified shell around it; meanwhile it begin to heat up.
- II. The steel shell achieves the maximum thickness when its temperature equals the liquid steel temperature and it starts to remelt. In this moment the ferroniobium particles reaches temperature higher than 1500°C and the eutectic regions melt down and begin to react with iron, forming a layer below the remaining solid shell. When the shell is completely remelted, the partially melted layer comes into direct contact with the liquid steel, starting its rapid dissolution in the liquid.
- III. In the final dissolution step the melting mechanism is accompanied by a liquid/solid diffusion, leading to the complete melt of FeNb.

The microstructure of ferroniobium is mainly characterized by two phases: primary lath of intermetallic Fe₂₁Nb₁₉ (μ) and eutectic zone. This is, in turn, formed by three phases: e1 Fe₂₁Nb₁₉ (a little less than 50% in the phase diagram), e2 niobium globes and e3 Fe₂Nb₃ (about 60% Nb, near the eutectic composition in the diagram). These have different melting temperature: the first melt form 1575°C and the latter from 1510°C. Therefore the usual steelmaking temperatures of around 1600°C are sufficiently high, in fact after the second stage in which the eutectic zones quickly melt, the temperature increase (due coming into contact with the hotter liquid) and also the remaining intermetallic μ phase can dissolve.

A successful dissolution depends on some factors: for example a higher temperature on the liquid steel leads to more rapid melting rate, as well as a stronger degree of agitation; a longer time allows better dissolution, but this factor is related to the particles size. With the previous temperature it can be reached a dissolution more than 95% in less than 10 minutes.

As said before, dimension and shape of the particles affect the melting behaviour; lumps and briquettes are made in a wide range of size, for each applications. The mentioned study [8] presents a characterization of the dissolution rate and dissolution mechanism of fines lumps and briquettes, comparing industrial and laboratory trials. The last one was carried out dropping these two type of samples in a deoxidized low carbon steel bath, heated up to three different temperatures: 1560, 1600 and 1640°C. The dimension are 20, 30 and 40 mm in equivalent diameter for lumps, and a fine briquette (<2 mm). The industrial trial, instead, is more similar to the common practice; it is characterized by a steel temperature of 1570°C and three type of samples: lumps with size distribution from 5 to 15 mm and from 15 to 30 mm, and briquettes of 40 mm in equivalent diameter. Also in this case the steel has a low oxygen content.

The result of the tests are shown in figure 1.8, where are represented graphics of the niobium content in the steel bath in function of time. It's clearly understood that longer times makes the dissolution more complete, and also the reduction of the particles dimension have beneficial effect. For both industrial and laboratory briquette dissolve more quickly, even if its dimensions are larger; this is visible in the industrial trial where briquettes have the largest dimensions, but they dissolve more rapidly than lumps.

In the figure are represented only two representative graphics (industrial and laboratory trials at a similar temperature), since, by increasing temperature, the differences between the various dimension and shape is less remarkable; at the highest temperature (1640°C), in fact, the rate is similar and all FeNb particles dissolved in a few seconds.

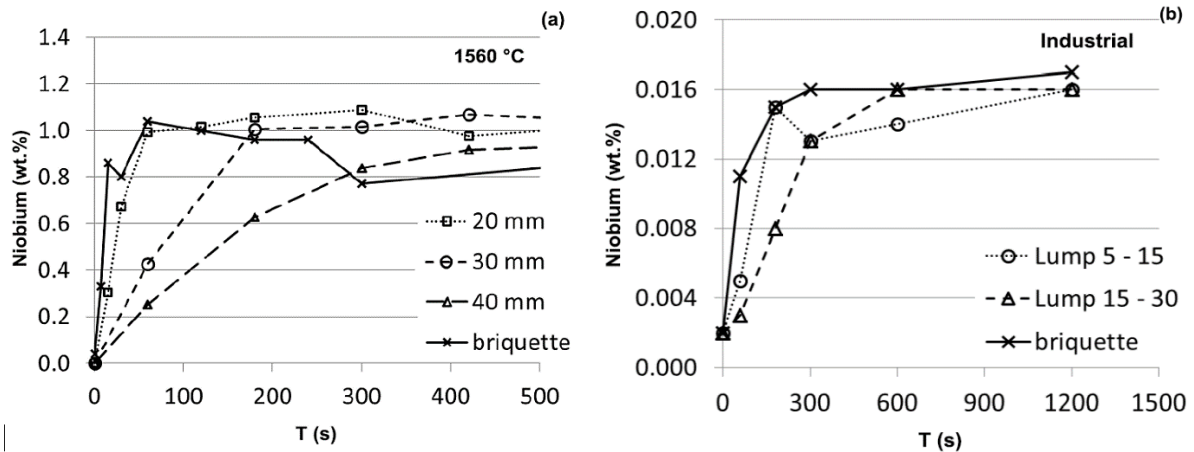


Figure 1.8 (a) laboratory trial and (b) industrial at 1570°C

A different behaviour is remarkable in the first test (fig. 1.8 a): the fine briquette for long dissolution time shows a reduction not negligible. This loss could be attribute to the very little dimension: this promotes a rapid dissolution, but in case of a time elongation, particles too small may be carried away by the convection current. For this reason it's important to keep under control the magnitude of the stirring (an agitation too vigorous could cause loss) and apply the correct time in relation with the particles size.

Almost total dissolution (the achievement of the plateau in the curves) occurs in about five minutes, and, obviously, this time drops when the temperature increase. The niobium addition at steel reaches high level of about 98% of the amount added as lump or briquettes.

The different attitude of briquettes to melting is investigate in a second part of the study, in which it's understandable the better behaviour. This part of investigation has the aim of describing the dissolution mechanism at the interfaces between the ferroniobium samples and the steel bath. For this purpose, the particles were immersed in the liquid steel, held for 10 seconds and water quenched for metallographic analysis.

The results are represented in figure 1.9; the melting is not completed, so both the samples formed the typical frozen shell around them.

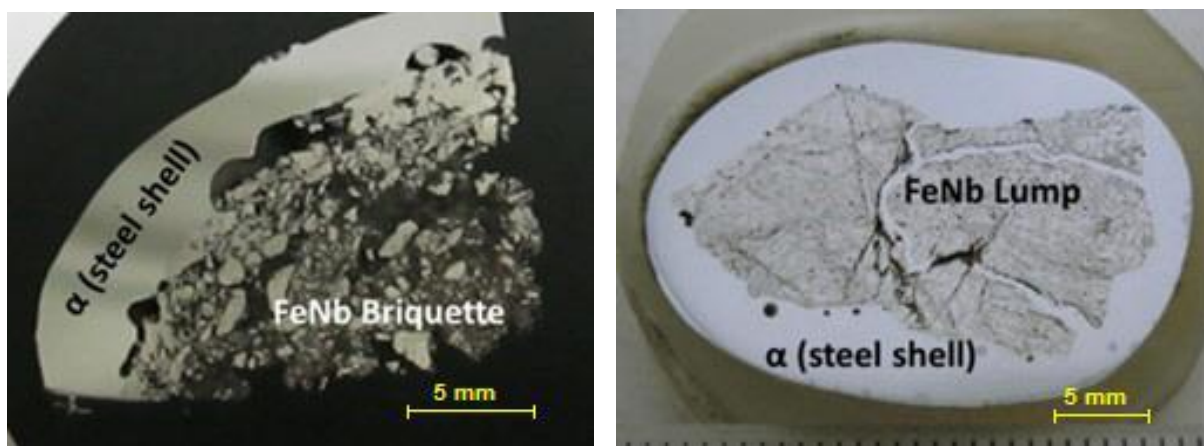


Figure 1.9 (a) focus on the section of metal with briquette and (b) with lump

The difference between the two trials lies in the larger number of particles that are exposed to the intermediate reaction layer formed below the shell; so briquettes have a higher reaction surface area of fine particles that are readily released and brought into contact with steel. In comparison with lumps the dissolution is faster because in the latter the reaction layer come into the FeNb core through pre-existing cracks, and it doesn't penetrate uniformly as the previous case. Probably the presence of more particle, visible in the example in figure 1.9 (a), is due to the more numerous processes of which the briquette is characterized.

Regarding the section shown in figure 1.9, it's should be said that the white region α (the steel shell) has the same composition of the surrounding steel bath, whereas the reaction layer is composed by an iron rich phase (α) and a low niobium content eutectic zone (which is the first to melt, as mentioned above). The internal region has obviously the composition of the initial FeNb piece, as it hasn't yet reached total dissolution.

1.5 Economical evaluations

[9] Niobium price has been remarkably stable in time, because it is essentially determined by the market leaders rather than being driven by supply and demand.

CBMM, being the most important producer of FeNb in the world, leads the market and its decision is to maintain the price in a limited range. In this way it is enabled a reliable market, oriented also at the development of applications and knowledge about niobium; for this purpose CBMM maintains two months of inventory at key distribution centre to ensure an efficient delivery even there is an unplanned demand.

Before the 60's the availability of niobium was restricted and its price was too high to allow most commercial developments; only with the discovery of large deposit in Araxá and the beginning of its utilization, price could reach a stabilization.

The diagram in figure 1.10 shows the price over the last decade [10].

For completeness it is mentioned the only significant variation happened around 2006: in this period CBMM made large investments in order to increase his production and the price moved from about 15/20 US\$/kg to the contemporary one. In addition another "ambition" was to make a one-off adjustment to a persistently price undervaluation environment (since in the same time demand was increasing and producers were expanding capacity) [11].

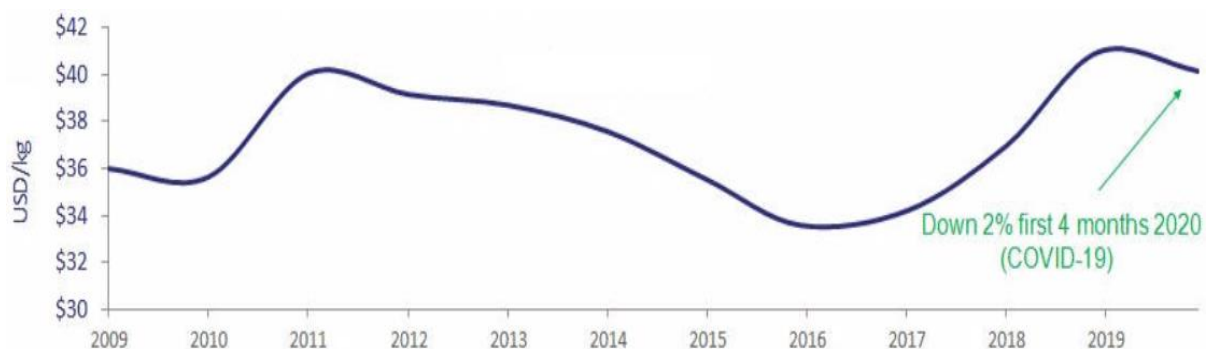


Figure 1.10 Price evolution of FeNb

Actually the quotations of Nb is around 35/40 US\$/kg and forecasts for future trend are stable. The global impact of Covid-19 has consequences for industry and also for niobium demand, which will decrease; however, contrary to the expectations, Chinese steel economy

will not fall, thanks to government measures. So the drop of the rest of the world will be mitigated by China’s resilience, and the demand will not fall too hard.

The price continuity is a own characteristic of niobium: the others alloying elements see volatility in their quotation. This derives from the fact that the reserve of these materials are not concentrated almost entirely in one area, but maybe they are distributed around various part of the world, and the leadership is not in the hands of a single company. In this situation, a variation in industrial usage could have significant effect on supply and demand, and the price could suffer drastic oscillations.

An emblematic example is given by vanadium [12,14]: in the last years this element has experienced a roller-coaster ride, as it can be seen in figure 1.11. In 2018 the Chinese decision to change standard for rebar in the building sector, gave a strong impulse to the price growth, reaching a historic peak of 120 US\$/kg; this request for rebar made with microalloyed steel in seismic zones, started the supply of a microalloying element, and since vanadium was the cheapest in that moment, his demand grew up exponentially, together with the price. In addition, also the usage in redox batteries gave a contribution. Once the price has increased too much, the costumers changed their attention to niobium and vanadium price started to go down, approaching a price comparable to niobium’s one. The flattening in the production of steel in 2020 has also contributed to this price drop (not totally visible in the graph).

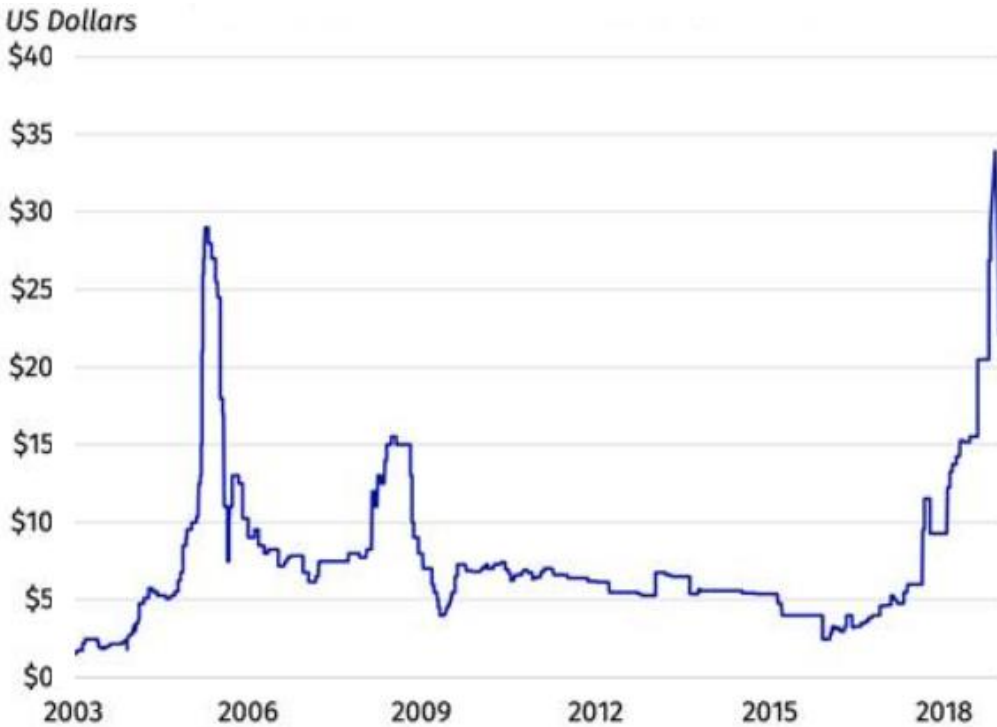


Figure 1.11 Trend of vanadium price

The previous peak in 2005 was already “caused” by China, whose steel production grew considerably and also the consumption of vanadium. Before this situation there was an excess of vanadium production and this justifies the low price. Therefore, this made a gap between supply and demand, surplus stocks were exhausted and the price increased. This condition changed quickly when substitution of vanadium with niobium, and others causes, leads to supply exceeding demand once again, and the subsequent price collapse.

[15,16] The third principal microalloying element, titanium, is considered a strategic raw material, and its production is concentrated in Asian continent and USA, although Russia, Japan and China alone account for more than three quarters of global output. Due its geographical distribution, titanium quotation has more fluctuation than niobium, but less than vanadium. In addition it's remarkable to say that these fluctuations are often triggered by change in sponge and scrap availability, in particular the titanium dioxide is a key factor for titanium price, since this is the most used type of material.

It has a wider market than niobium and vanadium, in fact its application are, for example, in aerospace and military sectors, so there is a special attention to it (for example titanium is included on the US Department of the interior's list of mineral products considered critical for economic and national security). Regarding the utilization in aerospace industry, although the last years saw an increase in trade, the outbreak of Covid-19 led to an unprecedented drop in air travel aviation: therefore the operators, due to the uncertain period, stopped the future order, affecting the demand. However, apart from this unexpected period, the titanium industry is on a long-term growth trend: for example the continuing advance in the field of additive manufacturing generates interest.

In steelmaking titanium is use as ferrotitanium; also in this field the global pandemic had influences in market, pushing down the price (due to a weak demand), after a period of stability. Nevertheless in the future, the growing requests for advanced high strength steel in automotive will increase the demand.

2. STEELS: PROCESSING AND PROPERTIES

2.1 Steelmaking

This chapter aims to introduce processes, metallurgy notions and main features of the steels before going into the effects of niobium; these arguments are exhaustively treated in [17,18].

Actual steelmaking is based on two processes: basic oxygen furnace and electric arc furnace. The latter is characterized by the use of steel scrap instead of coke or hot metal: iron recycling is adopted by long time because it has the advantage that it only needs to be remolten and not reduced from oxidized to metallic state. Steel scraps are charged into the furnace, in which graphite electrodes are inserted; an electric current passes through these electrodes to form an arc, which generates the heat necessary to melt the scrap. In this phase, if required, appropriate alloying elements are added to give the chemical composition required to obtain desired properties. The molten steel is then poured into a ladle, where it can be subjected to casting or secondary steel making operation, such as desulphurization or deoxidation; so it's possible to produce high quality steel, even though the source is scrap with various composition and some elements cannot be removed. This technique is profitable because of the reduced need of energy and the low equipment cost, but it is related to availability of scrap (steel demand has increased over time and so only scraps are not sufficient).

Basic oxygen furnace is, conversely, the main process for steel production, in fact about three quarter of the total (more than 1800 million tons per year) is made in this way. The actual method, introduced in the second half of the twentieth century, uses as raw material the "pig iron", which is produced in blast furnace by the reduction of ore. Pig iron, then is refined in steel with less carbon content in the basic oxygen furnace, and finally the product is cast.

The first step is the reduction of the ore (usually iron oxides) with coke, that is carbon produced from coal by heating it to expel undesired organic matter and gasses. The ores are previously dried and calcined to eliminate water or CO₂, and they are palletized with coke to form sinter, a porous agglomerate that makes the process more efficient. Another third element is added: limestone, mainly calcium carbonate, which acts as a flux for easier melting and slag formation (it absorbs many impurities floating on top of the molten iron and it is easily removable). These materials are charged into the top of the blast furnace, whose dimensions are approximately 30 meters in height and 10 meters in diameter. At the bottom of the furnace hot air (also 1600°C) is blown through nozzles called tuyeres and goes up heating the materials. In the first stage (from top to down in the furnace) the chemical reductions occur: carbon monoxide removes oxygen from the iron ore and leaves metallic iron; the newly formed CO₂ and the remaining CO come out as exhaust gases.

At a lower location these reactions are completed and the slag formation begins; meanwhile others secondary reactions occur and the solid iron starts its fusion. Below this, there is the inlet of hot air: oxygen reacts with coke to form carbon monoxide (which takes place in the reductions mentioned above), and generates a great amount of heat, that supports the process. This section is called combustion zone.

The resulted molten iron is deposited on the bottom and a layer of slag floats upon it. These two products are tapped at regular interval and collected separately in containers, by opening a hole in the bottom of the furnace. In figure 2.1 is represented a complete scheme of a typical blast furnace, in which are shown all the devices and the zones outlined in the process.

The performance of a blast furnace is indicatively 50%, in fact to obtain one tonne of molten iron, two tonnes of ore are necessary. Exhaust gases, resulted from reactions between air, coke and flux, are extracted and used as fuel in other operations during steelmaking. A considerable quantity of slag is also produced, and it can be recycle as inert material.

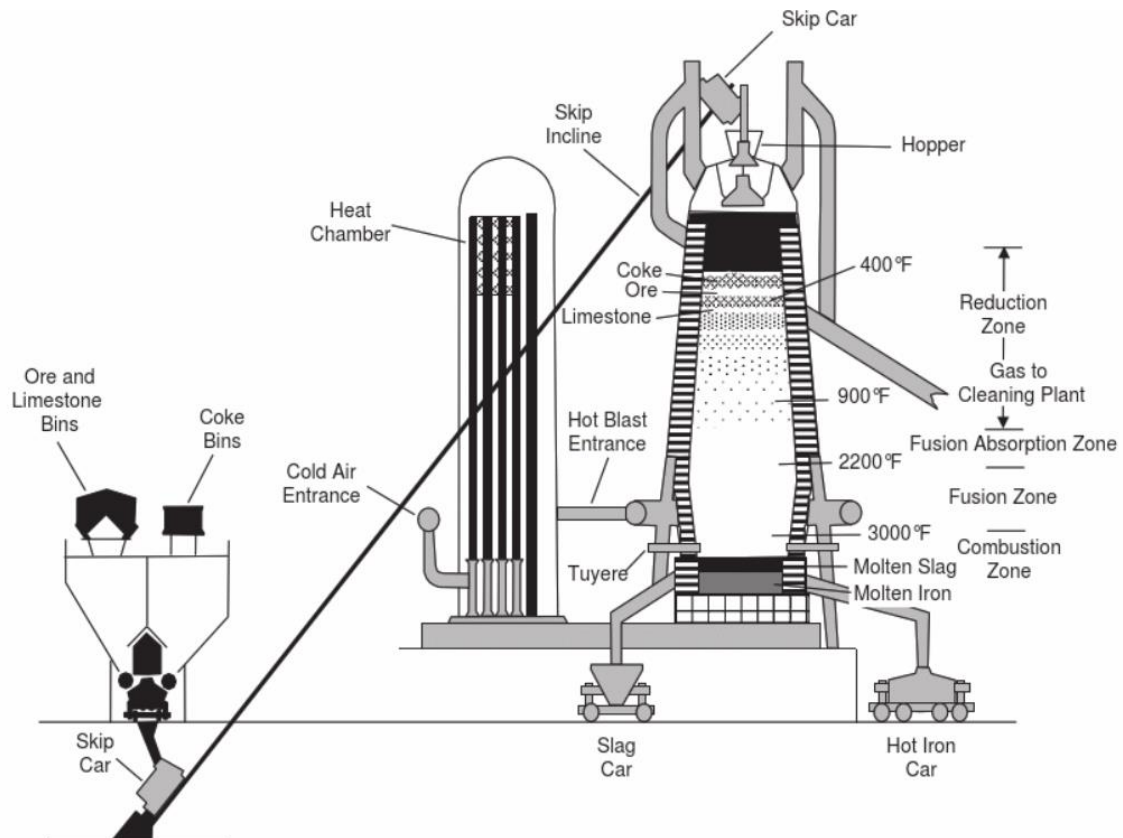


Figure 2.12 Representation of an iron blast furnace

The liquid iron obtained at this moment is not the final steel, but it has a high carbon content (about 4%) and others impurities; it's called pig iron and it has to be "converted" into steel. This operation happens in a large vessel, but sometimes it's made an intermediate operation of desulphurization. The vessel is called converter, and liquid pig iron (coming from the blast furnace through refractory containers at about 1200°C) is poured in; some iron scraps are also charged.

An oxygen lance is then lowered into the vessel, and pure oxygen is blown at high pressure. The oxygen insufflated reacts with the molten pig iron: this operation allows to eliminate carbon and generate heat. In fact the oxidation reaction between O_2 and C in liquid steel, is exothermic and releases a large amount of heat, that increases temperature up to 1650-1700°C (necessary to keep the steel liquid). Therefore carbon in the steel reacts with oxygen to form iron carbon monoxide; in addition other impurities are oxidized, forming the slag. Pig iron is finally converted in steel with low carbon content (< 1%). The converter is tilted and steel is tapped into a ladle, separately from the slag.

Once the final steel is obtained, there is the ladle metallurgy, in which take place the refining operations. Firstly the remaining unwanted elements (such as O, H, N) are deleted, with the aim of achieving the desired cleanliness. Then there is the addition of appropriate alloying elements, according to the final chemical composition.

After ladle metallurgy, the final product is continuously cast in a continuous casting machine. This method has replaced ingot casting because for mass production like automotive industry, it is more efficient and economical. Molten steel is transported above the casting machine and it is poured into a tundish (fig. 2.2); an opening in the bottom of the tundish allows steel to flow into a water-cooled mold. Here the solidification begins, with the formation of a skin on the metal surface. The solid layer thickens by advancing, and the remaining liquid at the centre of the ingot is solidified by spraying cold water. In this way the solid metal forms a

long billet, that is pulled by support rollers so that a continuous steel slab is produced. At the end of the machine slabs, blooms or billets are cut to the required length.

These products tend to have a non-homogeneous microstructure and composition, due to a stratification of the alloying elements (composition) and different cooling rate through thickness (microstructure). These aspects and other issues during casting will be investigate in a subsequent paragraph.

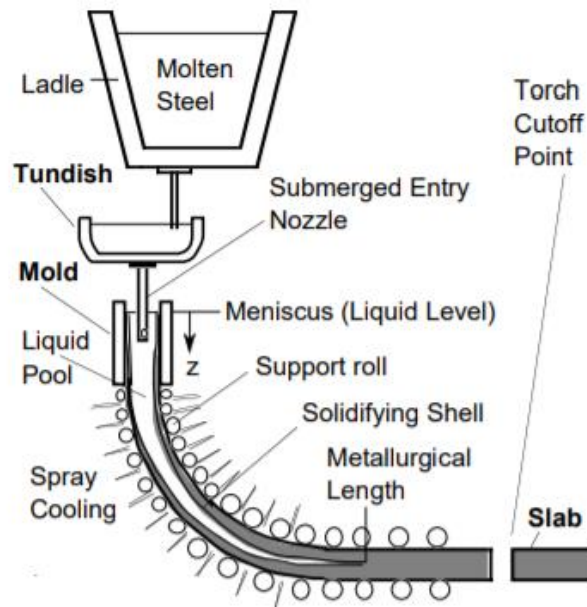


Figure 2.2 Continuous casting process

2.2 Hot rolling

[17-19] Semi-finished products are transported from the steelmaking plant to the rolling mill, where there is a reduction in thickness or the final shape it's already reached. Billets are reheated at 1200°C and then are passed through a series of rolls. The first pass is called roughing and going forward for the rolling direction, thickness is gradually reduced approaching shape and dimension of the finished product. The amount of deformation that can be achieved in a single pass depends on the frictional conditions along the interface: if the deformation is too high, rolls will be unable to squeeze the steel, and they will skid. During progression temperature decrease and the rolls speed increase (simple mass balance since there is a thinning), so it is required a computer control of the speed at each stand of rolls. At the end of the operation there is the possibility to wrap the strip in a coil; this is called coiling and it will be seen that its parameters have importance on mechanical properties.

With hot rolling it's possible produce plate or strip mills from slab and long product from blooms and billets (these are used in building sector for example as railway rails and bars with cross sections shaped like an "H").

The preliminary reheating is made to act in the austenite range, which provides a more uniform grain size and a better distribution and size of constituent particles; roughing, in fact, has the aim of "break" the structure of the "as cast" steel, that is inhomogeneous. During hot rolling the grain structure becomes elongated in the rolling direction, and some processes take place: material is subjected at high deformation that causes an increase in dislocations density and crystalline imperfections. Thanks to high temperature, material tends to lowering its free energy through a set of restoration processes that lead very quickly to the formation of new

austenite grains. These processes (that occur during annealing operation in which temperature is higher, so they result faster) are mainly:

- **Recovery:** it can be defined as a sequence of event that involve annihilation and rearrangement of defects. The high number of dislocations leads to a rearrangement into lower energy configuration, which annihilates many of them. Dislocations climb and slip to line up into low angle boundaries. These form internal subboundaries surrounded by subcrystal, which are free of dislocations because when dislocations of opposite sign meet, these cancel each other out. After the initial formation, two or more subboundaries migrate and meet to form a single one. This encloses a subgrain that increases with time and temperature. Recovery is initially very rapid and, with time increasing, it becomes slower.
- **Recrystallization:** it is a mechanism of nucleation and growth of new strain-free grains. It can be divided in dynamic and static recrystallization: the first takes place during deformation, while the latter occurs after deformation (obviously while the piece is still sufficiently hot). Usually for hot rolling the deformation time is short, so grains rearrangement is accomplished only by static recrystallization; its driving force is the remaining stored energy that was not deleted during recovery. It is a different process than recovery: this one, in fact, starts slowly with an incubation period (where stable nuclei are formed by the coalescence of subgrains) and proceeds faster with grain growth, while recovery process is opposite.

Recrystallization is a softening mechanism and it is affected by many factors, such as time, temperature, degree and rate of deformation, original grain size and metal purity: at higher temperature recrystallization starts before and it occurs less time to achieve a specific recrystallization fraction. If the amount of deformation is higher, then recrystallization occurs at lower temperature and with shorter time, because there is more dislocation density and thus more stored energy. In fact there is also a critical value under which there isn't a sufficient amount of energy to initiate recrystallization; on the other hand there is a ϵ_{cr} value at which steel can be strain at which dynamic recrystallization is initiated, due to high deformation.

Pure metals exhibit lower recrystallization temperature, and grains can grow more. Lastly, the finer initial grain size before deformation, the shorter time and the lower recrystallization temperature, since there are more stored energy and nucleation sites. These aspect will be treated again when the role of niobium is investigated.

- **Grain growth:** this process is characterized by the migration of grain boundaries, in fact they still have an interfacial energy. If there is a sufficient time (for example long interpass time or holding the workpiece at elevated temperature), the metastable material will recrystallize and grains will grow, ideally tending to form a single grain or monocrystal. However, the effect on growth rate of increasing temperature is more relevant than increasing time

It can occurs in two type: normal and abnormal grain growth. The first occurs by the movement of grain boundaries resulting from diffusion of atoms: grains with convex curvatures grow and incorporate those with concave curvature that are more instable and tend to shrink themselves. Conversely the abnormal mechanism takes place when few grains grow disproportionately. It occurs usually at high temperature (for example in carburizing of steel) when grain boundaries are initially pinned up by the presence of a precipitate second phase; nevertheless this resistance can be broken by elevated temperature because the second phase particles can coarsen or even redissolve, losing their force.

In figure 2.3 is shown an image of the grain evolution during hot rolling. In this case there is only a stand of rolls, but, if there is sufficient time and temperature, recrystallization phenomenon occurs within every stands. So, the “starting point” of a new reduction is the condition after recrystallization and grains growth of the previous pass.

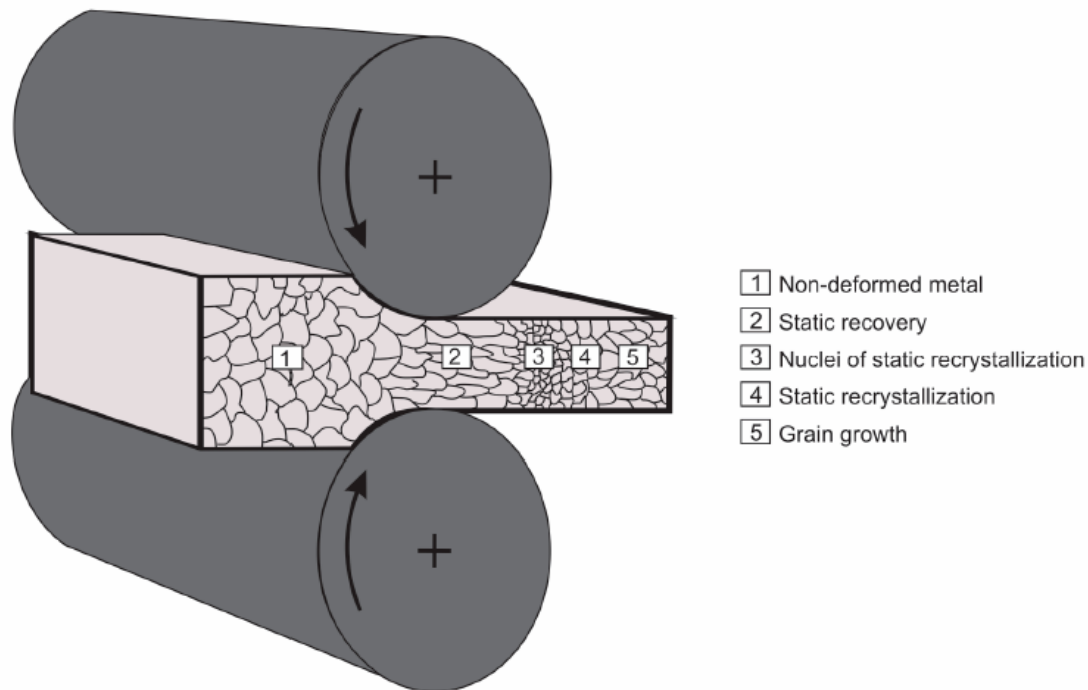


Figure 2.3 Schematic diagram of hot rolling

At this point it is useful to introduce the concept of “non-recrystallization temperature”; its relation with niobium will be a key point of this thesis.

As said before, hot rolling is made in austenite region in which high temperature allows recrystallization; nevertheless it exists a special one called T_{NR} , under which the phenomenon can no longer go to completion in the interpass interval or during cooling. Deformation below this temperature leads to appearance of elongated grains that forms a so-called pancaked structure (displayed in figure 2.5). All mechanisms and implications regarding T_{NR} (with niobium) will be treated in a future chapter, here it is described only a way to determine it.

T_{NR} is not an exact quantity because there is a range between recrystallization begin to be incomplete and it is arrested completely. A common investigation method for determining T_{NR} consists of carrying on a series of rolling passes and represent graphically the mean flow stress resulting versus the inverse of absolute temperature; the inhibition of recrystallization appears as a change in slope of the curve. This is visible in figure 2.4 where it's represented a multideformation test [20]; in this simulation a low alloy steel (0.02% C, 1.5% Mn, 0.26% Si, 0.043% Al) is subjected to 23 passes with an interpass time of 20 s, sufficient to allow an eventual recrystallization.

Since the curve is a function of the inverse of temperature, moving to the right temperature decreases, following the correct temporal evolution of cooling.

In the graph four different zones can be distinguished: initially stress increases slightly as temperature decreases; this corresponds to initial stage of hot rolling at high temperature, where austenite recrystallizes completely. The second zone shows a change in slope, so this is the point of T_{NR} : dislocations are no longer free to annihilate themselves, resulting in a more quickly increase of flow stress.

In the third zone it's manifested a drop in the flow stress, that corresponds to the start of the austenite to ferrite transformation, characterized by the temperature A_{r3} . In the last zone it occurs the rolling of ferrite ($T < A_{r1}$), with a small increase of the stress at lower temperature.

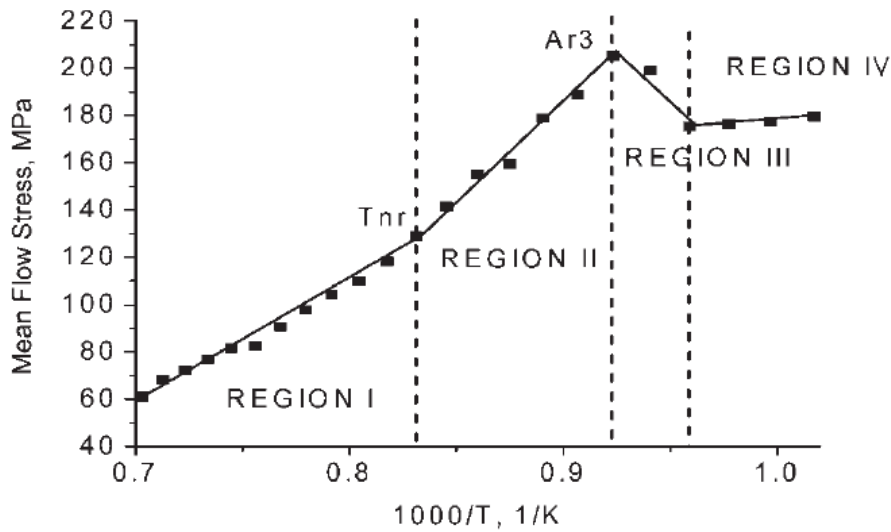


Figure 2.4 Results of the test for T_{NR} definition

For completeness it's opportune to say that in the industrial practice is usual to practice a thermomechanical controlled processing (TMCP) during and after hot rolling. The aim, in fact, is to provide a correct combination of temperatures and deformations, an addition of microalloying elements, a final cooling (less or more accelerated) to obtain the required microstructure and mechanical properties. This is the most efficient and profitable way to improve both strength and toughness of steel (through grain refinement, as it will be described).

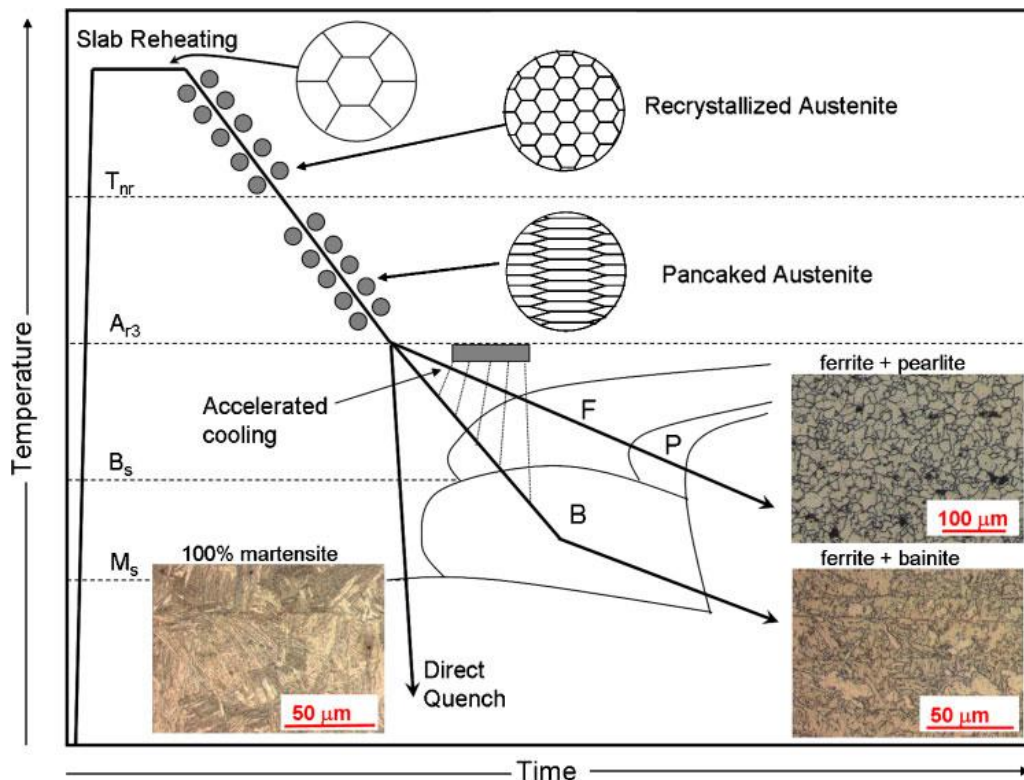


Figure 2.5 Summary diagram of TMCP and resulting microstructures

2.3 Inclusions effect

The microstructures obtained after hot rolling and thermomechanical processing can have intrinsic characteristics depending on the process parameters to which they have been subjected; nevertheless, other feature is important on finished products: inclusion. This occurs during primary processing, and it is introduced here because mechanical properties are affected by its presence. Additionally, also microalloyed elements can have influences on their evolution. Also this section takes many information from [17,18].

Inclusions are non-metallic particles (usually some type of oxides and sulphides) introduced in the liquid steel during steelmaking operations. Cleanliness is an important factor in view of producing steel with high mechanical performance, so a control of inclusions is required.

It's possible to identify two type of inclusions: indigenous and exogenous. The firsts are produced by reactions taking place in liquid or solidifying steel, their dimensions are small and their number is large; exogenous, instead, are larger and more irregular, and their occurrence is more sporadic, because these inclusions are originated from particles of refractories or other external material that come into contact with liquid. During steel production, in fact, liquid is transferred through vessels, tundish and other containers, and it is subjected to turbulence flow; in this condition steel can suffer slowdown and obstruction due to residual particles containing aluminium (this element in fact comes from deoxidation with Al for killed-steel). As a result, this deposit may erode the containers wall and become imbedded in solidifying steel as detrimental exogenous inclusions. An example is MgO-Al₂O₃-CaO crystal, or complex oxides of silicon and aluminium.

Studies regarding steel cleanliness found several sources of inclusion: in aluminium-killed steel, deoxidation products, from reaction between oxygen and aluminium, forms alumina, which is dendritic when it's formed in a high oxygen environment; slag entrapment during steel transfer produces spherical liquid inclusion. Other inclusions come from dirty lumps or broken particles by refractory brickworks; these are irregularly-shaped and can act as sites for alumina nucleation. Some example of inclusions are represented in table 2.

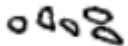
Type	As cast	After rolling
Al ₂ O ₃		
C ₁₂ A ₇		
CA ₂		
MnS		
C ₁₂ A ₇ (sulphide ring)		

Table 2 Inclusions in Al-killed steel. "A" represents Al₂O₃ and "C" represents CaO [17]

As seen in the previous table, inclusion change their shape during rolling: if these are globular particles, then they can stretch along rolling direction. Instead, in case of hard compound developed in a dendritic shape (such as alumina), then deformation during hot work may break them into cluster of particles.

A remarkable type is manganese sulphide; this is often present in steel since manganese is usually in the steel composition. MnS can take three forms: spherical shape randomly distributed in the steel matrix, cluster of fine protrusions in interdendritic distribution (dendritic solidification is promoted by rapid cooling), and angular geometrical shape.

One of many reasons why manganese is added to steel is its tendency to form MnS, thus preventing formation of FeS, which, because of its low melting point, severely reduces hot workability. Nevertheless this inclusion are to kept under control because in some situation are undesired: since they are easily extendable and flattenable along rolling direction during hot work, they can produce anisotropy in mechanical properties. For example resistance to ductile fracture is affected by this, and its reduction can be mitigated by the use of very low sulphur content. Another way is the addition of microalloying element: for example titanium forms sulphides with the same energy as manganese, so it can replace MnS with TiS. It is favourable because titanium decrease the plasticity of manganese sulphide, and may result in reduced elongation during hot rolling. Other materials that works as a shape controller (maintaining as much as possible a circular shape) are calcium or rare earth metals.

Elongated manganese sulphide can also act as a promoter of banding, microstructural condition manifested by alternating bands of different microstructures aligned parallel to rolling direction. In the micrograph shown in figure 2.6 is visible this status, in particular around the flattened MnS particles.

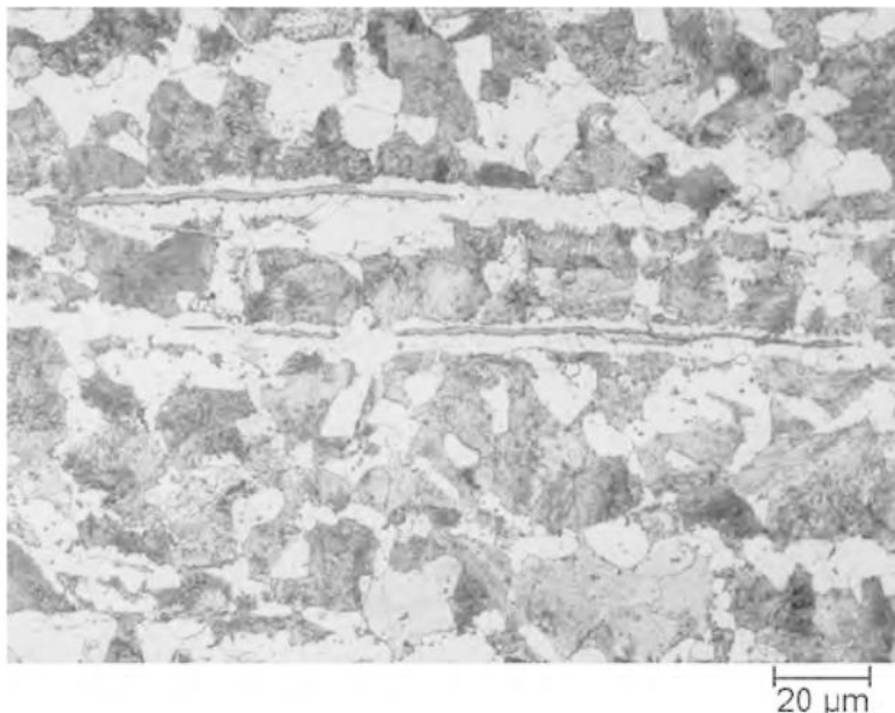


Figure 2.6 Ferrite bands with MnS inclusions [17]

A banded microstructure derives from interdendritic segregation during solidification, that causes difference in chemical composition within steel during dendrites development (it mainly depends on steel composition and cooling rate); with hot rolling this results in an alignment of

interdendritic variation, producing alternating region of high and low concentration of various solute elements.

In the steel with elongated MnS (like the example in figure 2.6), Kirkaldy et al. proposed an additional mechanism to consolidate the banding explanation: segregation to interdendritic regions occurs to both manganese and sulphur, and ferrite wouldn't be expected to nucleate in high-manganese zones. With decreasing temperatures, manganese concentrates in sulphide and its content around the inclusions is lowered; thus ferrite is stimulated to grow in this zone.

Although it is not certain that a banded microstructure has a significant influence on mechanical properties, an investigation is appropriate. Some studies compared the behaviour of low carbon steel with and without bands on some characteristic, and found, for example, that in impact test regarding ductile to brittle transition, energy absorption above the transition temperature was higher for the steel without bands (while below the temperature it wasn't noted differences). Other studies revealed that banding in martensitic steel could be deleterious to machining and cold forming operations. For these reasons a control of microstructure and elongated MnS content it's appropriated when chemical composition and applications could lead to issues. Here alloying elements take action: in fact in addition at the mentioned effect of controller by some elements such as titanium, alloying and microalloying elements in particular, make microstructure more homogeneous and refined (this is the main feature of niobium and it will be widely treated afterwards).

2.4 Properties and relation with applications

Steels have several application in many industrial sectors, and they must have a lot of properties in order to supply all the requests coming from all various uses. Nevertheless this thesis focuses on automotive steels, so in this chapter it will be given only the main features concerning this type of steel, in relation with their function in the vehicle. Several books [17,18,21] and documents [22-27] have been consulted for this considerable paragraph.

Firstly it's necessary to say that generally steel have alloying elements to obtain the required properties: these elements give, for example, strength, ductility, corrosion resistance, weldability, formability, machinability, endurance, ... Among these, in particular the tendency to delaying phases transformation it's important, because the final conditions are easier to achieve during cooling. Also the stabilization of austenite and ferrite is an important feature.

Microalloying elements can be described as a subgroup of alloying elements, because they are used in small amounts (<1% but also frequently <0,1%); they are mainly three: niobium, titanium and vanadium; their main characteristic is the formation of stable precipitates, which refine microstructure, in turn giving better properties (for example the stress-strain curve is lifted up). These aspect will be exhaustively explained in the following sections. Microalloying elements are typical in high strength low alloy steels (HSLA), a comprehensive category of steel, widely used in automotive industry. However this is an "intermediate" group regarding strength quality; in fact there are many typologies of steel, as it can be seen in a classical diagram strength-elongation inserted in figure 2.7. Here they follow a curve, where on the left there are low strength steel with high elongation (such as interstitial free IF, bake hardening BH and mild steel) while, moving to the right, tensile strength decrease and elongation increase (progressively there are HSLA, dual phase DP, transformation-induced plasticity TRIP, martensitic and other hardened steels). In the graph it could be added a new generation of advanced high strength steels AHSS, which have tensile strength's value similar to TRIP and martensitic, but higher elongation: these are in development thanks to the increasingly stringent demands of low CO₂ in automotive. These targets expand the use of higher performance steels, in order to reduce size and weight, and get lighter components in vehicles. Among them, for

example, there are twinning induced plasticity TWIP steels, in which nucleated twins induced by deformation, act as dislocations barriers and increase flow stress; the manganese content affects directly ductility and strength.

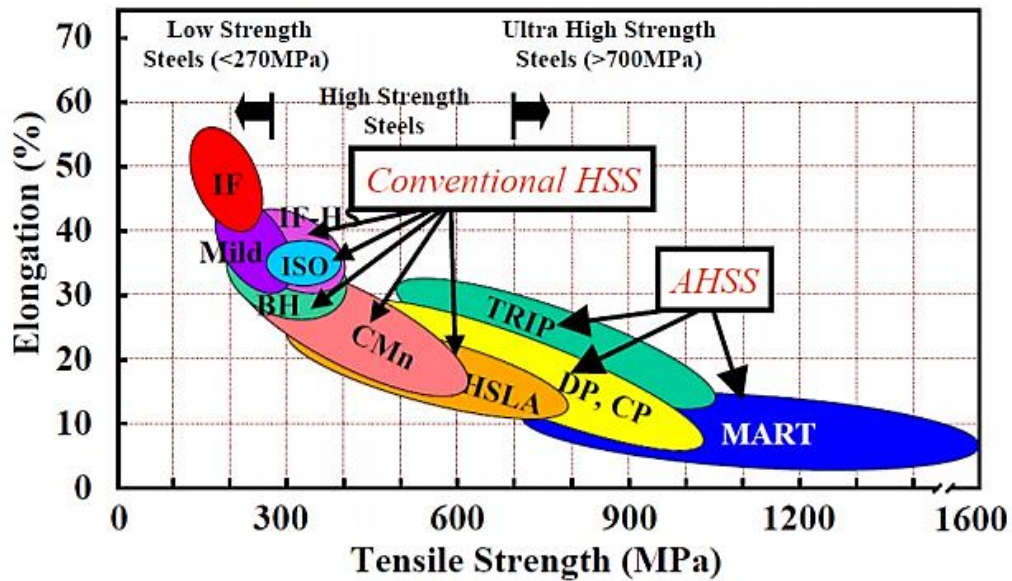


Figure 2.7 Overview of some steels typology

A passenger vehicle body is composed by a large assembly of metal components that accommodate specific and structural requirements. These demand a lot of features, such as stiffness, durability, crashworthiness and hardness. Generally components can be divided into two classes: parts that reacts to loads with minimal and significant deformation. The firsts have to accommodate road input load and they are controlled by stiffness and strength, which depends on material's modulus of elasticity and geometry; with AHSS it's possible to generate complex geometric forms to improve stiffness. Other components, instead, have to support loads with a controlled level of deformation, so energy absorption is a required features. In fact an automobile body has two main targets: to ensure the passengers safety through an impenetrable cell that support very high loads, and a dedicated crumple zone, which it deforms in a controlled manner, absorbing the maximum energy possible.

The occupant's safety is an essential requirement for automobile body: pillars, lateral roof beams and longitudinal beams for crash resistance, for example, are structural elements where high strength is a principal claim (the higher strength the better behaviour). The classical stress-strain curve is a marker for this property; it is obtained by a tensile test and it give two important parameters: the strain hardening exponent n and the energy absorption. The strain hardening exponent appears in the Hollomon's equation ($\sigma = K\epsilon^n$) that describes the plastic flow and determines the stress-strain curve. It gives an indication of how rapidly a metal becomes stronger when it is deformed; it represents the slope of the true stress versus true strain curve, plotted on a logarithmic scale. The exponent can give also information about formability, in fact metals with high n shows a good formability. Instead, the maximum value of stress depends on the steel structure and thermomechanical processes, and it could be increased with some methods, such as grain refinement, precipitation or solid solution; niobium's relationship with them, and the subsequent effect on mechanical properties will be explained later.

Energy absorption is directly connected with crash, during which it's necessary that a component collapse in a stable and desired way. It can be calculated by the area under the stress-strain curve: a high value of tensile stress, correlated with good achievable strain, increases the

area of the curve; the AHSS are designed to reach this objective and consequently with these it's possible to reduce, for example, thickness and cost of a specific component. A level of 10% of plastic strain is often used in crash test to compare different material, because it has been suggested that at this level the majority of energy has been absorbed. The exponent n is also important here, because with high n strain is distributed more uniformly and involves a larger volume of material; in this way local peaks of strain are reduced and the component can absorb more energy.

An illustrative component is B pillar, which is involved in lateral impact: it is usually made through hot forming and it's composed by high strength steel (also 1500 MPa) to avoid intrusion into the vehicle. An option is the addition in the lower area of the component of a softer steels energy-absorbing: in this way high rigidity for safety is combined with a controlled deformability.

Sometimes, therefore, strength has to be combined with ductility to exhibit good toughness. This aspect is to be kept under control also at lower temperature, so the ductile to brittle transition is a noteworthy properties (fig. 2.8). Ductile fracture occurs by tearing of the metal with a large consumption of energy; it is initiated by microvoids nucleation and coalescence, and proceeds only with a great deformation that leads to final fracture when the ligaments between microvoids are too smaller to support the load. However when temperature decreases, the fracture becomes brittle, which is a more destructive one, because it often starts with a not evident small defect and it propagates unstoppably approaching the speed of sound. It expends less energy than ductile fracture and it's a result of cleavage that occurs by breaking of atomic bonds. A typical reference temperature is the 50% ductile failure temperature; it has to be as low as possible, to ensure an adequate reaction to impact at every possible condition. It is influenced by some factors, such as the metal composition (for example high carbon level it gets worse, whereas microalloying elements enhance the situation)

An ordinary test to evaluate ductile to brittle transition behaviour is the Charpy test, represented in figure 2.8: an impact tester (a pendulum) hurts the specimen in the centre where there is a V-shaped notch. A portion of kinetic energy of the pendulum is transferred to the specimen which deform or broke itself; the energy absorbed by the specimen is determined by the height reached by the pendulum and its mass (mechanical energy conservation).

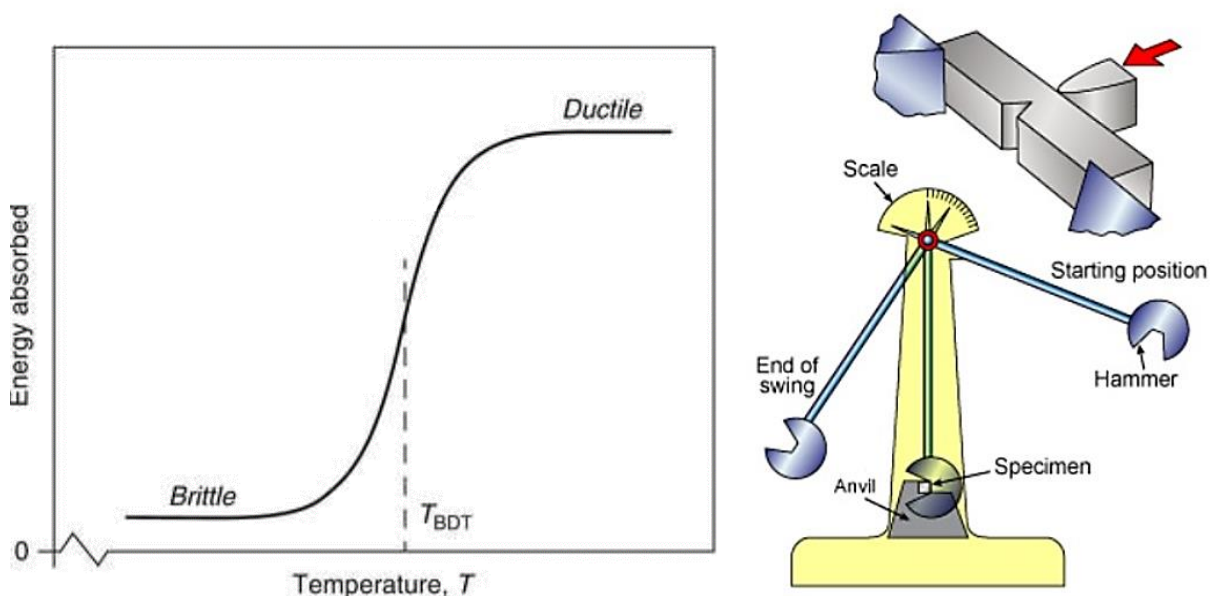


Figure 2.8 Ductile to brittle transition and representation of Charpy test

In addition to structural elements, vehicles are composed also by exterior panels, for which the main requirement is good formability, since their geometry is quite complex and are usually cold formed. Formability is characterized by several properties, some of which are exposed below.

First of all the process limits of a metal are given by the forming limit diagram, which is shown in figure 2.9 a; these limits are the major and minor stresses where local necking occurs. Determination take place on a sheet where is drawn a regular pattern of circles, lines or dots; sheet is deformed (until failure happens) and consequently also the grid deforms. Then the strain of the drawn profile is measured: the major is defined as the strain in the direction of the maximum strain, it's considered always positive, and it's plotted on the vertical axis. Minor strain, instead, can be positive or negative, and it determines the horizontal axis. Each material has its own forming limit diagram, but generally, a component is considered acceptable if it stands below the limit curves.

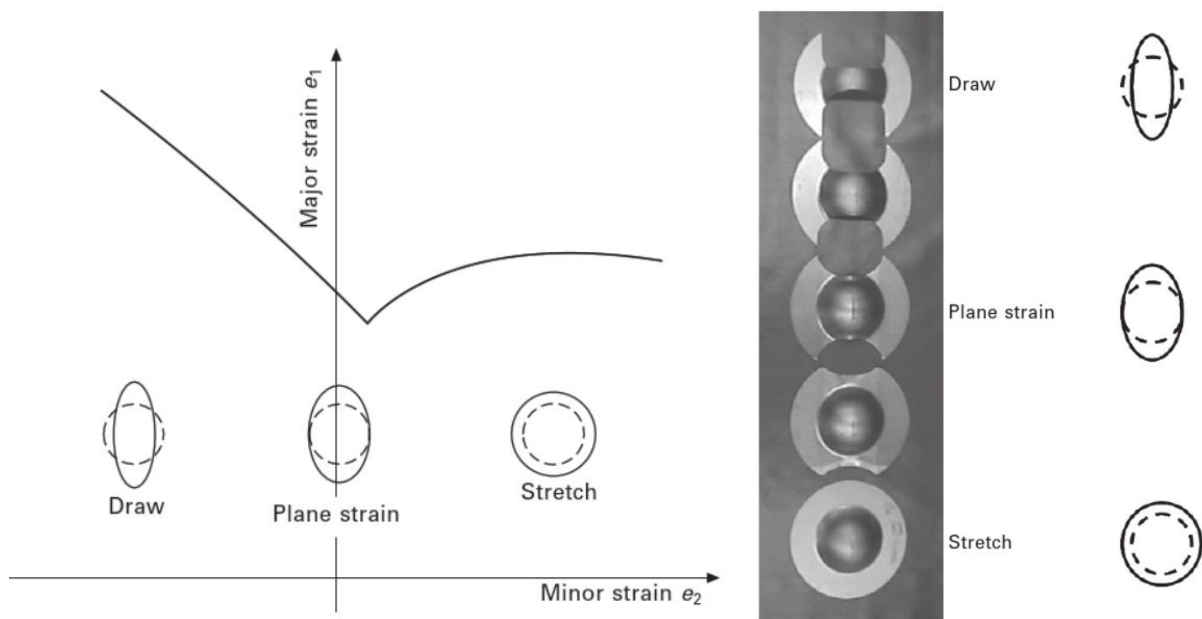


Figure 2.9 (a) Schematic FLD representation and (b) deformed Nakajima test specimen

Other ways to evaluate are the Erichsen test and the Nakajima test, where a steel sheet is deep-drawn until a failure occurs. In the Nakajima test, for example, blanks with different geometries to represent biaxial (stretch) and negative minor strain (draw) conditions, are punched until cracks (fig. 2.9 b); usually these test are accompanied by image correlation methods to generate or compare the FLD.

In figure 2.10, instead, is shown a simple bulge test, where it's evaluated the stretching behaviour of some dual phase steels. It is clear that greater strength afflicts formability.



Figure 2.130 Drawing depth limits for several DP steels and a draw quality steel (DC)

In a forming process other factors must be considered; among them there are anisotropy and springback. The first refers to discrepancy in strain behaviour along different directions during forming; this is primarily caused by rolling since the rolling direction confers to grains, more or less markedly, a preferential distortion direction. In particular in cold rolled strips this phenomenon is accentuated; in fact anisotropy is related to the crystallographic texture, so depending on the arrangement of the crystal respect to the applied force system, some slide system will be activated more easily than others. Anisotropy is expressed by coefficient of normal anisotropy r , namely the ratio of the true strain in the width direction compared to the true strain in the thickness direction ($r = \varepsilon_w/\varepsilon_t$). An unitary value represents an ideal isotropic material, in which the relationship between two sides of a section doesn't change during deformation, i.e. it occurs in the same way in both direction. Therefore, the higher r the better isotropic behaviour. DP, TRIP and TWIP are steels with good isotropic properties, and their r -values also tend to 2, especially in samples intended for deep drawing (where failure risk is higher).

Springback is the tendency of the metal to partially return to its starting shape after the removal of loads, due to elastic recovery. This is critical in joining operation where high precision is required, since marked springback can limit the options. For example in welding, pieces could be forced to join in the correct position, but severe springback may cause residual stresses that lead to consequential deformations.

Curiously the AHSS steels have larger levels of springback than these of mild steel less performing. The reason for that is visible in the curves in figure 2.11: the higher strength and strain hardening of AHSS lead to greater value of elastic recovery from the desired deformation point.

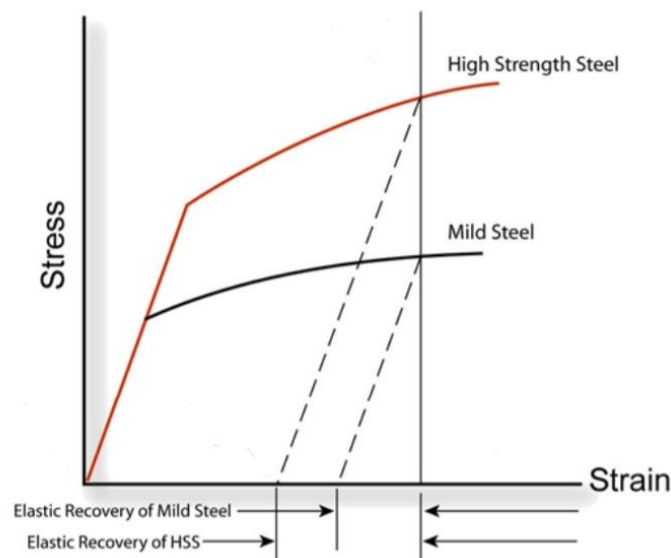


Figure 2.11 Simplified graph of elastic recovery

Springback occurs for example in V-bending, where it's given a formula [28] in function of radii before and after springback, respectively R_B and R_A :

$$R_B/R_A = 4(R_B \cdot \sigma_Y/ET)^3 - 3 \cdot (R_B \cdot \sigma_Y/ET) + 1$$

Where σ_Y is the yield strength and T is the thickness of the sheet.

To compensate this phenomenon for example it is possible to apply overforming; it requires previous analysis and modelling, because an excessive angle could lead to cracking in the

external side of the metal. Addition of niobium in steel has a favourable impact as will be seen later.

After forming or shearing processes, the remaining sheet free edges could be deformed through an elongation or an edge flanging operation (hemming), for example in an automobile inner panel. The material resistance to necking during flanging operation (when circumferential strain exceeds material limit) is evaluated by the hole expansion test, that quantifies the hole expansion ratio (final and initial diameter difference/ initial diameter). A representation of the test is shown in figure 2.12 a.

Many factors could affect the HER: the hole preparation (microfractures on the surface), the punch geometry, the mechanical property and the microstructure of the material. Again AHSS and other steels with hard phases like DP and TRIP, have the lower values of HER (figure 2.12 b), due to the presence of martensite. For this reason ferritic-bainitic steels are developing: some studies explained that an increase in volume fraction of hard phase has a moderate reduction of HER for these steels (voids initiate at bainite with higher strains than martensite). Additionally another study observed that in a TWIP steel cracks are triggered by decohesion between the matrix and the above mentioned MnS particles elongated along the rolling direction (due to the high manganese content of these steels).

However a microstructural control of fine and well distributed martensite phase is an improving method for HER gain.

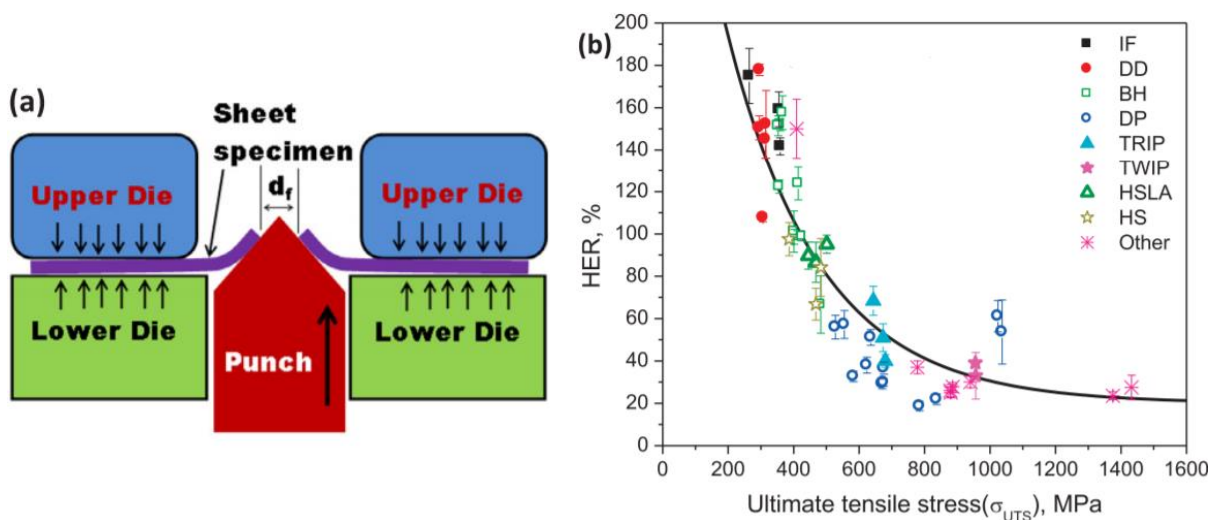


Figure 2.12 (a) Schematic representation of HET and (b) values for different steels typology

Many component in a car body, after forming need to be welded; welding process simply consists in joining two pieces of materials through a heat input that melts metal and allows them to join. In general welding can be described as the ability of a material to be welded, generating a strong and tough joint, without significant defects.

Although there are many welding processes, a common factor for good weldability is the pursuit of a low carbon content, in conjunction with a low carbon equivalent CE. It is a marker of weldability in relation to the content of some elements, and it given usually by the Dearden and O'Neill formula that is commonly accepted:

$$CE = C + Mn/6 + (Cr+Mo+V)/5 + (Ni+Cu)/15$$

The development over the years tended to decrease these two factors, as it can be seen in the historical evolution represented in figure 2.13.

The critical zone in a welding operation is the heat affected zone HAZ: this is the area adjacent to the solidifying melted steel and it is the place where defects can occur; due to the

rapid cooling, the HAZ can be affected by residual stress, hydrogen cracking (CE value is kept low to reduce this problem) and embrittlement.

About the latter inconvenient, microstructure is a key point, because it is required a good level of toughness to avoid failures; therefore microalloying element has a beneficial role in the microstructural control, to provide adequate properties.

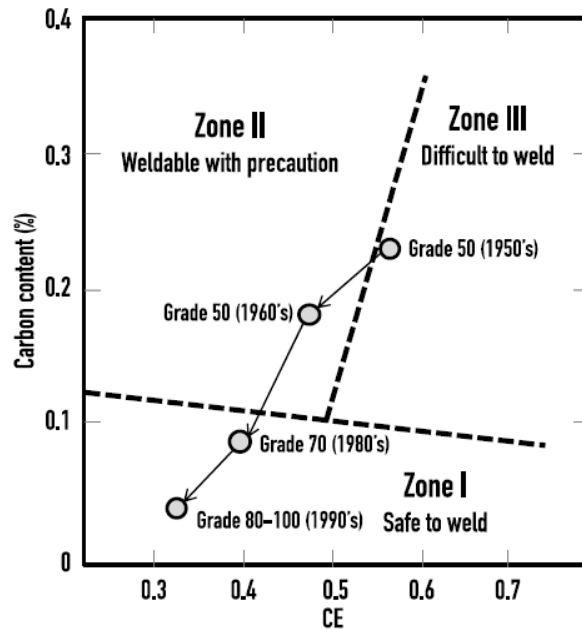


Figure 2.13 Graville diagram with historical steels evolution in weldability

Lastly, another property is required by some automotive elements: hardness. The gearbox components, for example, need to adequate wear resistance (so hardness), since they crawl each other in working condition. However a gear tooth require also toughness in depth, in order to have bending fatigue resistance: therefore high hardness is usually applied on the surface.

Namely hardness is the resistance to penetration, in fact the majority of test consists in a load application on the indenter, a hard material; depending on the test its shape changes (Brinell uses a sphere while Vickers adopts a pyramidal shape). The indenter penetrates the surface and the resulting indentation gives information about the material hardness: obviously small indentation indicates high hardness and vice versa.

Hardenability (the tendency to harden under various cooling conditions) depends on some factors: firstly more carbon content increases the amount and hardness of martensite, and the achievable depth; although with low C content (as in low carbon steels) a large section is not hardenable, an excellent combination of hardness on surface and toughness inside can be obtained.

Carburizing operation it's a common practice to enrich a surface with carbon: besides to C content, time and temperature affect widely the carburizing depth. Since this process is conducted at high temperature, the microstructure control could be a method to optimize the process itself and the results; so, again, use microalloying elements may represents an efficient option.

3. MICROSCOPY METHOD

The presence of a large number of images in this thesis makes useful to summarize the techniques of metals characterization that will be encountered in the next chapters. The tangible effect of niobium addition is at microscopic level, so these images must have a proportionated resolution to show the necessary specifications. Microscopy features, in fact, have a micrometric or nanometric size, therefore human eye can't resolve those elements; since it has a resolution of about 0,1 mm, other ways are necessary for microscopic investigations.

The book [29] shows exhaustively the following concepts.

3.1 Light microscopy

The first historical method for material examination has been used for a few centuries, and since the end of the nineteenth century metallurgists use light microscopy for microstructure analysis.

It basically consists of a set of lenses that magnify the image: an illumination system reflects the rays coming from a light source by a reflector to illuminate the specimen through a lens. The rays converge at the objective lens that focus them to generate the primary inverted image of the sample; this lens determines the final resolution and the total magnification of the microscope. At this point there are two possibilities: the rays are further converged by a second lens (projector lens) to form the final image on a screen or camera film or sensor that records or take a picture. If, instead, the purpose is to see directly with eyes, an eyepiece replaces the projector lens, and forms a virtual inverted image on the human eye retina. The eyepiece could be fitted with a graticule for measurement, and there are also various types of objective lens for the aberration correction.

Before microscopy viewing, however, the specimens must be prepared to display the microstructure; these are cut into cross sections with abrasive or electric discharge machine, and then a grinding operation removes any damage caused by sectioning. With grinding, the surface is smoothed through a series of abrasive papers with abrasive particle size gradually more fine; the last pass is made with a fine diamond past or alumina, up to reach a mirror-like surface (polishing). Lastly metal is subjected to etching, a controlled corrosion process in which chemical agents dissolve certain areas of the specimen surface due to the difference in electrochemical potential; an ordinary etchant is nital, a solution of nitric acid, water and alcohol.

The corroded areas reflect light differently and appear in other colours; grain boundaries are an example of element revealed by this method, since they are severely attacked the agents and they looks like dark lines.

Light microscopy can reach a maximum resolution of 0,2 micrometres, so it is an appropriate process for characterization of microstructure (for example grain size) and metal phases; nevertheless other components such as precipitates have smaller size (in nanometer range) and require more magnification, therefore electron microscopes are used.

3.2 Transmission Electron Microscopy

TEM is a powerful microscope that allows to obtain images of very fine microstructural features. It is somehow similar to the previous one described, but source and lenses: the light rays are replaced by electron rays, and the glass lenses are replaced by electromagnetic ones. Figure 3.1 represent a simplified scheme to better understand the description.

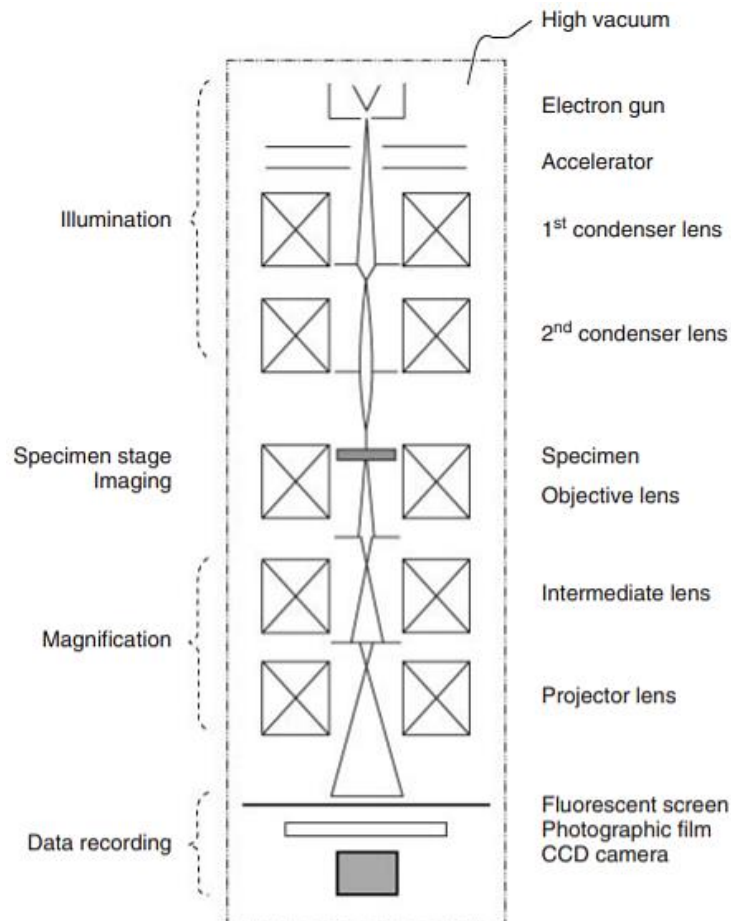


Figure 3.1 Illustration of a TEM structure

The source of a TEM is an electron gun that generates an electron beam for specimen “illumination”. The electron gun is composed usually by a tungsten filament (which works as a cathode) heated by a current to high temperature; this provide sufficient energy for electrons to leave the filament (alternatively electrons are pulled out by applying a very high electric field to a metal surface). Then, they are accelerated by a high electrical voltage (commonly 200 kV) toward the anode, to form an electron beam. Its intensity (determined by the filament temperature and the voltage) defines the resolution, because intensity determines the wavelength of the electrons that, in turn, determines the resolution.

The gun works in high vacuum condition (about 10^{-4} bar) in order to avoid the interaction with the possible particles in the air, which could distort the beam.

Subsequently the beam goes through various lenses: unlike the light microscope where they are made of glass, these lenses are electromagnetic because glass can't deflect or focus an electron beam. Electrons interact with magnetic field, generated by a solenoid, and they are focused and deflected by field's magnetic line of force. Regulation is simply because it's only necessary to change the current in the solenoid.

Beam invests the specimen and electrons are diffracted depending on the crystal structure. An additional set of lenses is located beside the specimen to ensure the correct magnification. Lastly the diffraction pattern is projected onto a fluorescent screen for the final observation.

The specimens of a TEM must be electronically transparent, i.e. it must be able to transmit electrons: for this reason the sample thickness is very thin, at least about 100 nm. It is initially pre-thinned through grinding techniques, then final thinning (electrolytic thinning or ion milling) allows to reach the required thickness. Specimen is therefore mounted in a special holder that holds and tilt it for better scanning.

The TEM resolution can reach value of 0,1 nm, so this microscope is very useful for revealing ultrafine details or defects; an example is dislocation, which appear like dark lines. Dislocation generates a local lattice distortion that deflect electrons into diffraction direction different from the normal direction of a crystal without defects. Diffraction intensity changes in some portion of the lattice plane, resulting in areas of different colours. In figure 3.2 is represented the attitude of the beam when it passes through a dislocation: due to the “separation” in the path of electrons, in *a* there is a lowering beam intensity, which results in a decrease of the bright field (BF) intensity, near the dislocation core *b*.

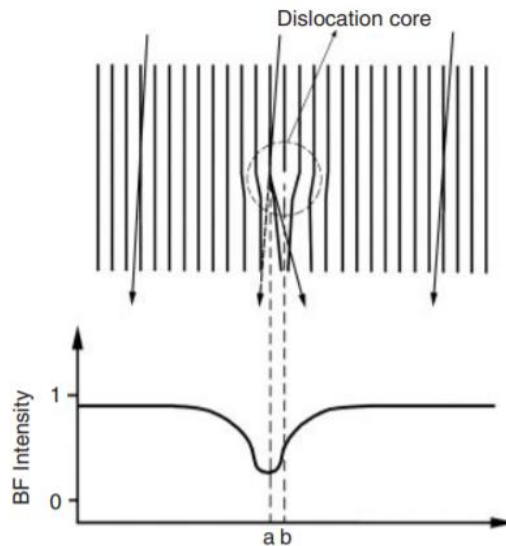


Figure 3.14 Formation of a dislocation image

3.3 Scanning Electron Microscope

This type of microscope has a wide use in microscopic structure examination, thanks to its high resolution and great depth of field, which allows to obtain three-dimensional appearance. Its instrumentation is similar to that of TEM, but here the electron beam is condensed to a fine probe for surface scanning. The acceleration voltage for the beam is an order of magnitude less than that for a TEM and the electromagnetic lenses are located before the specimen; in SEM, in fact, lenses are for electron probe formation that will impact the material surface, while in TEM a portion of lenses forms directly the image and magnifies it. Here the electron beam is reflected in various direction by the surface and a detector collects the signal electron emitted by the specimen. The scanning probe moves over the surface along parallel lines and generates a rectangular raster.

The signal detection is based on electron scattering: when high-energy electrons hit a specimen, it produces elastic or inelastic scattering. The first generates backscattered electrons, typically deflected from the specimen at large angles and with a little loss of energy. Instead, inelastic scattering produces secondary electrons (electrons with sufficient energy to leave its orbital and to be ejected from atoms) deflected at small angles and with greater energy loss.

The electrons collected by the detector are used to reconstruct an image, according to a relation between the scanned points and the picture points on a screen (amplification of electron signals converted in photons).

SEM resolution depends on the size of the electron probe scanning, and it can reach values in the nanometer range.

This type of microscope is quite easier to operate and maintain compared with a TEM; specimens, for example, don't require specific preparation claims. Simplicity of processes is, in fact, a motivation for its large utilization.

3.4 Electron Backscattered Diffraction

[29,30] Within the SEM analysis (also in TEM but to a lesser extent) there is the EBSD technique, whose main purpose, for metals, is the identification of the crystalline orientation of grains. EBSD is based on the principles of backscattered electron emission and Kikuchi band: these are lines of intersection between the detector screen and the surfaces of diffraction cones, which are generated by electrons scattering from a location of the surface to a certain crystallographic direction that satisfies the Bragg's law. These bands have a width proportional to the planar spacing and each band represents a specific crystallographic plane. To ensure a large number of backscattered electrons generated (in order to obtain more accurate analysis), it is used an high acceleration voltage in the range of 15-30 kV.

The determination of the structure of a crystal is possible by indexing all the bands and the resultant intersection pattern; this indexing is made by an appropriate software. With the scanning of the entire specimen surface, all the EBSD patterns are indexed and collected, and the differences between them reveal the crystal orientation among grains. The orientation differences are represented with colours, so it is generated a map that shows great colour contrast where the difference in grain angles is high.

In EBSD analysis the support of the specimen must have a large tilt capability, because the surface has an ample tilt angle (about 70°) with respect to the electron beam. The detector consists of a phosphorus screen and a CCD (charged couple device) camera that records the fluorescent patterns.

A requirement for the EBSD analysis is the crystalline state of the material, because amorphization may disturb diffraction pattern acquisition. The surface polish should be similar to that of specimens for light microscopy.

3.5 Atom Probe Tomography

[31-33] Tomography aims to obtain a three-dimensional vision of the internal structure of an object, at an atomic level. In APT, in fact, the purpose is the identification each atom and its position in the analysed volume.

Historically this technique derives from the field electron microscope (FIM), whose principle is the electrons emission from a solid that occurs when it is exposed at a high electric field; the sharp needle specimen is mounted on a vacuum system (there are traces of helium or

neon image gas) at cryogenic temperatures. The image gas atoms is polarized and attracted to the specimen, and when the electric field is sufficiently high, the resulting ions are “expelled” and projected towards a phosphor screen positioned in front of the specimen. The image is the result of field ionization of gas atoms over individual atoms of the surface.

The study of this technology began in 1935, and the atomic resolution was achieved in 1955. Over the time methods and instrumentations were developed and actual APT is a field electron microscope combined with a time of flight mass spectrometer: the ionized atoms, evaporated (through DC voltage or laser pulses) from a hemispherical surface of the sharp needle sample, are accelerated by electric field and detected on a position sensitive detector, which records each hit coordinates. A local electrode is located between the specimen and the detector, and it is used to reduce the energy deficits over the field and to improve the mass resolution. In figure 3.3 a, it’s represented a typical instrumentation for APT analysis.

The area for the analysis depends on the diameter and the distance of the detector, and the specimen tip radius, which determines the angle at which electrons evaporate (as it can be seen in fig. 3.3 a, the suitable area is identified by the acceptance angle $2\theta'$).

Atoms evaporate layer by layer, so the final result is a 3D reconstruction that match the shape of the material (fig. 3.3 b). The achievable resolution is 0,2-0,3 nm, so several tens of millions of atoms can be collected in a typical volume of $50 \times 50 \times 200 \text{ nm}^3$.

As said before, material for APT reconstruction have to respect a fine needle shape with a hemispherical apex and a moderate shank angle. Surface must have a high quality: some methods for TEM preparation can be utilized also in these specimens, or additionally, electropolishing and micropolishing operations are adopted.

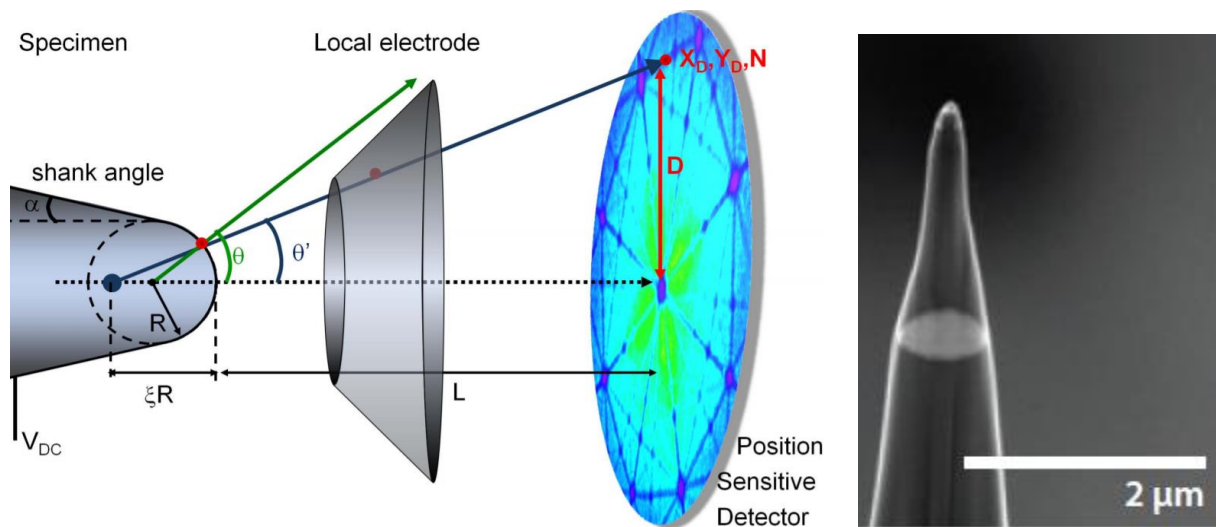


Figure 3.3 (a) Scheme for APT analysis and **(b)** magnification of a sample

4. NIOBIUM EFFECTS ON STEEL

The necessity of stronger and lighter steels led to the use of microalloying elements niobium, titanium and vanadium thanks to their effects of solid solution, precipitation and grain refinement. The latter two are the most important and will be discussed in the next pages. Therefore this chapter represents the central part of the thesis, since there is the presentation of the main mechanisms by which niobium works on steel. The relation between mechanism and mechanical properties, obviously, will be present, as well as the comparison with the other elements Ti and V.

4.1 Delay of recrystallization and grain refinement

[20,34,35] Niobium's main attribute is the best microstructural control among microalloying elements; this, combined with a thermomechanical controlled process, allows to obtain grain refinement. It is the best strengthening mechanism for increase both strength and toughness and also the most cost effective way.

The starting point for grain refinement is hot rolling: historically it was conducted at high temperature (both roughing and finishing) in order to work in the region where the steel is softer, but with the introduction of controlled rolling (due to undesired fractures) the aim is the refinement of austenite, operating at lower temperature. Limiting the soaking temperature during slab reheating has already the advantage of reducing grain growth, but especially finishing rolling below T_{NR} leads to the formation of fine microstructure. As it can be seen in figure 4.1, niobium expands the operational window where recrystallization doesn't occur (or it is strongly retarded), in which is beneficial to accumulate as much deformation as possible.

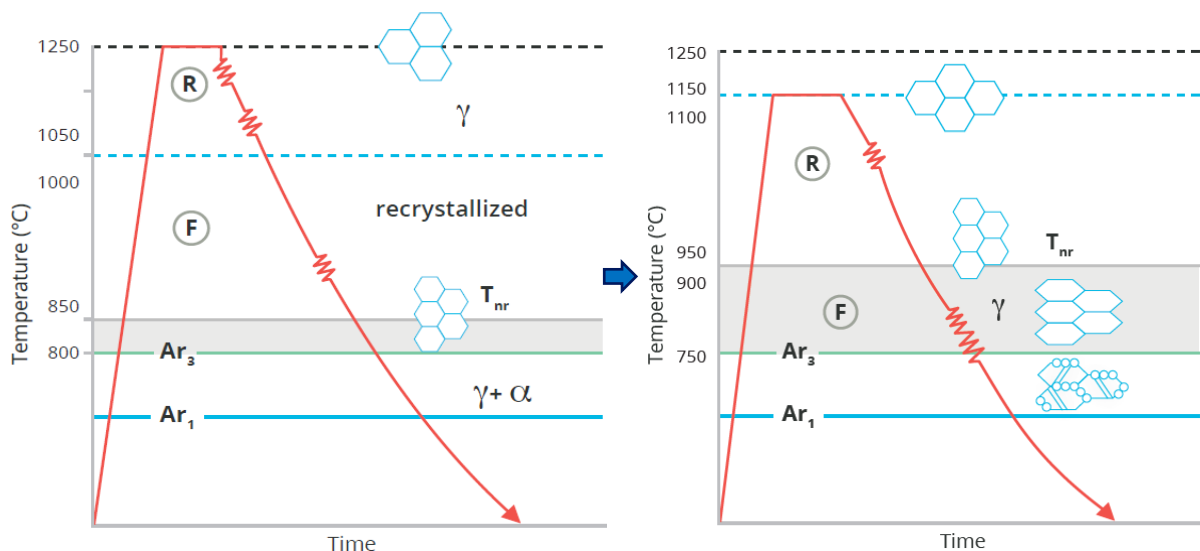


Figure 4.1 Enlargement of the temperature range for controlled rolling, where recrystallization doesn't happen (coloured region)

Creation of pancaked austenite grains comes from accumulation of strain hardening below T_{NR} and results in more grain boundaries, which are nucleation sites for the austenite to ferrite transformation. The formation of deformation bands within the grains is also a further element for increase of nucleation site. Figure 4.2 shows this phenomenon: with niobium ferrite will be finer because the transformation starts from finer elongated austenite grains, where the ratio of grain boundary surface area (that is a nucleation site) to grain volume is increased.

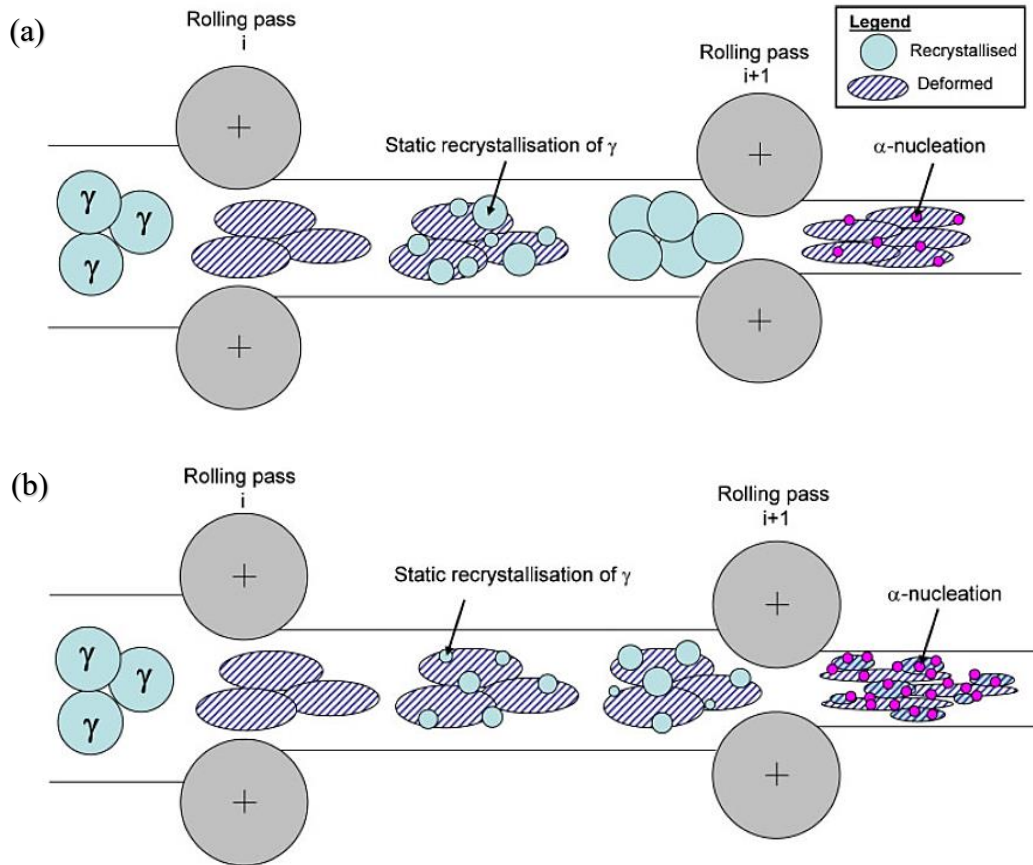


Figure 4.15 (a) Deformation above and (b) below T_{NR}

Rolling in an enlarged pancake window it's easier because there is more operating margin, and niobium is very effective in this: it increases T_{NR} and decrease A_{r3} . The latter phenomenon is attributable to segregation of Nb and C at the grain boundaries that leads to reduction in carbon activity and interfacial energy for nucleation, and it depends also to the cooling rate and the niobium content in solid solution; the more content, the more drop in temperature. With a low A_{r3} it is possible to finish rolling lower, so the achievable deformation is larger and the microstructure is finer.

Increase in T_{NR} , instead, is correlated to more factors, principally solid solution and precipitation (that will be widely investigated in the next section): the first affects recrystallization due to the friction effect originated by the difference in atomic radius (for example niobium is 15,6% larger than iron). Precipitation, instead, practices a pinning force in obstruction to grain boundary and dislocations motion; this effect is stronger than the solute drag, and it causes a decrease in effective grain boundary area that leads to less surface energy for recrystallization. This force is also called Zener force, since he proposed an explanation of this mechanism. Other studies were carried out and it can be summarized that there is a “driving” pressure for recrystallization that comes from the stored energy of the deformation applied, and a “pinning” force of the precipitates that contrasts grain growth by decreasing the grain boundary surface energy. The greater of the two establishes the progress or the stop of recrystallization.

Some studies conducted by Medina [35] revealed that the two “resistance mechanisms” are quantifiable by an increase in activation energy for recrystallization by solute drag and precipitation for a Nb-steel: this gain is respectively:

$$\Delta Q_{SOLUTE} (\text{J} \cdot \text{mol}^{-1}) = 109731,9 \cdot [\%Nb]^{0,15}$$

$$\Delta Q_{PRECIPITATION} (\text{J} \cdot \text{mol}^{-1}) = 1577000 \cdot [\%Nb \%C^{0,7} \%N^{0,2}]^{0,15}$$

The values confirms that the pinning force is stronger than the solute drag.

The delay in recrystallization is visible in the graphs in figures 4.3: in (b) the addition of niobium in a 0.02% C, 1.5% Mn steel results in higher temperature for 50% recrystallization (that is equivalent to a gain in T_{NR}). Nevertheless there are other factors that affect the behaviour: higher temperature, in fact, leads to faster recrystallization, and at certain values (namely $>T_{NR}$) also the previous mechanisms are almost ineffective, as it can be seen in fig. 4.3 (a). Here is represented softening (= recrystallization) over time, in function of various deformation temperature for a low carbon steel with niobium. The plateau in the curves represents the temporary recrystallization stop: it occurs only after some time because precipitation requires time to become effective in pinning. At the higher temperatures, presumably above T_{NR} , softening is completed after relatively short time, and probably precipitation didn't take place. In this case it is tested the same steel, but maybe for the steel without niobium, the curves would be translated to left, which means that both solute drag and precipitation wouldn't be present. Therefore this is a reason for the development of controlled rolling: knowledge and application of correct rolling parameters leads (for example also the amount of strain has influence, as said previously) to better results.

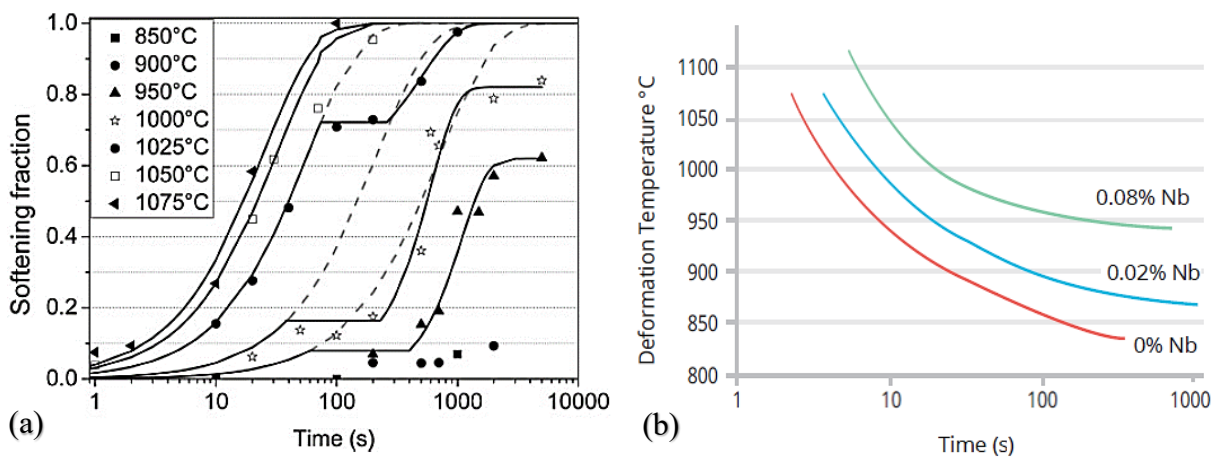


Figure 4.3 (a) Recrystallization curves and (b) time for 50% recrystallization

Microstructural refinement is clearly visible in figure 4.4, where a small addition of niobium (0,025%), in a low alloy Cr-Mo steel, decreases and homogenizes grain size [36]. The results (fig. 4.5) show that size distribution is shifted downwards: the “peak” is located in the range 5-10 μm , while without niobium it is in the subsequent range and the distribution is flatter, synonymous for more inhomogeneity.

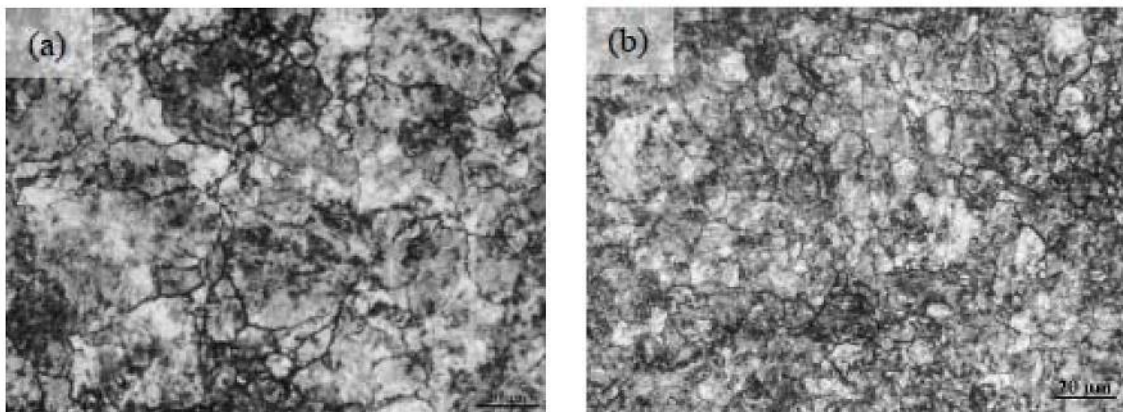


Figure 4.4 (a) Austenite grain without Nb and (b) with 0,025% Nb

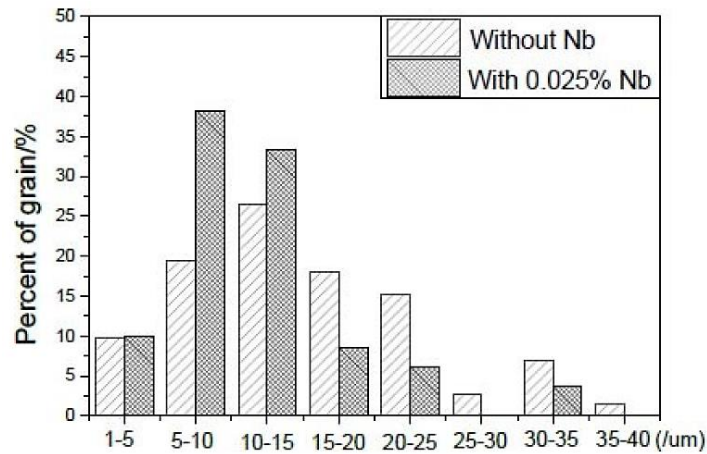


Figure 4.5 Size distribution of the previous micrographs

Niobium, as seen in the images, is strong in microstructural refining, but it doesn't work alone: in fact it's not certain that only increasing its content, mechanical properties and microstructural features will be better. Thermomechanical process parameters, in fact, are to be taken into account to find out the optimum niobium amount (not necessarily the maximum).

Generally metals strengthening by grain refinement follows the Hall-Petch equations:

$$\sigma = \sigma_0 + K \cdot d^{-1/2}$$

where σ_0 is the friction stress and K is a material constant that depends on composition and other factor such as the Burgers vector; d is the grain size and obviously for smaller values strength is increased because dislocations pile up and stop their movements against a greater number of grain boundaries.

Improvement in toughness is also obtained, and it is understandable from figure 4.6: a groove, maybe originated by a little crack, require more energy to propagate due to a longer path and more "arresting points". Thanks to this, there is a better behaviour at lower temperatures: in fact it occurs a drop in ductile to brittle transition temperature, and Gladman et al. [20] quantified the grain size and other factors contribution in a formula to determine DBTT:

$$DBTT = -19 + 44 \%Si + 700 \cdot (\%N_i)^{1/2} + 2,2 Pe - 11,5/d^{-1/2}$$

In which N_i is the weight concentration of interstitial nitrogen, Pe represents the volume fraction of pearlite, and d is the gran size. A smaller value of the latter is beneficial, while impurities raise the ductile-brittle temperature.

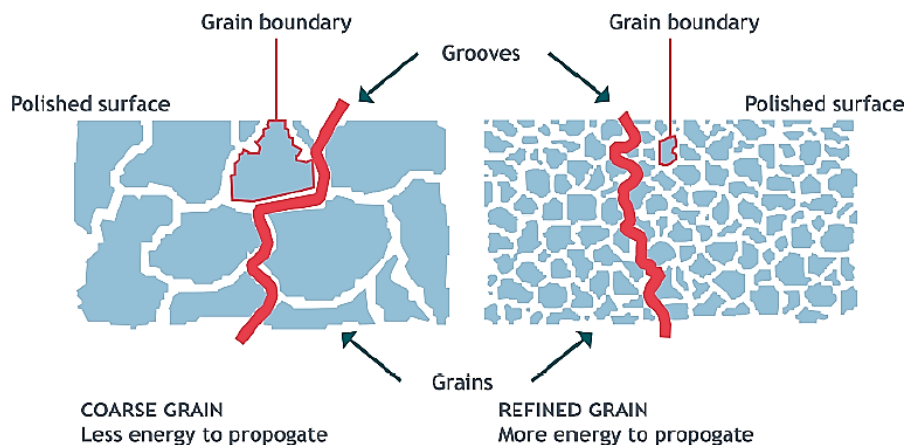


Figure 4.6 Enhanced toughness

Pearlite is also detrimental, so, for applications that work at low temperatures, it's useful to keep it under control. A study [37] revealed that the presence of degenerate pearlite could enhance the toughness behaviour. This type of pearlite is obtained by an accelerated cooling, and niobium increases drastically its fraction. It is formed by cementite nucleation at the ferrite-austenite interface, with the cementite particles that are enclosed by ferrite, in the transformation temperature between normal pearlite and upper bainite (which is more easier to obtain since alloyed steels have a CCT diagram with transformation curves shifted to the right, so it's applicable a slower cooling).

Formation of degenerated pearlite is based on diffusion process and the difference to the conventional lamellar pearlite is attributed to the insufficient carbon diffusion to develop continuous lamellae. In addition, the ferrite-cementite interface, in degenerated pearlite, is wider than in the normal one: thus the grain boundary area is larger and it can act as dislocations and fractures arrester.

Figure 4.7 shows the microstructure and a magnification of degenerated pearlite: the non-continuous lamellae and their finer thickness compared to the conventional ones, allow to experience more uniform strain distribution during deformation. This is the reason why it is believed that better toughness is achieved.

Microstructure, however, is mainly composed by ferrite, which is acicular in case of high cooling rate; this type confers more strength than conventional polygonal ferrite. A good level of toughness is maintained thanks both the presence of degenerated pearlite and the refinement operated by acicular ferrite. To give some numerical data the fraction of degenerated pearlite rises 16% with high cooling rates (from 8%) and impact toughness is increased by more than 35% compared to conventional cooling; steel has a tensile strength of about 500 MPa, and an elongation value of 23-26 % [37].

In the study is presented a comparison with vanadium, and the results show that niobium is better in toughness, in fact the latter has an almost double amount of degenerated pearlite, both with normal and accelerated cooling.

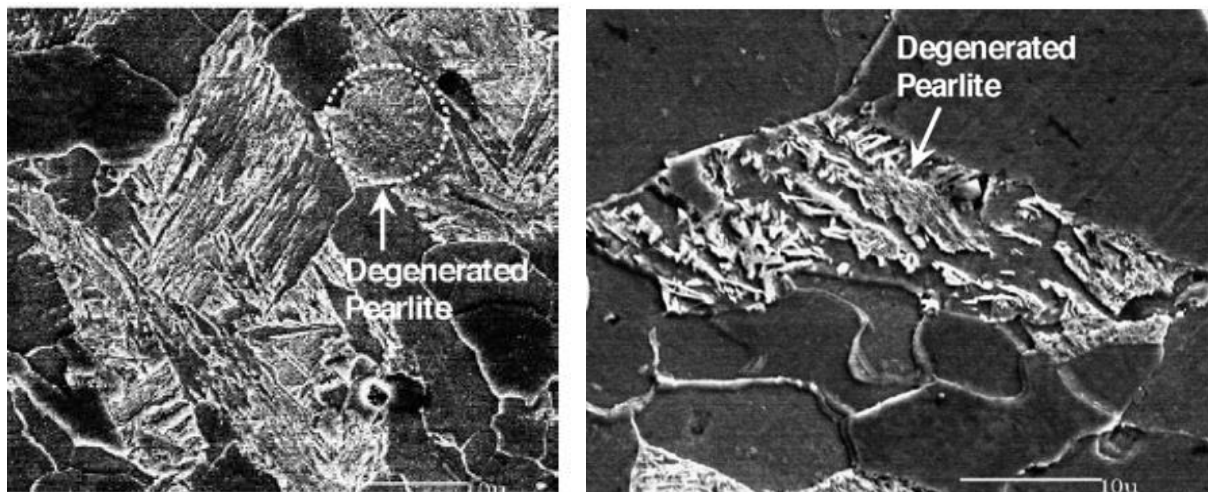


Figure 4.7 SEM image of microstructure and magnification of degenerated pearlite

4.2 Precipitation

[38] Precipitation is based on the fact that during cooling process niobium (as the other microalloying elements) combines itself with available atom of carbon and nitrogen, to form niobium carbo-nitride Nb(C,N). This depends strongly by the solubility of niobium in the matrix, that allows to calculate the temperature below which Nb precipitates, in relation with the C and N content. Professor Mohrbacher in [39] explains largely many notions in the following pages.

Solubility of Nb in austenite, in relation to the amount of C, can be evaluated from the diagram in figure 4.8.

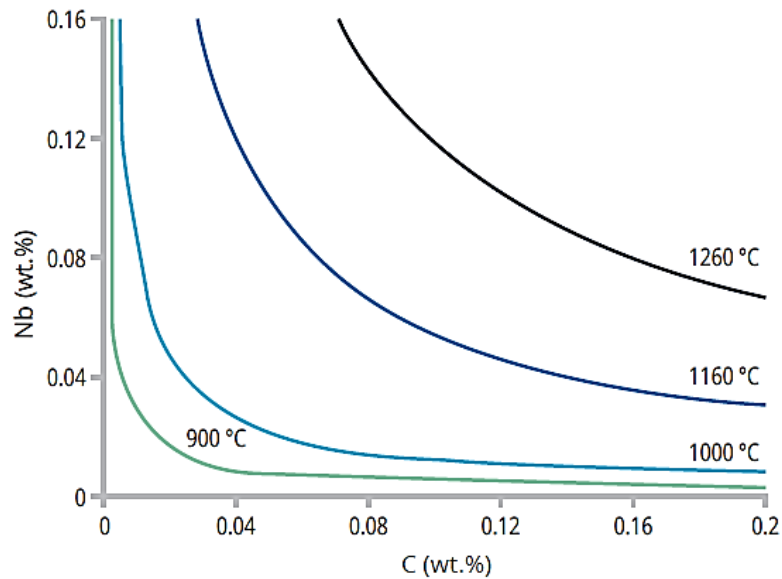


Figure 4.8 Niobium carbide solubility limit in austenite, as a function of temperature and carbon content

With this diagram it is possible to graphically calculate how much niobium can be in solution with a given amount of carbon, at various temperature; obviously with an increase in temperature, more Nb can be in solution. At typical reheating temperature for hot rolling (about 1100-1200°C), up to 0,12% Nb is dissolved in austenite.

Behaviour of the graph is confirmed by some analytical formulae in literature [40] that allow to calculate the dissolution temperature, or conversely the element concentration, in an analytical way. One of these, widely used, was published by Irvine et al. in 1967, and it represent the solubility product for carbonitrides:

$$\log [(\%Nb)(C + 12/14 N)] = 2,26 - 6770/T$$

where T is the temperature in Kelvin. If, instead, in the steel is not present nitrogen (or more probably it is fixed by titanium), thus niobium carbide will be formed; Kunze proposed an equation for solubility in Fe-Nb-C steel:

$$\log([\%Nb][\%C]) = 2,783 - 7407/T$$

When the temperature drops, the austenitic matrix becomes supersaturated, and precipitation can start; basically it follows three stages: clustering of solute atoms, nucleation and growth of second phase (consisting of more elements), and coarsening of precipitates.

Precipitation can occurs homogeneously into the matrix, or heterogeneously on microstructural defects such as dislocation and grain boundaries. The second type is considered an order of magnitude quicker than matrix precipitation, because the large mismatch between the lattice of NbC and the matrix increases the probability of nucleation at defects, where part

of the free energy is reduced. For example in dislocation, solute atom concentration is increased by the dislocation movement, in particularly when two of them react or annihilate each other.

Here the precipitates growth can be contained thanks to a large surface energy of the precipitates-matrix interface; their size stops growing as soon as it is sufficient to pin the dislocation (the pinning force mentioned above that retard recrystallization). Instead, nucleation at grain boundary (especially at grain corner), reduces the free energy because a small part of the boundary disappear when a nucleus is formed on it; this reduction in combination with the difference in solute concentration could increase the precipitates size (until the surrounding matrix is depleted). The strain associated with the volume growth promotes a vacancy flux toward the particles to reduce the local internal stress; grain boundary, so, could represent a vacancy sink, but the flow can be obstructed by large particles and nucleation of precipitates could be delayed. An equilibrium level, therefore, is determined by some factor, such as the solute supersaturation, vacancy concentration and atoms mobility.

In figure 4.9 (a) is shown a scanning transmission electron microscopy (a type of TEM) in which precipitates at grain boundary are clearly visible. They arose from cooling the specimen from 1200 to 950°C, followed by quenching to fix the steel feature. The steel is a Nb-Ti microalloyed steel, with 0,042% C - 0,085% Nb - 0,017% Ti and other alloying elements [41].

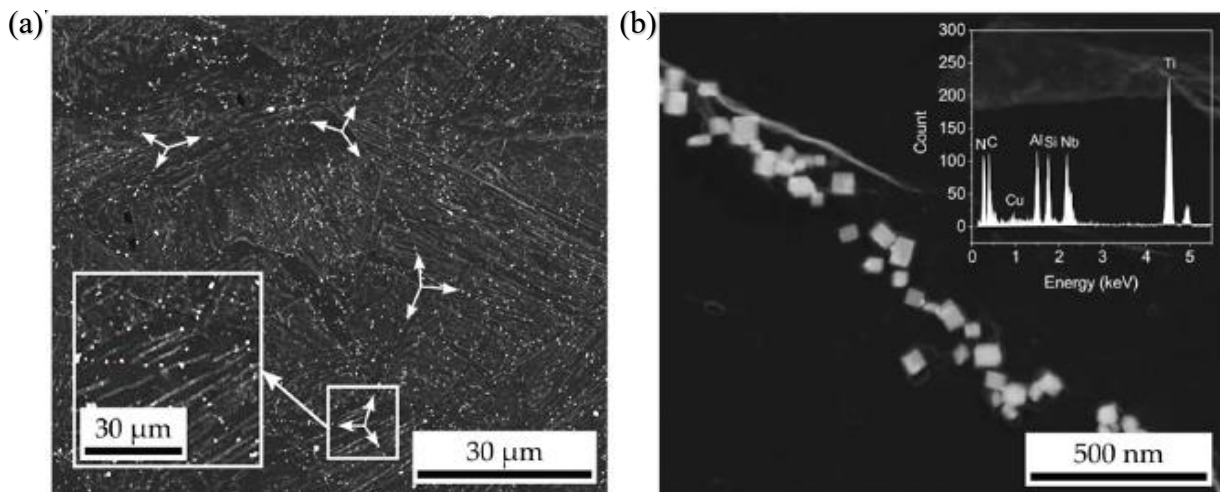


Figure 4.9 (a) STEM of a portion of microstructure and (b) magnification of a precipitates population

A detail of precipitates along grain boundary is represented in figure 4.9 (b), where it's integrated an energy dispersive x-ray spectroscopy (EDS) that allows to identify the particles composition. Precipitates in question have a relative large size, in fact they are cube-shaped with sizes of up to 80 nm.

EDS analysis reveal that the particle are Nb-rich TiN, while Al, Si and Cu signals had their origin from the STEM setup. Therefore, titanium nitride can represent a sort of nucleating element, since its great stability: in fact it is undissolvable up to 1300°C. For this reason TiN is beneficial in austenite grain control, because it can exert a pinning force over grain growth, also at very high reheating temperature.

Figure 4.10 show a particular case: niobium accumulates on TiN, but in this case the Nb-rich layer grows along two opposite direction on the pre-existing TiN cubes. Probably this phenomenon is due to dislocations, which, as said before, are nucleation sites, so it's possible accumulation and growth along their direction.

These precipitates are smaller, and they are better in reducing recrystallization: the progress of precipitation leads to particles coarsening, which can remove Nb from solution and consequently affect the grain boundary mobility (less solute drag for recrystallization delay).

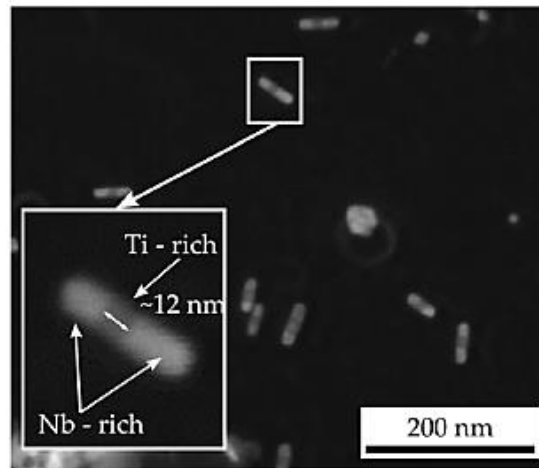


Figure 4.10 Precipitates with Nb-rich caps

The precipitation process could be slow if spontaneous: sometimes it could require also an incubation time of some minutes. To induce a faster precipitation, “dynamic” precipitation can be achieved through deformation, as it can be seen in the representation of figure 4.11, where there are sketched start and finish precipitation curves, for deformed and undeformed austenite.

Basically when steel is deformed, the dislocations increase their density; consequently also the chance of particles precipitation grow up (since dislocation are nucleation sites) and precipitates population augments.

Numerous studies were carried out regarding precipitation induced by precipitation, and that of Dutta and Sellars [42] is representative. The classical C curve (visible in figure 4.11) and its apex depend on the nature of the heterogeneous nucleation sites, resumed in a coefficient that includes interfacial energy, precipitates volume and other physical constants. Precipitation induced by deformation generally reaches a maximum at temperatures between 925-900°C because there are more energy stored that requires a lower temperature for supersaturation (that leads to precipitation), and, in turn, there are more nucleation sites that shorten time.

Deformation temperature, strain ϵ and strain rate $\dot{\epsilon}$ are important in precipitation kinetics: for example the Zener-Hollomon parameter (which is used in equations and empirical approximation) contains strain rate and deformation temperature.

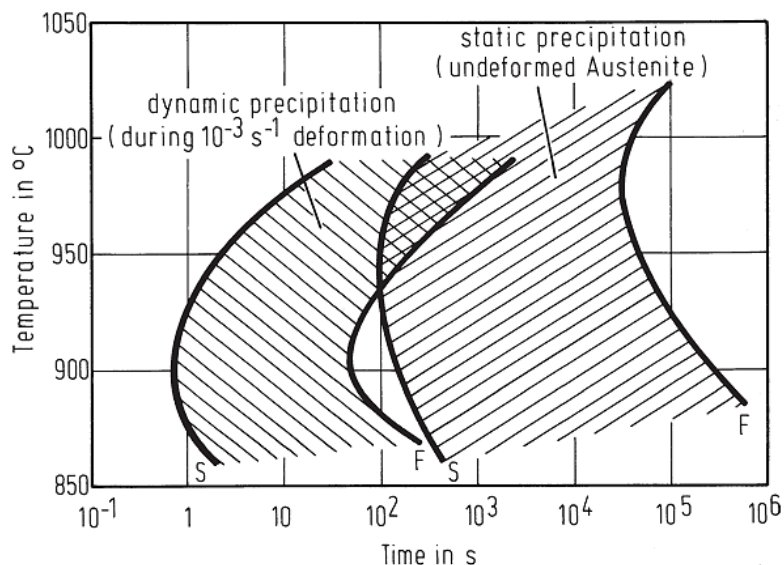


Figure 4.11 Simple representation of faster precipitation induced by deformation [40]

In general an increase in strain (at temperature below which recrystallization occurs before precipitation) promotes shorter times. For high values of temperature, due to the high driving force, recrystallization takes place before the beginning of precipitation and this is amplified by higher strain and strain rate; therefore, the recrystallization delay and the increase in T_{NR} could be afflicted because there are more dislocation that annihilate each others. If, on the other hand, particles can precipitate before recrystallization, then this is stopped due to the pinning force and solute drag.

Precipitates induced by deformation are generally smaller than those of the non-deformed condition: this depends by time and atoms mobility in the steel, since precipitation after deformation is conducted at lower temperature and/or in a shorter time, the mobility is reduced and coarsening is more difficult. Obviously the holding time after deformation can increase the particles size.

The particles shape this time is ellipsoidal, as it is shown in figure 4.12 (a): the sample is a microalloyed steel (0,078% C, 0,067% Nb, 0,02% Ti, 0,056% V) deformed at 900° C by a true strain of 0,67. These precipitates are not formed on the pre-existing TiN, in fact the attached EDS analysis (fig. 4.12 (b)) revealed that they are composed mainly by niobium and carbon, so they are “pure” NbC (the peaks related to Cu are caused by the supporting grid and the structure of the analysis equipment). For this reason the shape is ellipsoidal and is not dictated by the cuboidal TiN. The size range is 10-20 nm with some tiny particles of less than 10 nm; their dimension are retained because the specimen were immediately quenched without holding time necessary to coarsening; this represents the precipitation quickness.

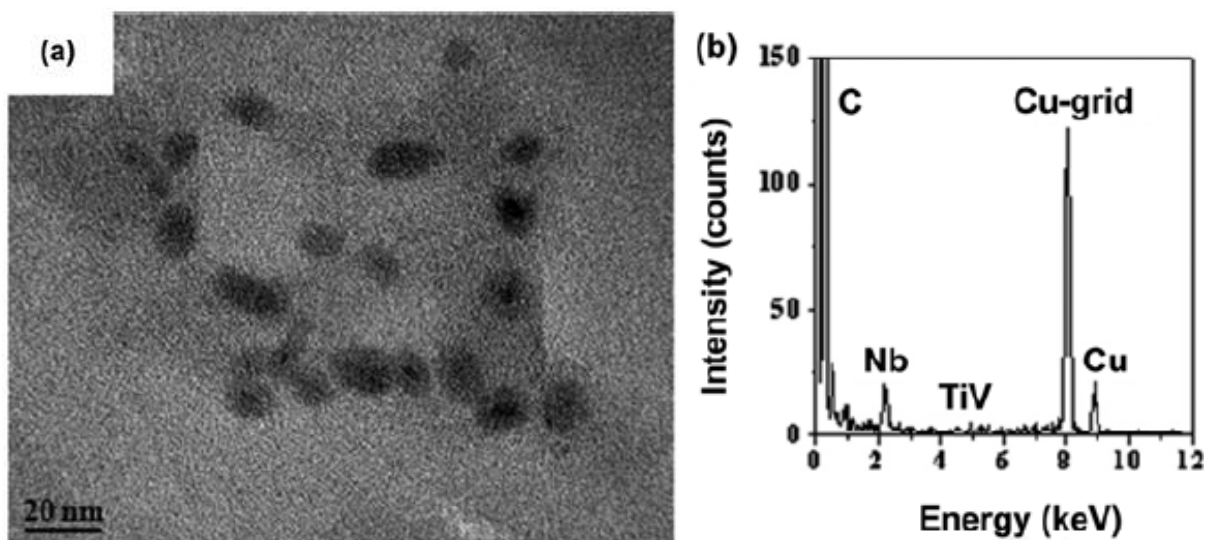


Figure 4.12 (a) TEM image of NbC precipitates and (b) their EDS analysis

Kinetics of precipitation is not influenced exclusively by processing parameter, but also by steel composition: some elements, in fact, retard the phenomenon. For example with molybdenum the precipitation curves are shifted to longer times. This is related to the lower activity of carbon caused by these elements, which leads to delay in Nb precipitation.

Atoms mobility is connected to the diffusion coefficient: their diffusivity increase with more carbon at higher temperatures, but molybdenum leads to lower diffusivity values. Chromium and manganese have similar effect to Mo, while the presence of nickel increase the coefficient.

Lastly, a reduced silicon content is considered a sort of promoter for fast precipitation, because it allows a better formation of nano-cementite particles that serve as precursors for NbC nucleation.

The niobium content is not completely expended in the austenite precipitation: a significant portion remains in solution and it is available for subsequent precipitation during temperature reduction and phase transformation.

During the austenite to ferrite transformation, it takes place an interphase precipitation that lets to the characteristic formation of row-type precipitates. This phenomenon is ruled by elements partition on the austenite boundary while the ferrite front is advancing: figure 4.13 exhibits clearly the dynamic of this precipitation. Partition on the austenite side leads to local supersaturation of carbon concentration, as in (a); solute drag slows down boundary movement so carbide can precipitate (b) and the carbon concentration decrease, allowing again to boundary migration. A typical line of carbide particles is left behind (c) and the process repeats itself. Metallographs of emblematic interphase precipitates are inserted in figure 4.13:

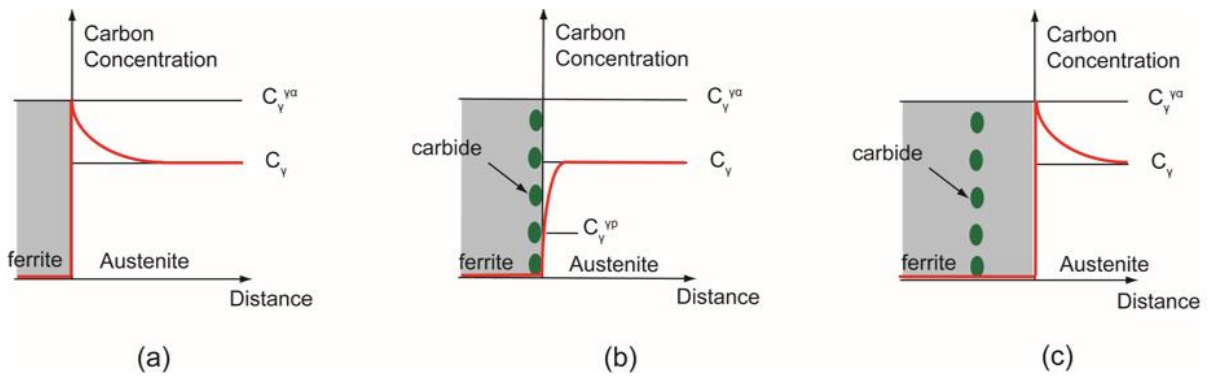


Figure 4.13 Progression of interphase precipitation

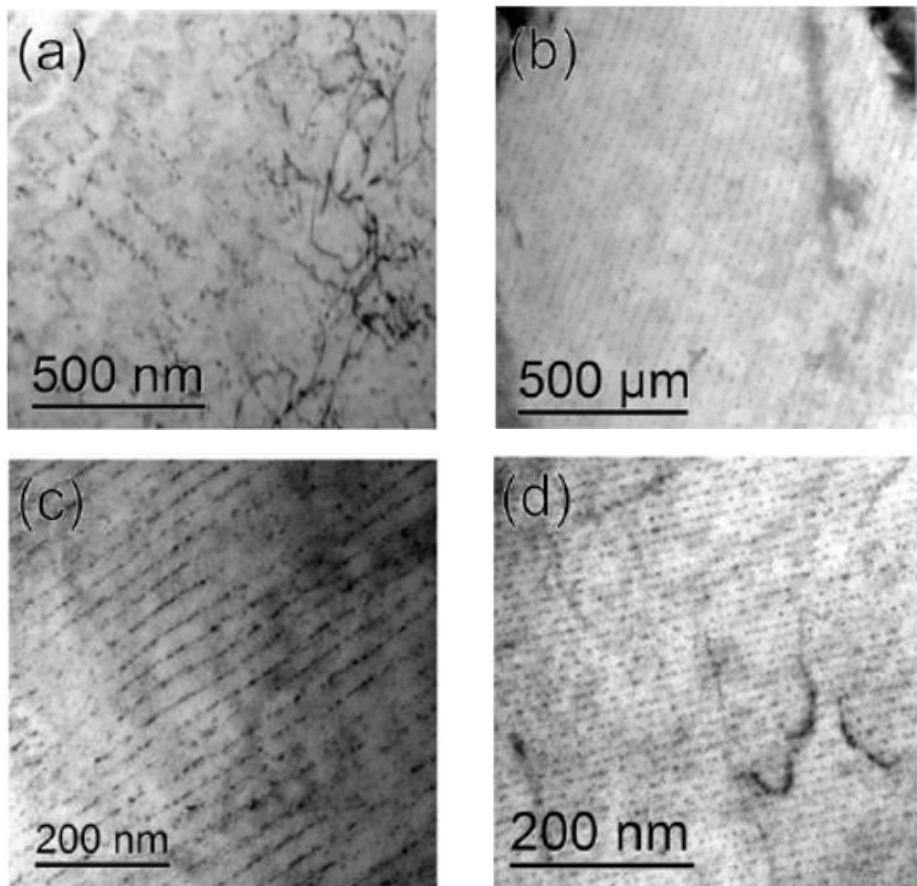


Figure 4.14 Example of rows precipitates at (a) 720°C (b) 700°C (c) 680°C (d) 650°C

The spacing between layers depends on the temperature (samples are held for 30 minutes to allow a complete precipitation): with a decrease in temperature there are closer lines; also particles size follow this trend (their dimensions drop with temperature and stand on some nanometres). In addition, their occupational density along the rows increase with lower temperatures.

A peculiarity is that the imagine of the distinctive rows are visible only at certain orientations, since from different angles, particles could appear randomly distributed in the matrix.

Molybdenum, again, obstructs the mobility of the γ to α interface: this results in a delay of phase transformation, which, however, leads to a more complete precipitation process (time required, in fact, is higher than that in austenite without Mo). Manganese and chromium have the same consequence but in a minor way; niobium, instead, has a stronger effect than Mo, but its amount in solution is lower for two reasons: firstly Nb, as microalloying element, is added in smaller quantity, then it has stronger affinity to carbon to form precipitates (which deplete matrix).

As the temperature drops, the atoms mobility decreases, in fact times for precipitation and particles coarsening is higher than those demanded in austenite range (in particular in the undeformed condition and elevated temperatures). Sometimes, in effect, transformation occurs too quickly for interphase precipitation, so it is established a niobium supersaturation in the newly formed ferrite, which results in high nucleation density for subsequent nucleation. Alternatively fine cluster within ferrite grains with size of even 1 nm could form in place of interphase precipitates.

Anyway a certain percentage of niobium (also with interphase precipitation) remains in solution and it could precipitate in ferrite in the form of fine dispersed particles. The precipitation process has to be expected analogous to carbo-nitrite formation in austenite, since is determined by solubility products. In ferrite, in fact, solubility of niobium it is lower, and it follows the next expression [40]:

$$\log([\%Nb][\%C]) = 4.90 - 11030/T$$

With low supersaturation level precipitates nucleate heterogeneously on the grain boundaries; at high supersaturation level, instead, it's possible both homogeneous (within the matrix) and heterogeneous precipitation, although the second is again preferential. These is characterized by the formation of prior transient iron carbide clusters on grain boundaries; these are metastable and disappear to the benefit of the stable NbC. Segregation induced by short range chemical interaction and long range elastic stresses of the Cottrell atmosphere (formed by C atoms), causes an alteration of the concentration near the dislocations. When concentration reaches a certain level, FeC precipitate, which act as transient clusters prior the effective precipitation of niobium carbides; the remaining carbon atoms left in solution are not sufficient to form NbC, due to the previous extensive segregation. However niobium atoms are present in solution and when they reach the dislocation (driven by the elastic field), they replace iron in FeC and finally equilibrated niobium carbides are formed.

Growth and coarsening it's possible but the atoms mobility is slowed down, so generally particles remain tiny, even having a size of 2-5 nm; solute segregation energy, instead, determines the more or less elongated shape.

[43-45] In the industrial practice after finishing rolling, an operation of coiling is carried out, and here precipitation takes place. During this operation the cooling rate of the coil is smaller than that during rolling, because here the sheet is wrapped on itself and, being the layers in contact, temperature decreases very slowly spontaneously. The properties of the precipitates are influenced by coiling temperature and cooling rate, as it can be seen in figure 4.15.

The early precipitates formed before in the high austenite range will not contribute secondarily, because now they have grown up and their main effect of control of the austenite grain size is almost completely expired.

If coiling is conducted at high temperature (about 700°C or more) precipitation occurs before the austenite to ferrite transformation, but at around 600°C, the formation of precipitates is maximum; lower coiling temperatures don't bring advantages with an optimal precipitation, because it may not happen at too low values. This condition is observable in figure 4.15 where is displayed the increase in strength as function of cooling rate and coiling temperature.

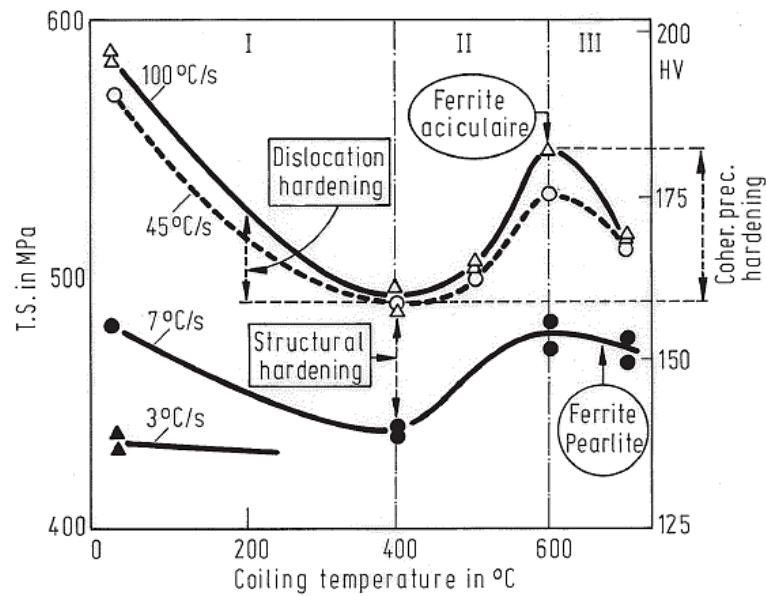


Figure 4.15 Strength as a function of coiling temperature and cooling rate

The mentioned peak at 600°C is attributed to coherent precipitates, which bring a greater increase in strength, as it will be seen in the next section. The great rise of the curves at very low temperature is not attributed to precipitation (because at this range it is inhibited) but to a work hardening effect.

Low coiling temperatures allow to obtain a finer microstructure, as in the graph in figure 4.16, where is represented a microalloyed HSLA steel with Nb and Ti. This reduction is attributable to the containment in the particles growth.

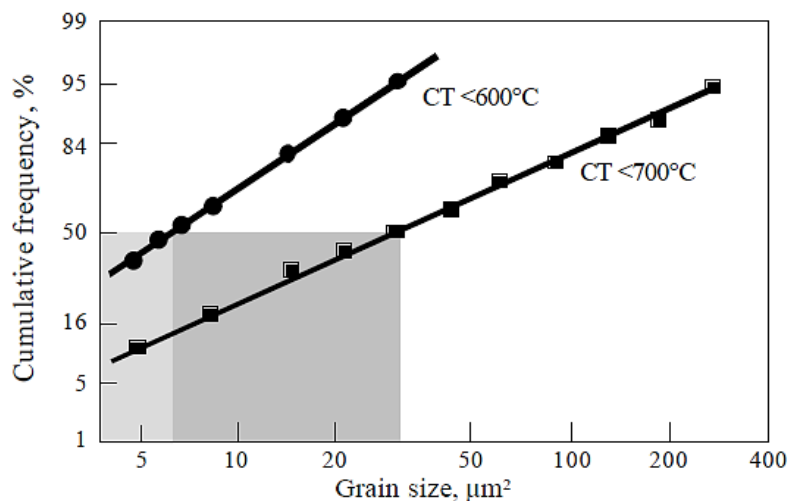


Figure 4.16 Grain size distribution for two coiling temperatures

At coiling temperature $< 450^{\circ}\text{C}$ precipitation is likely to be suppressed leaving a quantity of microalloy in solution, which, anyway, will give a strengthening contribution of solid solution.

The choice of the coiling temperature and condition sometimes is more important than the amount of niobium, in order to meet the property requirement: it has been found that niobium content over 0,06% doesn't have further contribution, so in these case a good accommodation is to adjust the coiling temperature.

Cooling rate (between the end of hot rolling and the beginning of coiling) is also an important attribute: in addition to microstructure refinement and formation of harder phases (acicular ferrite), at an high one a large amount of niobium is in solution and it is available for precipitation; in fact the more Nb present, the more precipitates possible to give the peak at 600°C . Low cooling rates, instead, allow particle coarsening and promote formation of incoherent niobium carbonitrides, which are less effective in strengthening than those coherent.

Regarding the steel typologies that requires high cooling rate, nevertheless, it can results in the opposite achievement (respect to particles coarsening): when steel is subjected to quenching to obtain a hard (martensitic) structure, precipitation is avoided. These steel (for example martensitic) are typically cold rolled to sheet and then are formed, so they need a restoration of ductility; in order to achieve this, an annealing/tempering operation is carried out, which returns the necessary ductility and also allows precipitation. In addition, also a traditional method uses water quench to investigate precipitates in ferrite, and also in this case, an annealing operation is required.

Treatment usually is conducted in the temperature range between 600°C and 700°C , but a typical condition is 670°C for 1 hour; it is remarked in figure 4.17. However the time processing is variable and it may even take a few days. Combination of time and temperature determines the final condition of the steel and the status of the precipitation. This is clearly understandable in figure 4.17: intersection of annealing time and temperature provides the completeness of precipitation; for higher temperatures it is achieved in shorter times (this is the case of continuous annealing).

Diagram shown in the figure represents a scheme of precipitation kinetics: three different curves represent various percentage of precipitation in function of time and temperature. Obviously, time need for an elevated level of completeness is long due to the slow kinetics. It is remarkable that a contained reduction of 70°C in temperature, almost halves the precipitation percentage.

In this kinetic graph it's possible to "superimpose" curves that represents thermal or mechanical treatments (such as coiling or heating before hot forming): their intersection with the precipitation curves gives information on the status of the accessible precipitation. For example, coiling would be illustrated by a curve in the low temperature region that extends over long time due to the slowness of cooling in the coil, and, therefore, higher percentage of precipitates can develop.

The diagram in the figure is referred to an experimental steel that has 0,011% C - 0,08% Nb - 0,001% N. It was soaked at 1250°C and quenched, and figure 4.17 exhibit precipitation for the typical annealing treatment mentioned just above.

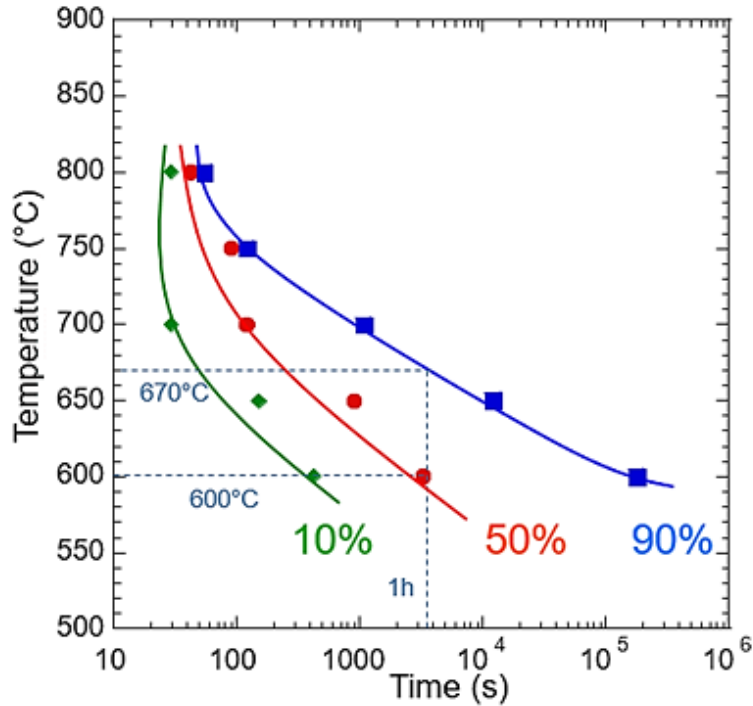


Figure 4.17 Precipitation kinetics of Nb during annealing

The process marked by long time and low temperature is called batch annealing, while for the opposite condition, the annealing is continuous; in the graph it would be in the region between 750-800°C and around hundreds of second. This operation has the advantages of economic benefit and reduced scatter in successive mechanical properties.

In both cases the process involves a reacquisition of diffusivity that allows atoms aggregation and precipitation. The results are represented in figure 4.18 (a) and (b), respectively the amount of precipitates and their size at some annealing temperatures. An exemplary annealing trial carried out, on the previous steel, at 700°C for 3000 s, gave as outcome particles whose average size was 2,3 nm.

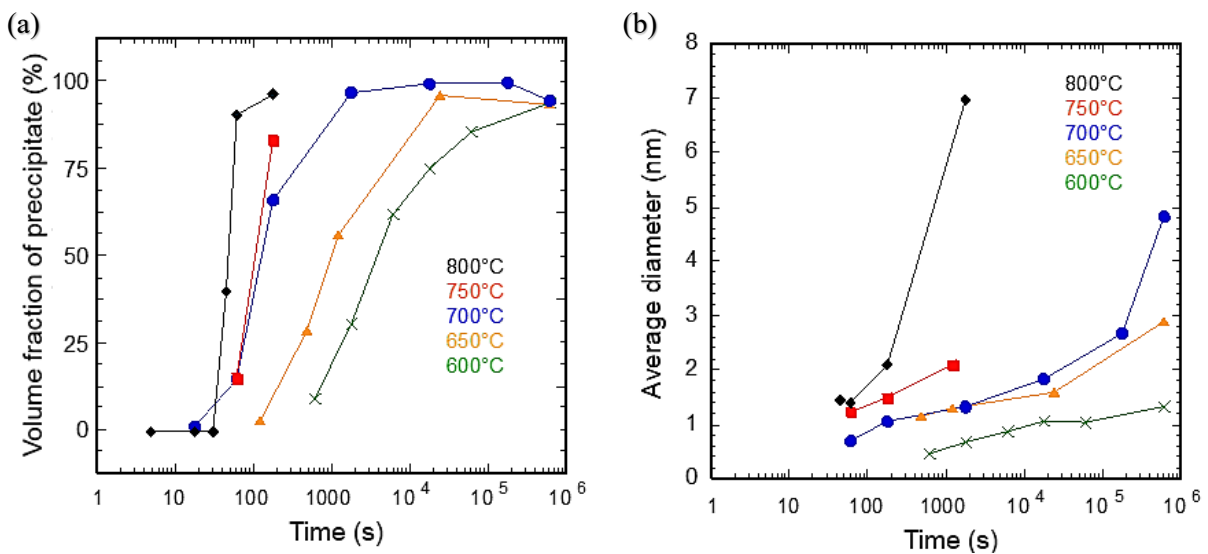


Figure 4.18 (a) Kinetic and (b) size of precipitates

Lastly in figure 4.19 is represented a summary scheme of niobium precipitation and its effects in grain refinement and strengthening. It should to be said that at the end of the process, there is the possibility of a remaining amount of solute niobium: this will be available in succeeding precipitation (for example in the steel ageing), or it will contribute at strengthening through the solid solution mechanism.

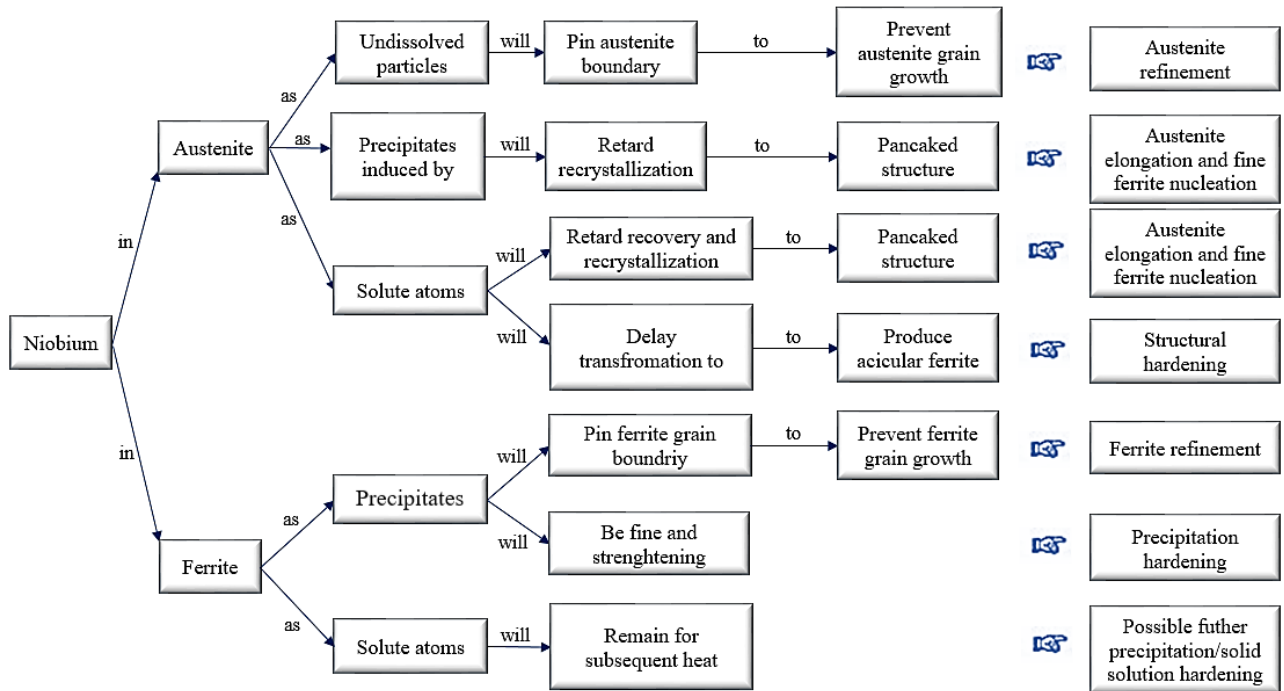


Figure 4.19 Nb role in thermomechanical process

4.2.1 Precipitation strengthening

[18,40] When a particle is formed in the steel, it interacts with the surrounding elements giving strength by hardening mechanism. Mainly it consists of the interaction between the precipitates and the motion of dislocation, with the firsts that act as a barrier to the latter, and provide resistance to slip.

However it is identifiable also the misfit strengthening, that comes from the lattice mismatch between the microalloyed carbonitrides and the iron lattice. Even the crystallography of precipitates plays an important role, since the crystal orientation in the matrix give a more or less marked contribute.

Concerning niobium carbide, its structure it's a layering of niobium and carbon, with an octahedron of Nb around every C and vice versa, without C-C bonds. The lattice parameter of NbC is 0,447 nm, and it is larger than those of the matrix: in fact the austenite lattice is 0,3596 nm and the ferrite one is 0,2866 nm; these differences generate a misfit respectively of 24,1 % and 55,7 %. If instead precipitates are nitrides, the lattice value drop to approximately 0,435 nm, so their effect, for example in pinning recrystallization and grain growth, is weaker, and for this reason carbide are preferred to nitride. Additionally niobium precipitates have the largest lattice constants compared to titanium and vanadium, so it has the stronger effect. Titanium nitride, for example, has a lattice parameter of about 0,425 nm, so it isn't the most powerful precipitates, but it is the only one that is present at high temperature; in fact after pinning austenite grain growth initially, its effect becomes marginal (also because particles grow).

Table 3 resume some precipitates features during the precipitation process described earlier.

Precipitation	Precipitates crystallography	Orientation relationship
In austenite	Incoherent	Arbitrary orientation
Induced by deformation (in austenite)	Incoherent	Cube-cube (100) _{ppt} // (100) _γ and [100] _{ppt} // [100] _γ
In ferrite	Coherent or semi-coherent	Baker-Nutting (111) _{ppt} // (110) _α and [011] _{ppt} // [010] _α

Table 3 Matrix-precipitates connection

The most effective interface relation for precipitation strengthening is coherent or semi-coherent: with these type of precipitates there is a local strain field that acts with the surrounding structure, creating a stress; the combination with fine particles impedes dislocation motion. Precipitates formed in austenite, in fact, are more effective in delaying recrystallization and preventing coarsen microstructure, than in hardening the steel. The shape is another aspect regarding effectiveness: spherical shape is preferred than elongated or needlelike because stress-concentration is prevented.

The strengthening mechanisms (concerning interaction between precipitates and dislocation) are two: cutting and looping (represented respectively in figure 4.20 (a) and (b)). The first follows the expression:

$$\sigma_{cut} \propto \gamma^{3/2} \cdot f^{1/3} \cdot r^{-1/2}$$

where f is the volume fraction of precipitates, r is their radius and γ is the anti-phase energy that increases with size increasing; it is proportional to the anti-phase boundary that is a portion of the atomic grid out of phase, where a lateral shifting has moved atoms, breaking their order (usually atoms of the same type became flanked). The source of anti-phase boundaries is a dislocation that causes the shifting during its motion; the formation of this boundary increases the energy (due to the atoms repulsion), so further dislocation transit is more difficult. The strengthening attribute is the energy required by a dislocation to cross and split a particle (fig. 4.20 a). This mechanism is not the strongest, but growing up the volume fraction, it can give a contribute.

If precipitates, instead, are too hard to be crossed (such as the non-metallic phase like niobium carbonitrides), then it takes place a looping process, that follows the Orowan process that is shown in figure 4.20 (b). When a moving dislocation runs into a particle, it loops the latter, leaving a sort of dislocation ring around the particle. Gradually these build up and the distance between dislocations (the space free of them) decreases, until further looping is impeded by work hardening. This mechanism observes the Orowan equation:

$$\sigma_{loop} \propto (G \cdot b) / L$$

in which G is the shear modulus, b is the Burgers vector and L is the average particles spacing; it is proportional to the radius r .

With a shorter radius and a dense population, the contribute will be larger. So this is a reason to avoid coarsen precipitates, in particular the so-called Ostwald ripening, which both reduces the precipitates number and increases their radius: the smaller ones, in fact, are dissolved and the solute is redistributed to the larger. From the equation it's clear that, in this condition, L grows up and σ decreases.

For completeness it's reported a "correction" that is the Ashby-Orowan mechanism, in which it is taken into account the interaction between two dislocations with opposite signs in the vicinity of the particle. This can take a reduction in the effective strengthening value due to their annihilation.

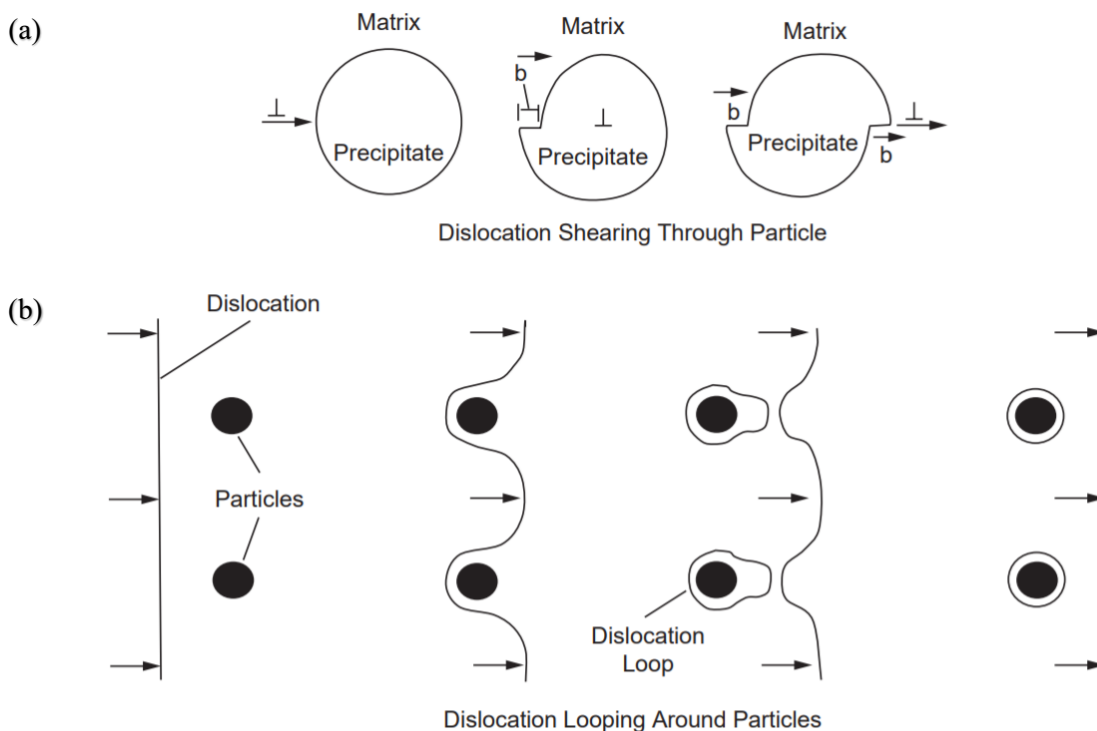


Figure 4.20 (a) Cutting and (b) the Orowan mechanism

The ideal point in strengthening is the intersection of the two curves of the mechanisms (cutting increases with radius while looping decreases): the radius relative at this point represents the peak strength, in which they both contribute.

As described before, annealing may allow precipitation in case of previous cooling so rapid that it didn't occur; in this situation, precipitation during annealing operation could give a contribute in hardness. As in can be observed in the graph in figure 4.21, after a certain period the particles show their effect and hardness is increased; intuitively time drops at higher temperature, but the maximum contribution is similar. This is due to the dependence of two factor: volume fraction and particle size, that increase with longer times. Since the measures were carried out on the same material, the optimum dimension (and quantity) is the same, but is reached at different times. After that, hardness decreases due to the precipitates coarsening (when they become "overaged").

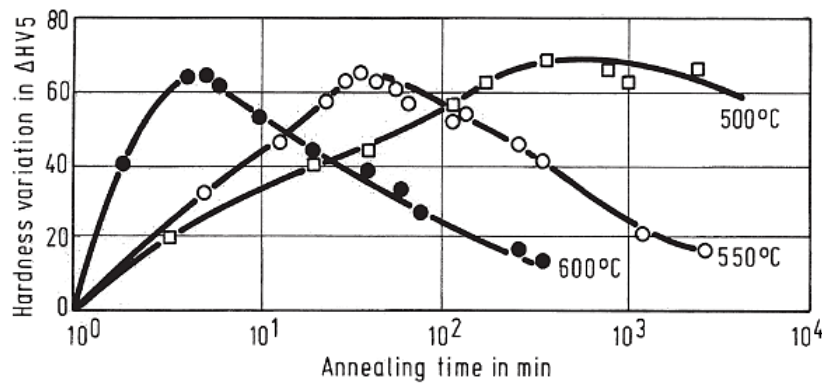


Figure 4.21 Hardness increase of a 0,11% Nb steel

There is another important aspect regarding the mechanical properties: interphase precipitation could cause toughness degradation as a result of their arrangement; along the direction of a particles line, cracks may find a preferential path to expand. However grain refinement provided by niobium enhances toughness, so precipitation strengthening is utilizable (if application requires strong toughness control, for example, interphase precipitation could be avoided by fast cooling obtaining more dispersed particles).

Finally it's remarkable to said that uniformity in the mechanical properties is a target to be achieved in order to satisfy the increasingly stringent demands of the market. In hot rolling, in fact, it can be developed different condition along the length and across the width of the strip.

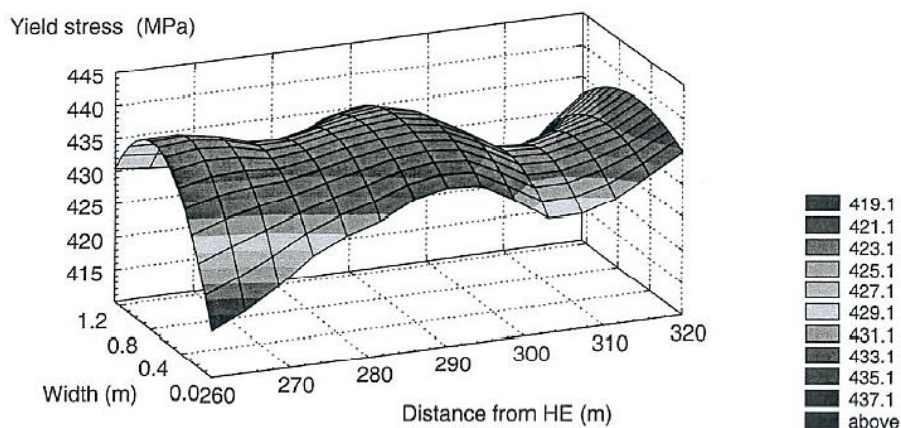


Figure 4.22 Topological strength distribution in a HSLA steel strip (HE=head-end of the strip)

During cooling and coiling, for example, the edges may be 20°C colder than the centre, and this could lead to different properties, as in the illustration in figure 4.22. Here it's suggested that insufficient time at temperature was experienced in the edges which are cooled quicker and exhibit softer strength values [43].

Also the head and the tail end of the strip could manifest gradient in properties, due to the exposure related effect to inner and outer laps. To reduce these effects it is possible to apply a catenary, which involves a reduction in the level of cooling applied at the head and tail of the metal. So the rapid cooling experienced by the exposed inner and outer laps will be reduced, producing a balance in the run-out-table.

4.2.2 Investigation method for precipitation

Shape and size of precipitates are detectable by using powerful SEM or, more appropriately, TEM, but this is not effective in evaluating their total amount (due to the restricted area of analysis and the impossibility to examine a whole specimen of big dimension). One common technique is the extraction of precipitates by dissolving the metallic matrix in acid; with this it's also possible to quantify the amount of remaining solute niobium that will be available for further precipitation or strengthening by solid solution. This method consists in the dissolution of the material, then filtering and measurement of the precipitates. The reliability is statistically significant, but there is the possibility that the smallest particles (that give the larger contribute) pass through the filter, "falsifying" the analysis.

Electrical resistivity is an alternative useful method to evaluate precipitation in steel, and it relies on the principle that solute elements are consumed while the process advances; consequently the matrix is depleted and the electrical resistivity drops because solute elements are stronger scattering centers for electrons in comparison to precipitates [41]. This phenomenon is clearly visible in figure 4.23, where it's illustrated a diagram that compares electrical resistivity in combination with niobium solute, with the progress of precipitation. The result in the graph comes from a study conducted on a microalloyed steel with 0,042% C - 0,085% Nb - 0,017% Ti - 0,005% N. The specimen was soaked at 1200°C for 10 minutes, then it was cooled down to lower temperatures, deformed ($\epsilon = 0,3$ and $\epsilon = 0,6$), isothermally held and quenched to characterize the strain-induced precipitation. In addition, one sample was held at 670°C for one hour after cooling from 1200°C and subsequently quenched to fix precipitates. This process was made for the evaluation of the precipitation status before the austenite deformation and after the interphase precipitation (in this way the only permitted precipitation is spontaneous in ferrite).

In figure 4.23 only the results of two trials are displayed: one was deformed at 950°C ($\epsilon = 0,3$), and the other isothermally held at 670°C. Despite the small number, they represent correctly the evolution, since in other diagrams the trend was similar.

The resistivity decreases with reduction of Nb solute (which means that particles are getting larger): at the same time there is less electrons dispersion, so the resistivity is diminished. Isothermal holding for one hour leads to precipitation that is more complete. Application of a more extensive deformation ($\epsilon = 0,6$ in the examined case) results in lower values of resistivity, because, again, the number of precipitates is higher and the matrix is solute exhausted.

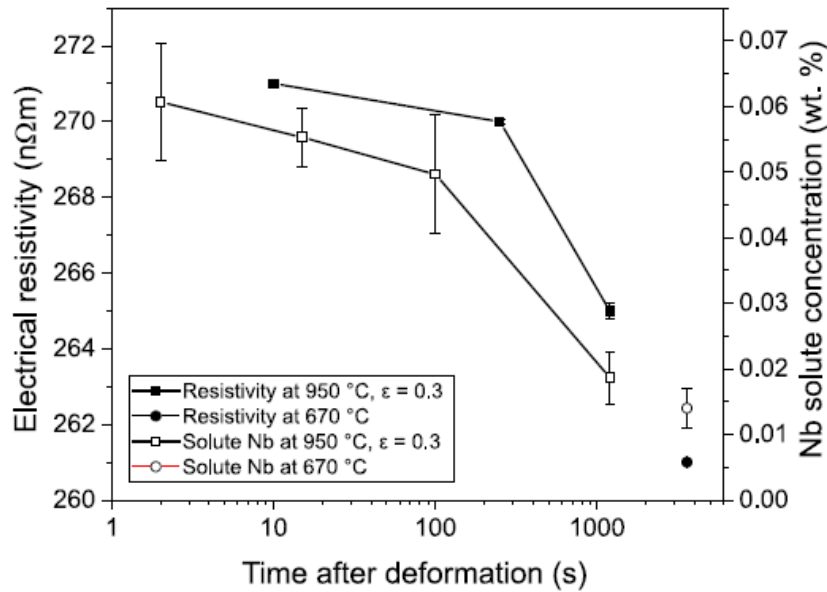


Figure 4.23 Correlation time-resistivity-solute concentration

Jung et al. [46] carried out another study, in which it's studied the dynamic precipitation kinetics in a complex Nb-Ti-V microalloyed steel through electrical resistivity measurement. The fraction of the microalloying elements is respectively 0,067%, 0,02% and 0,056%; the amount of carbon is 0,078%, while manganese percentage is 1,85.

The specimen was treated at 1200°C for 900 seconds, slightly deformed twice ($\epsilon = 0,08$) at 1150°C and rapidly cooled (-50°C/s) to 900°C; in this range precipitation doesn't occur. Then it was compressed with true strain of 0,15 - 0,34 and 0,67 and subsequently quenched at room temperature. Similarly to the previous trial described, a specimen was annealed at 900°C for 1800 seconds, after a compressive strain of 0,67.

An advantage of this analysis is the subtraction of the contribute of interstitial atoms and crystal defects (called ρ_d) to the electrical resistivity ρ_r . Therefore, it is quantified a corrected resistivity measure ρ_c only dependent upon solute microalloying elements. The adjustment is perceptible, as it can be noted in figure 4.24 where the curves are quite separate.

Deformation was conducted under the T_{NR} (approximately 950°C for this steel), so the microstructure was largely deformed, resulting in numerous band in the grains: this provides many nuclei for clustering and precipitation. Figure 4.24 shows the electrical results: with a strain of 0,15 resistivity didn't change appreciably, so it can be assumed that dynamic precipitation has not yet started. Increasing the strain magnitude, precipitation occurs and it leads to decrease in resistivity, as explained before. The noticeable fall regarding the annealed specimen confirms the supposition of a more complete precipitation thanks to longer times; in fact, a software calculation estimates that only about one quarter of Nb-rich particles has precipitated after compression of 0,67.

In comparison to other steels, it was found that in this one precipitation kinetics is faster, and it is probably related to the higher concentration of niobium and carbon.

[47] The last years saw a strong increase in computational power of the software, which are useful method to preliminary investigate thermodynamic and precipitation behaviour quickly, and without test. Those programs are embedded with the classical solubility and dissolution kinetics equations, but sometimes these are not sufficient, because comparisons with experimental trial show discrepancies (for example a more or less precise equilibrium between precipitates and matrix or a lack of homogenization insides the carbonitrides, could affects the

prediction of computational analysis). Hence many factors must be taken into account for an accurate analysis, and some databases and additional modelling have been developed by researchers. For example interfacial energy is a critical parameter in precipitate evolution, due to the difficulty in calculating it, also in relation with the coherent or incoherent interface type.

It is believed by some authors that acquisition of better information on the critical variables entering the theory could be a better way than introducing a lot of adjustable parameters; in order to express the correct behaviour, a general modelling that includes the classical theory and controls the critical factors it's better than adjusting each time some factors.

Just to name few software, it's possible to mention DICTRA, CALPHAD, Thermo-calc, ...

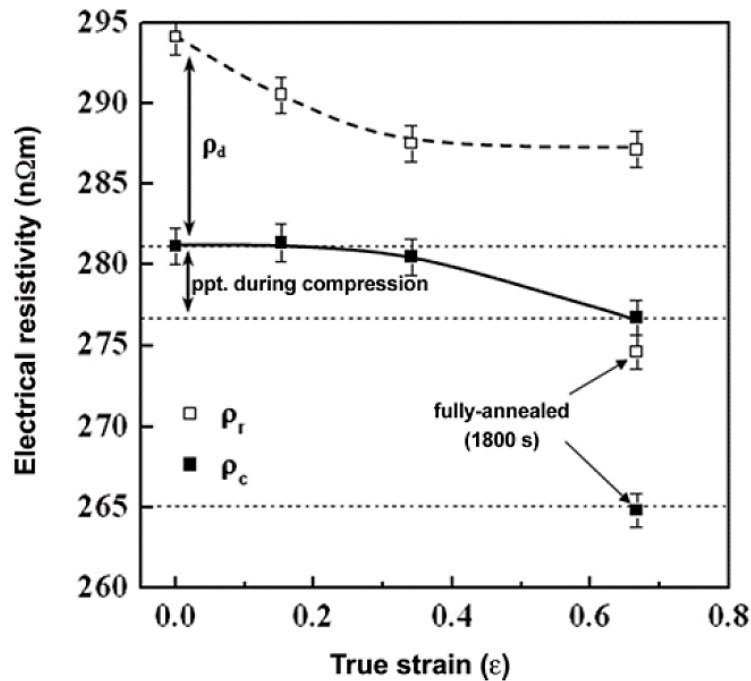


Figure 4.24 Corrected resistivity as a function of compressive strain

4.2.3 An example of a case study

In this section is provided a complete investigation performed by A.G. Kostryzhev et al. [48], in which is examined the effect of niobium precipitation in a Nb-Ti microalloyed steel, correlated to microstructure and process parameters.

The steel processed has the following composition: 0,081%C - 1,20% Mn - 0,27% Si - 0,021% Ni - 0,019% Cr - 0,1% Mo - 0,016% Cu - 0,037% Al - 0,064% Nb - 0,021% Ti - 0,003% V - 0,001% S - 0,012% P and 0,0047% N.

Process was conducted in a laboratory thermo-mechanical simulator, using small samples. Six trials were studied, and they are graphically summarized in figure 4.25; the three deformation temperatures (1075°C, 975°C and 825°C) for the single compression hit at $\epsilon = 0,75$ were chosen because they represent three particular condition: above, near and below the T_{NR} ($\approx 975^\circ\text{C}$). After this deformation, process follow two ways: cooling to 800°C (above $A_{r3} \approx 775^\circ\text{C}$) and water quenched, or cooling at 600°C (below A_{r3}), holding for 300 s, and then air-cooling to room temperature. These two options aim, respectively, to investigate the precipitates in austenite and in ferrite.

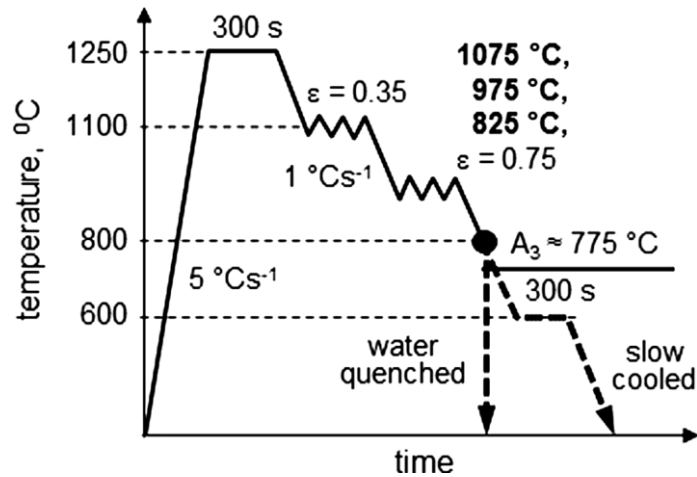


Figure 4.25 Thermomechanical controlled process schedules

The obtained microstructure has ferritic grains that get smaller as the deformation temperature decrease; in the sample held at 600°C their size drops from an average of 13 μm , to 11 μm and to 9 μm .

Precipitation happens all the time, in a size range 20-170 nm; it's possible to separate them into two groups: particles >70 nm, which are cuboidal $(\text{TiNb})(\text{C},\text{N})$ or ellipsoidal carbonitrides, and particles <70 nm, spherical NbC characterized by the absence of titanium. An overview of the size distribution is represented in figure 4.26.

It is clear that the deformation temperature is a key factor: 1075°C is too high for strain-induced precipitation, since, according with the precipitation kinetics diagram (C curves) for this steel, it starts below 1000°C. The total precipitates number of this condition, in fact, is the smallest.

In austenite the particles size decrease with lower temperature due to the slower diffusion and dislocation annihilation that obstructs coarsening. Another aspect it's noticeable: the maximum time available for strain-induced precipitation occurs at 975°C (where it's located the "nose" of the curve); therefore, particles fraction >70 nm will be higher than the other temperature because for 825°C the atoms diffusivity is lower (so particles don't grow), and for 1075°C this type of precipitation doesn't take place (so their number is smaller).

In ferrite, particles density increases per μm^2 due to longer precipitation time. The maximum values of finer precipitates is obtained for 975°C; coarsening this time is avoided because the temperature of isothermal holding is lower.

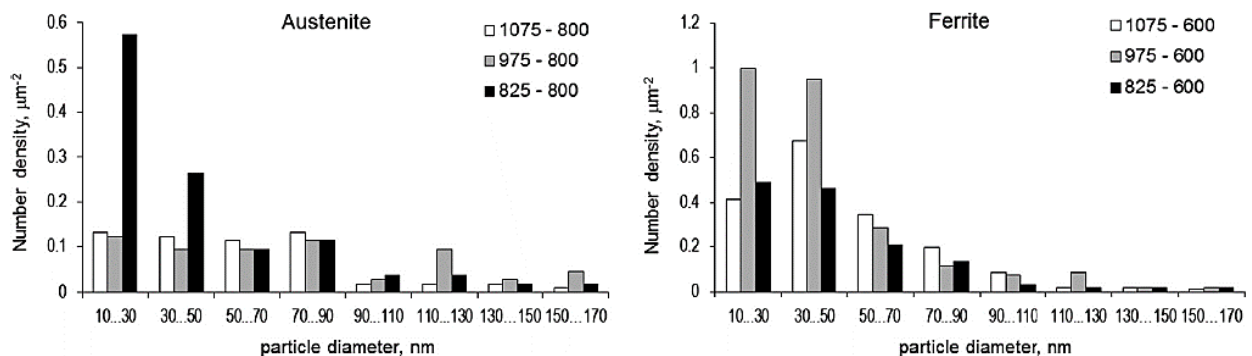


Figure 4.26 Precipitates size distribution

In addition APT analysis was applied to study the precipitates composition; in figure 4.27 is visible a reconstruction of precipitates on the trial deformed at 1075°C and held at 600°C. The investigated area is limited but niobium carbide are easily detectable in the aggregation zones of both carbon (a) and niobium (b).

The analysis revealed that are formed fine Nb-rich cluster with size between 3 and 13 nm; these particle gave a wide contribution to strengthening. Cluster are aggregates of atoms held together by metallic bonds; the number of atom “species” that compose them is limited, and it could be even just one. Their size could be very small when the number of atoms reaches level of a few dozen (for example in the study it has been detected clusters composed by around 30 atoms). Chemical study reveals that their density decrease with deformation temperature, and larger clusters contain less niobium.

A small Nb amount remain always in solution after all processes practiced in industry; keeping this in mind, it’s understandable that in this type of precipitation analysis, sometimes, it’s more important a focus on the process parameter rather than on the niobium quantity. It is bound by the solubility limits, so a disproportionate addition is unnecessary and inappropriate. Knowing its beneficial effects it’s opportune to optimize the process.

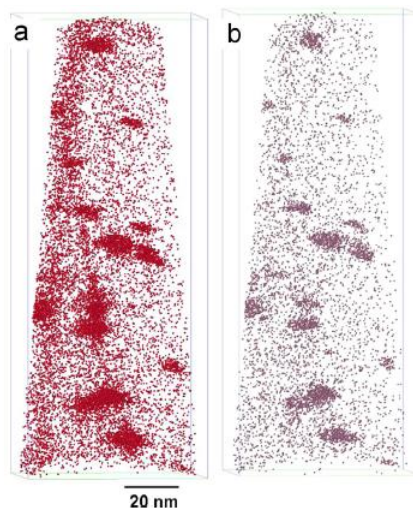


Figure 4.27 (a) Carbon and (b) niobium atom map

Lastly, it was quantified the effects on mechanical properties. There are several contributes to strengthening: these are now treated separately, and they are resumed in table 4. The exposure refers to the final ferritic condition, i.e. after holding at 600°C for 300 s.

- Grain size work through grain refinement; the large increment in σ is given by Hall-Petch equation: it has been calculated to be 204, 220 and 240 MPa respectively for the three decreasing deformation temperatures. This is attributed almost exclusively to the smaller ferrite grains, because the possible increment attributable to pearlite was negligible.
- Precipitation strengthening was evaluated using the Ashby-Orowan equation. As explained previously, smaller particles confer more contribute, in fact for the >70 nm, it is 24-28 MPa, while for the <70 nm, the values range is 45-62 MPa.
- Clusters act with the same mechanism of precipitates: in this study, however, their increment is estimated via subtraction of the others mechanisms from the measured yield stress. The results are 127, 78 and 47 MPa for the three temperature (as said their number decrease with lower temperatures). These confirm that finer particle are more effective in strengthening. Cluster contribution could be even slightly higher, as

evaluated in other Nb microalloyed steel; this is due to the presence, in this case, of titanium, which leads to the formation of large (TiNb)(C,N) that lower the amount of available niobium for clustering. Another cause is the reduced dislocation density compared to other steel cooled more rapidly.

Application of analytic method instead of contribute subtraction from yield stress, results in significantly higher values. This might be caused by overestimation of cluster number due to the small area of APT analysis, and their non-uniform distribution.

- Solid solution strengthening mainly derives from the contents of Si and Mn within the matrix. Its increment is around 40 MPa.
- Hardness is increased at higher deformation temperature; this can be attributed to increase in precipitation and clustering strengthening.

TMP schedule	Calculated contributions to the yield stress (MPa)				Measured hardness (HV)	
	Grain size	Solid solutes	Precipitates			Clusters
			< 70 nm	> 70 nm		
1075-600	204	44	51	28	127	197 ± 14
975-600	220	39	62	28	78	186 ± 13
825-600	240	42	45	24	47	174 ± 7

Table 4 Summary of the various contributors

4.3 Comparison with other elements

As said, niobium is not the only element to have the above described effects on steel; the other main microalloying elements are titanium and vanadium. Many time it's used a multiple addition, because each material has an own feature, so they may complete each other.

[17,35,39] Nb, Ti and V have in common the tendency to form precipitates during cooling, which prevent grain growth and strengthen steel; moreover they are added in small amounts. The development of precipitates depends on intrinsic characteristic of the elements: mainly, solubility controls the process. Figure 4.28 display the solubility product as the temperature rise; in can be observed that the trend for precipitation is Ti > Nb > V. In the figure are shown also boron and aluminium, because they are often used in low alloy steel (for example, Al deoxidize steel) and could generate precipitates.

Solubility product is based on the reaction between substitutional (those in the chart) and interstitial elements (carbon and nitrogen); their ratio is the factor n, and frequently is unity. The expression

$$K = [X][Y]^n$$

in the y-axis of the graph, represents the solubility product that is the logarithmic term in the equations seen previously. Lower values indicate higher tendency to precipitation.

Titanium nitrides have low solubility in austenite, so it form stable particles that are not dissolvable unless high temperature, thanks to which it is the best element to control grain size in high austenite region. For this reason it is usually always used in addition to niobium (that, in turn, refines better at lower temperatures); for example, Ti is required in welding due to the huge heat involved.

The size of these precipitates is larger than the others formed subsequently, and it is also related to the ratio Ti/N: size presents a minimum when this value is near but slightly lower than the stoichiometric ratio 3,42 (that is the ratio of the molecular weight of C and N). This optimum value is approximately 2, so this hypo-stoichiometric ratio enables the ideal particles that exert the higher pinning force to austenite grain growth. A “critical” dimension beyond which the force is too weak could be considered around 100 nm.

Ti/N ratio influence also other parameters, such as energy for deformation and activation energy for recrystallization. These curves have a parabolic trend, and it is related to the best condition for precipitation: in fact, their peak occurs at a hypo-stoichiometric ratio that leads to small particles (although it has been observed a delaying effect of solute drag at very high Ti/N values). Hence, a control of this value is very important to prevent undesirables coarsen particles.

Finally, it could be resumed that titanium performs its function mostly at high temperature, while at the lower ones it has to be accompanied by others elements; it can delay recrystallization, but in a lesser way than Nb and V, because the driving force is bigger than the pinning force (sometimes, in fact, in Ti-steel doesn't exist a T_{NR}). Ti precipitates are larger than the Nb and V ones and they can even become detrimental if their dimensions gets too big: they could even act (at high Ti/N ratio) as nucleation sites for recrystallization. In addition they could be harmful for toughness, as potential nuclei for cleavage fracture.

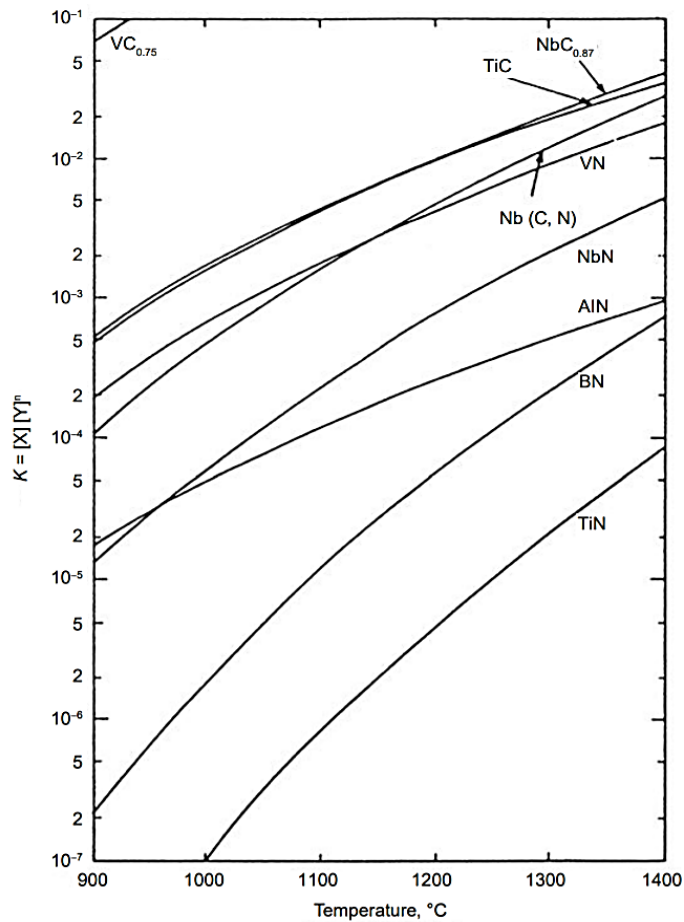


Figure 4.28 Solubility product vs. temperature in austenite

Aluminium could form precipitates smaller than TiN, but larger than NbC or VC, and their power in recrystallization inhibition is insignificant. Higher solubility temperatures and larger diffusion coefficient (almost two order of magnitude) compared to other elements are the reason

for particles coarsening. Indeed, a reduced amount of Al may be preferred to have more N available for precipitates that are more efficient. Aluminium, nevertheless, could be important in steels for deep-drawing (typical ultra-low carbon that will be presented in a subsequent chapter): its precipitation stabilizes nitrogen and enhances the formation of a correct texture for good formability.

Vanadium has the lowest solubility temperature, so its interest is in ferrite grain refinement. V(C,N) can precipitate during interphase precipitation, or directly in ferrite in which they can act as nucleation site for fine ferritic grain. Interesting precipitates are the intergranular ones and those formed in the ferrite to austenite grain boundaries and dislocations.

Niobium precipitates, anyway, remain the most efficient in grain refinement and precipitation strengthening. They have, in fact, the greater mismatch in the lattice constant, which results in larger strain field in coherent precipitation. The values are:

- NbC: constant lattice = 0,447 nm; misfit in austenite 24,1% and in ferrite 55,7%
- TiC: constant lattice = 0,4329 nm; misfit in austenite 20,3% and in ferrite 50,9%
- VC: constant lattice = 0,4154 nm; misfit in austenite 15,3% and in ferrite 45%

For completeness it should be said that for all three elements, the lattice parameter is higher for carbides than nitrides, so the first are more effective in pinning force and strengthening.

In figure 4.29 is shown a representative diagram that confirms what has just been said. For example, in order to obtain an increment of 150 MPa in yield strength (considering both the effect of precipitation and grain refinement) in a mild steel, it's required an addition of 0,03% Nb, or 0,08% V or 0,1% Ti. The discrepancy decreases considering the atomic percentage: niobium, in fact, has almost a double atomic weight, so the atomic % is respectively 0,05%, 0,07% and 0,086% for Nb, V and Ti.

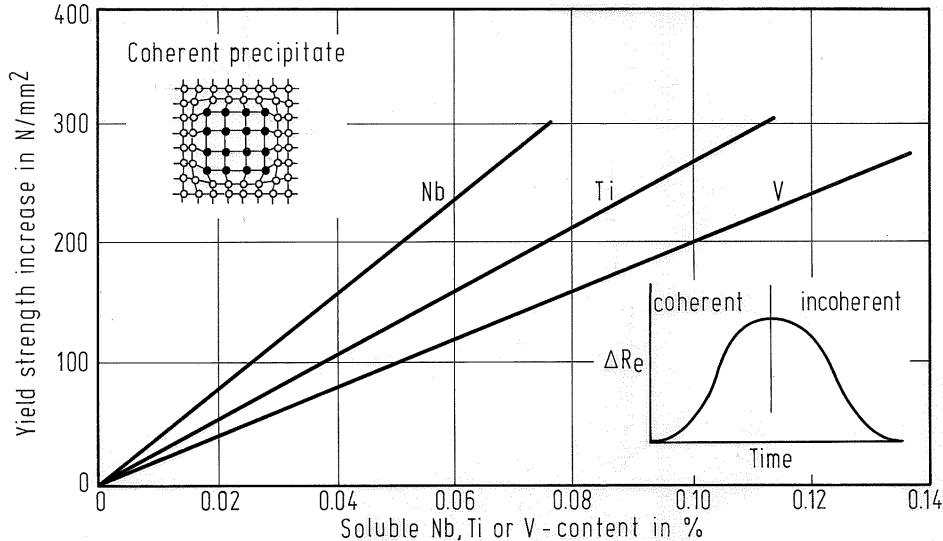


Figure 4.29 Strength increase for the three elements

Precipitates, as remarked before, has the effect of increasing T_{NR} and consequently obtaining a finer microstructure. In the past Boratto et al. [20] estimated the following formula for the T_{NR} :

$$T_{NR} = 887 + 464 \cdot C + [6445 \cdot Nb - 664 \cdot (Nb)^{1/2}] + [732 \cdot V - 230 \cdot (V)^{1/2}] + 490 \cdot Ti + 363 \cdot Al - 357 \cdot Si$$

Influence of microalloying elements is clear, as well as the prevalent importance of niobium. Nevertheless this is an empirical formula, so it must be take care in its application, because it

neglects some aspect of microalloying; for example it considers a too much linear trend as the amount of elements increase, while at certain point their effect reaches a limit. Additionally, as repeated more times, chemical composition alone doesn't determine T_{NR} since a great contribution is given by processing conditions.

Another element that is often used in steel is molybdenum; this alloying element is mainly added because it prevent embrittlement phenomena related to phosphorus segregation during thermal treatments. Then, it improves hardenability, by shifting to longer times the curves of formation of polygonal ferrite and pearlite, and promoting the development of harder phases like bainite and acicular ferrite.

The mentioned characteristic of slowing down the atoms mobility and the carbon activity, results in increased niobium precipitates solubility in austenite. This translates into more microalloying elements in solid solution, which leads to delay in γ to α transformation, and better precipitation of fine niobium carbonitrides in ferrite.

Mo in combination with Nb, at high temperature of roughing rolling retards the rate of recrystallization [49]; this is visible in the graph in figure 4.30, where are displayed the effect of these two elements. Niobium has the strongest effect with less amount (one tenth of Nb it's better than one unit of Mo), but also molybdenum gives a remarkable contribution.

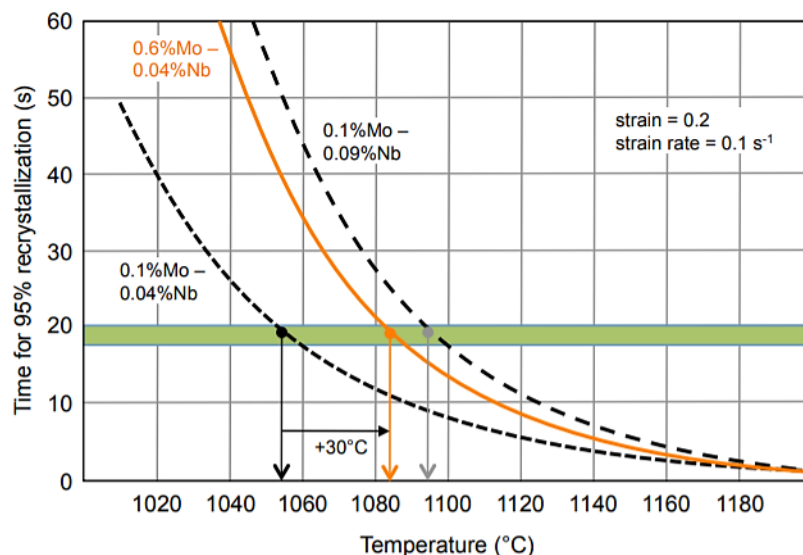


Figure 4.30 Influence of Nb and Mo on recrystallization

Mo has been revealed being a hardenability element: this is related to interaction with boron. Briefly, boron provides hardenability through its segregation at grain boundary where it obstructs the formation of grain boundary ferrite, in favour of harder phases. This is possible if B is in solid solution, so it's should be avoided formation of complex boron precipitates, and Mo, with reducing carbon activity, is effective. Niobium, with the creation of NbC, has similar effect, but molybdenum is better.

Another work was performed by H. Pan et al. [50], who studied the influence of microalloying elements on microstructure and mechanical properties in a warm-rolled medium-Mn steel. They made a comparison between the steel in the basic condition, with niobium (0,05 %) and with niobium and molybdenum (0,22 %). The amount of carbon is around 0,19 %, while the manganese one is 5,6 %. After the warm rolling at 700°C with a heavy reduction, trials were intercritically annealed at four temperatures (550°C, 600°C, 650°C and 700°C) for 30 minutes, and lastly cooled to room temperature.

The resulted microstructures are composed by ferrite and retained austenite (γ_R), whose volume reaches a peak at 650°C, and it is influenced by niobium and molybdenum (it decrease with addition of Nb and especially with Nb-Mo co-addition). The mechanical stability of γ_R is important for the mechanical properties of TRIP steel, that will be treated subsequently; for the moment it could be said that with niobium and molybdenum, it is necessary higher stress for martensitic transformation (thanks to smaller grain size), and the steel can maintain good ductility with the reduced amount of γ_R .

The yield strength of the steels with Nb and Mo presents higher values especially at 600°C and, again, with the combination of both; this is attributed to enhanced precipitation. It has been identified that molybdenum promotes formation of further finer precipitates; at 600°C their average size is about 6 nm, and increasing temperature also their dimensions grow up. This improved precipitation at 600°C is due to the increased density of fine dispersed particles allowed by molybdenum: its relative precipitation “C” curve is that one shifted most on the left, so the available time for precipitation is the longest because, in addition, at 600°C the curve presents the typical “nose”.

The multiple Nb-Mo addition results in the aggregation of (Nb, Mo)(C,N), which have a niobium concentration smaller than the simple Nb(C,N). An APT analysis in figure 4.31 illustrates this condition.

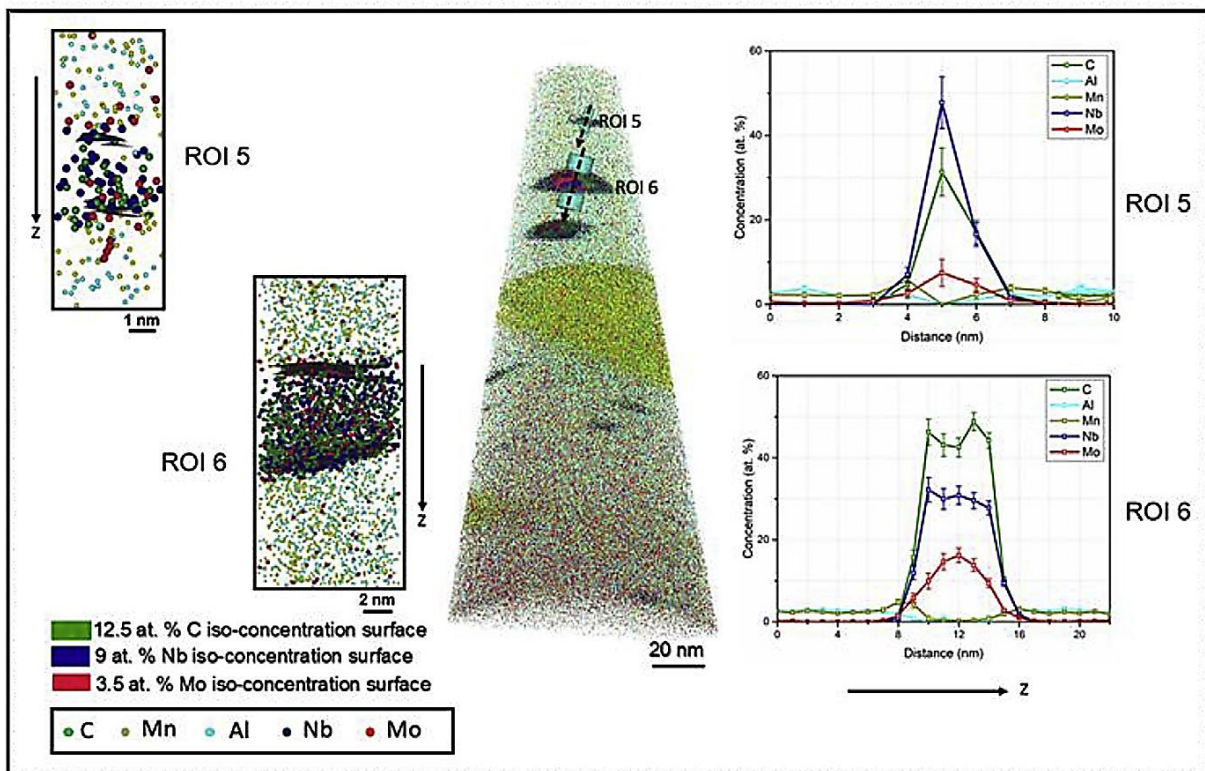


Figure 4.31 APT characterization of two region of interest (ROI) and corresponding concentration distribution

It was found that the replacement of Nb with Mo in the complex (Nb, Mo)(C,N) could reduce the interfacial energy for these precipitates, and this could be a reason for the higher density of fines particles.

Lastly it was performed quantification of the contribution of the strengthening mechanisms to the steel strength; the two most influential are grain refinement and precipitation. The latter is not present in the Mn-steel, and, confirming what has been explained before, its percentage is greater for the steel with both niobium and molybdenum.

4.4 Weldability

[19,25] In the last half century there was a development in technologies and process of welding operations; numerous application requires this technique, and the quality demands of strength and toughness are increasing. Several studies were conducted about welding in pipeline for oil and gas transport, because usually they work in severe condition (high pressure and low temperatures), so they require excellent properties in the welded zone, in order to avoid damages harmful for the environment. However, also the automotive industry needs accurate welding process for structural integrity and passenger safety.

Although niobium doesn't appear in the common carbon equivalent formulae, its effect on steel is helpful for the HAZ, that is the critical zone for defects. Grain refinement performed by niobium is the only mechanism that simultaneously improve strength and toughness, therefore its attendance enhances the steel behaviour in the HAZ. This is the area immediately adjacent to the solidifying metal and it mainly consists of three zones: grain growth, recrystallized and tempered zone. The first is the most important, because here the heat input to the material is higher, and also the probability of formation of a hard phase (like martensite that is brittle) during cooling grows up. As the heat input increases there is the risk of grain coarsening, and niobium tends to control the microstructure; this is beneficial for toughness, as it can be seen in figure 4.32 where are compared two steel with and without niobium: the first has only a slightly drop in the energy absorbed before fracture.

Martensite is the lowest temperature transformation product and hardness is related to its carbon content (another reason to keep the C level low); the higher content the higher hardness but also the lower toughness. So it should be preferred a softer phase like bainite. Nevertheless, if cooling rate decreases (in response to higher heat input that slow down cooling due to higher starting temperature), then there is the possibility that the transformation temperature may not be low enough to develop an appropriate microstructure for adequate strength and toughness. However niobium, when precipitates are dissolved and enter in solution, exerts its favourable effect on hardenability and fine grained bainite can be obtained since Nb ensures that transformation temperature remains low enough.

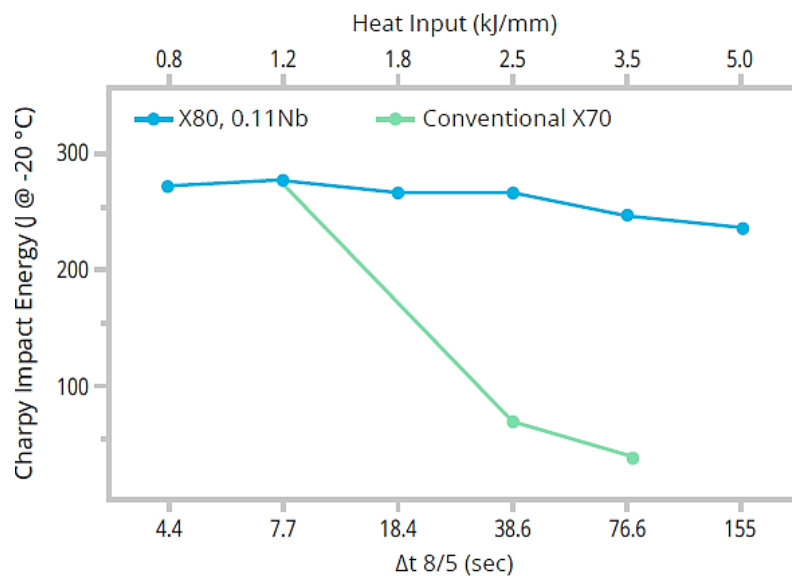


Figure 4.32 Impact energy of welded specimens vs time between 800 and 500°C

In general, the aim of a good toughness in HAZ is reached with a reduction in the ductile to brittle transition temperature and an increase in the upper shelf energy. In addition to microstructural refinement and carbon reduction, improving cleanness of non-metallic inclusion is another salutary aspect.

Some studies observed that acicular ferrite, that is promoted by niobium, is better than polygonal ferrite, because the first one has more grain boundary that serve as trapping for defects or microcracks.

Addition of molybdenum is convenient also in this case: in combination with niobium, it provides a good refinement of acicular ferrite, and it strengthens metal, as in figure 4.33 (a). Here it is understandable that an appropriate co-addition of Nb and Mo results in best properties: Nb lowers the transition temperature, and with Mo (and Mn) higher strength values are achievable.

Niobium precipitation in welding operation (in particular during post-weld heat treatment) could affect the properties shown in figure 4.33 (b): the reduction of area. This is an indicator, since it indicates how much deformation the steel is able to withstand during tensile test; an high value results in better behaviour. The deterioration experienced with niobium could be attributable to precipitates that may obstruct dislocation and reduce the ductility of the matrix. Fast precipitation kinetics accentuates the phenomenon, so the strong effect of molybdenum is probably due to its retarding consequence on precipitation. Also the control of the post welding parameters alleviates problems.

Nevertheless, precipitation could results in other beneficial aspect: the consequently delayed recrystallization leads to more efficient redistribution of carbon due to the shorter diffusion distance between grains. This translates into lower probability of formation of brittle phases like martensite (or at least they are reduced and better distributed). Since molybdenum increases the hardenability of carbon enriched austenite, when niobium is added, toughness is enhanced for the reasons stated above.

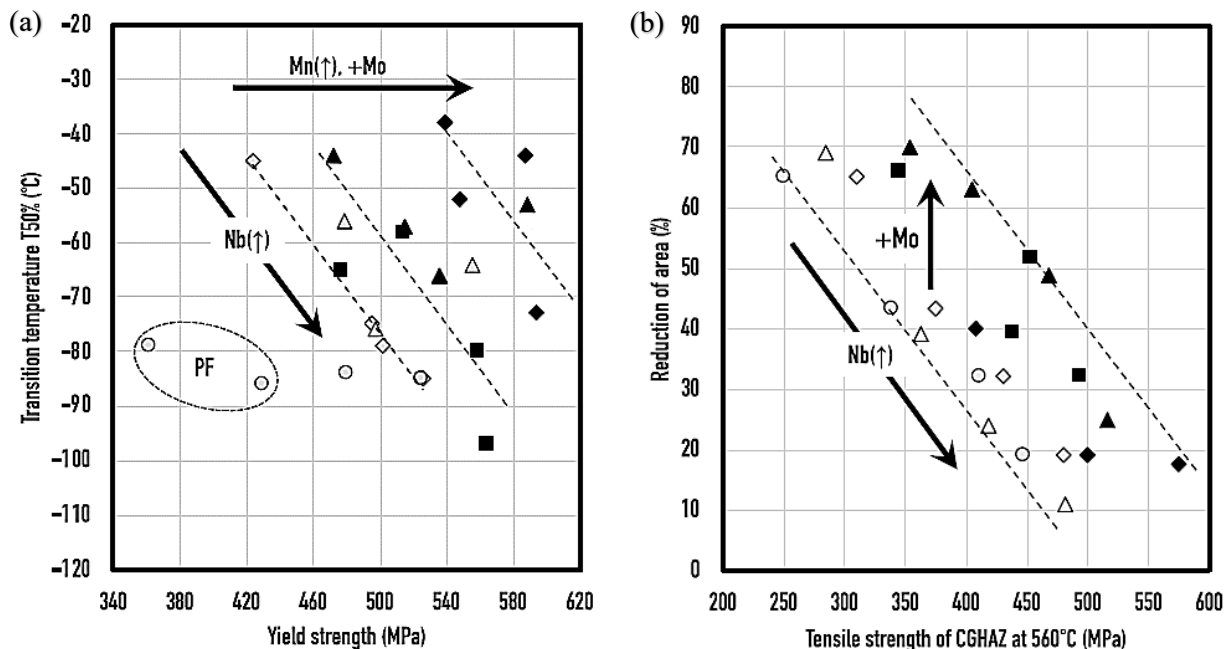


Figure 4.33 Influence of Nb and Mo on (a) toughness and (b) reduction of area in the coarse-grained zone

Keeping adequate mechanical properties is important, since in the heat affected zone the temperature reached are high, so the microstructure and the characteristics previously obtained

could be deleted. With niobium, the metal softening is less pronounced than in the Nb-free one.

Homogeneity in grains size is important for toughness: abnormal grain growth is detrimental and it results in higher ductile to brittle transition temperature. This can also occur with excessive amount of niobium: in the second study mentioned [25], in fact, with the addition of 0,1% Nb there is the formation of inhomogeneous individual large grains. It has been found that addition of smaller quantity was favourable, but when the percentage reaches 0,1% there is an increase in DBTT. Whereby, greater Nb addition doesn't bring automatically advantages, but customized evaluation are necessary.

Titanium is considered an improver for that condition: this element, in fact, forms nitrides stable at high temperatures, which don't dissolve in the heat-zone and, therefore, the prior austenite grain size is smaller compared to Ti-free steels. Transition temperature is decreased and this is experienced in the downward shift of the transition temperature curve in function of the niobium amount (initially decreasing, then increasing at 0,1% Nb).

In addition, also titanium was found as promoter of acicular ferrite, because the fine carbonitrides have a low particles-matrix interfacial energy that facilitate its formation.

Subramanian et al. [51] carried out an EBSD characterization of HAZ region in welding, in a niobium microalloyed steel for linepipe application. Their purpose was to research the target microstructure with an optimum density of crystallographic high angle boundaries, which are considered microcracks arresters.

In the study are presented some trials with different condition (for example single or multi-pass welding, or different concentration of some material), but here it will be reported an illustrative case. The low carbon steel (0,07% C) has 0,08 % Nb and the welding operation is a single pass. Specimens were subjected at different heat inputs (from 8 to 50 kJ/cm) and the micrographs show that the austenite grains size increase with heat input.

The Charpy impact energy for high heat inputs follows the expected trend (decrease at higher values due to coarsen martensitic product) and it presents a maximum at 20 kJ/cm. This is attributable to the wider and uniform distribution of high angle boundaries within a packet, due to large misorientations between different Bain groups in the austenite grains. This condition is represented in figure 4.34, where in the first level it is shown a coloured EBSD map of the Bain groups; the yellow outlines in the second images band symbolize the high angle boundary, which are formed when crystallographic units meets, as it is understandable in the relative figures below. It's clear that the optimum density occurs when the heat input is 20 kJ/cm and the cooling rate is 15 °C/s, which enables a good temperature window for transformation. At high heat inputs one Bain group dominates, which results in poor distribution of high angle boundary: microstructure in this condition is mainly bainitic or acicular ferritic, but the poor distribution drops toughness (graph in figure 4.34). Instead, at lower input, their presence (anyway reduced and with less misorientations than the optimum) comes from island of martensite, since the cooling rate is greater. These high angles associated to martensite product should be avoided, due to the brittle behaviour of the phase, because they cannot arrest cracks propagation; this translates into lower Charpy energy, as it can be seen in the linked graph.

Therefore, the differences in crystallographic structures, related to cooling rates and heat inputs, show their effect on toughness properties; in this case 20 kJ/cm is the best choice.

Niobium addition is beneficial because it lowers the transformation temperature of austenite to other phases through solute drag and precipitation that inhibit nucleation and growth of ferrite. Thus, the best structure is achievable easier because the operative window is larger.

Some micrographs confirm the fact that for heat input of 20 kJ/cm the impact energy is greatest: for this condition the fracture is found to be ductile, while in the other cases, it appears brittle.

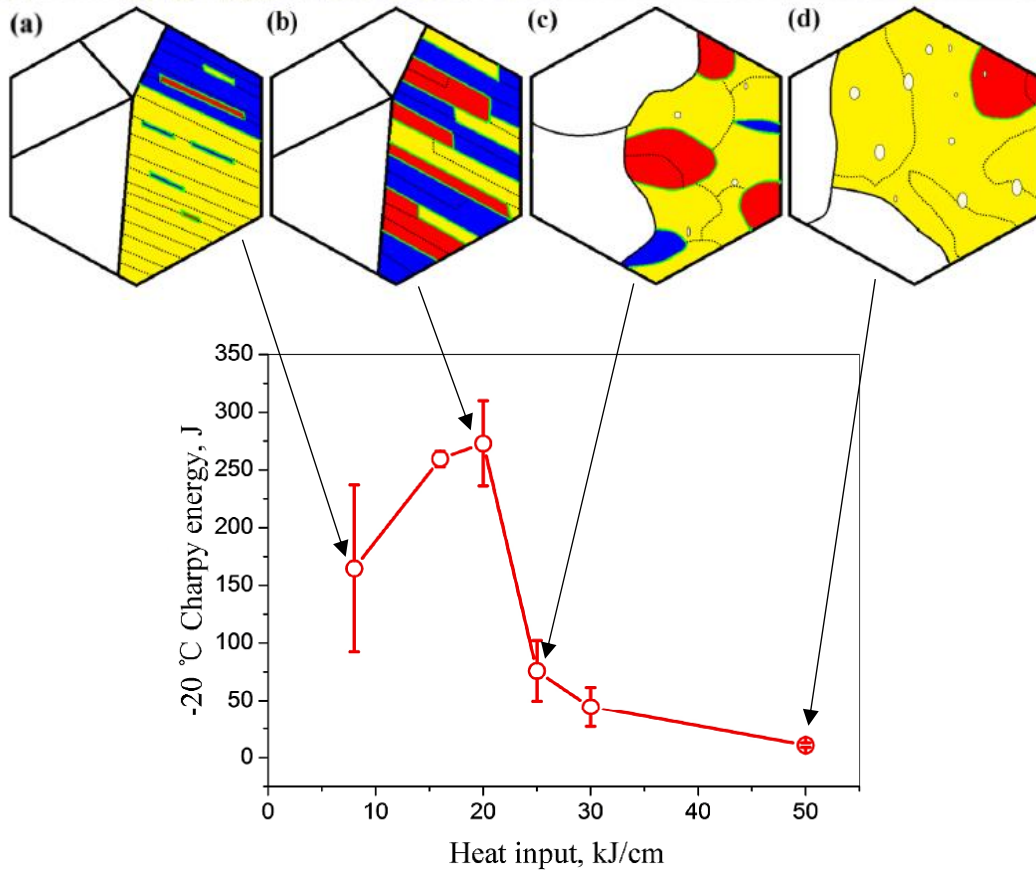
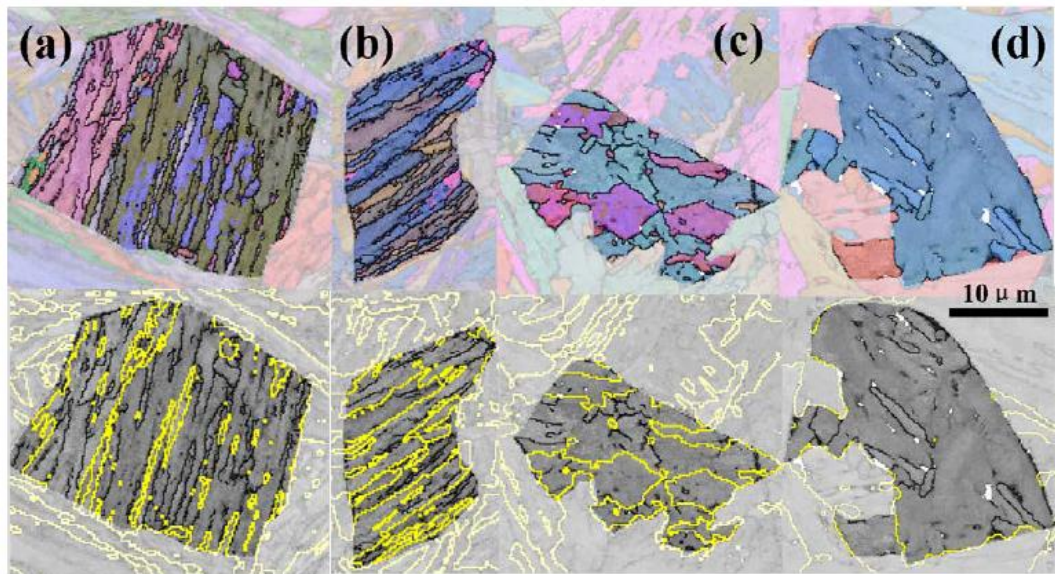


Figure 4.34 EBSD analysis for (a), 8 kJ/cm (b), 20 kJ/cm (c), 25 kJ/cm and (d) 50 kJ/cm

4.5 Hydrogen embrittlement

Hydrogen embrittlement is an issue that affect steels and it has been known for a long time; numerous report were carried out about this topic, and researches still continue today, in order to study adaptation to the new demands (for example the growing attention to replace fossil fuels with hydrogen gas).

This phenomenon is caused by the absorption of hydrogen in the material, which negatively affect its performance and mechanical properties due to reduction in ductility and occurrence of failures (delayed or unpredictable). Improving resistance to the hydrogen induced cracking (HIC) is related to chemical composition, metallurgical operation and microstructure of the steel. Resistance optimization is crucial for successful steel usage.

Some researches show in general terms this mechanism [52,53]: it starts with the penetration of hydrogen atom in the material, and its diffusivity is important, in fact only the diffusible hydrogen is harmful. In general the body-centred-cubic BBC steels have higher H-diffusivity than the face-centred-cubic FCC, so their resistance to embrittlement is lower. If hydrogen can penetrate it follows process of physical, chemical absorption and dissolution (that depends on type of alloys and temperature); additionally it could immigrate through dislocations movement during deformation, when their velocity rate is below a critical value that is related to diffusion coefficient, activation energy, Burgers vector and temperature.

Once inside the metal, hydrogen is expected to accumulate near or into the cavity of a defect, such as those in figure 4.35, including atomic vacancies, dislocation, grain boundaries and inclusion. Therefore, as said in previous chapter, their control is essential for good properties; for example the mentioned MnS or Al₂O₃ particles are potential strong sites for aggregation. When there are pre-existing microcracks on the metal surface, the phenomenon is accelerated because hydrogen has larger micro-zones to diffuse and reach the tip of the fracture or some defects. Then hydrogen cannot escape anymore due to the low diffusivity, and it is accumulated and redistributed in the cavity of the defect as a conglomerate of gas. As visible in figure, the internal pressure grows and if it exceed the material resistance, fracture expands itself.

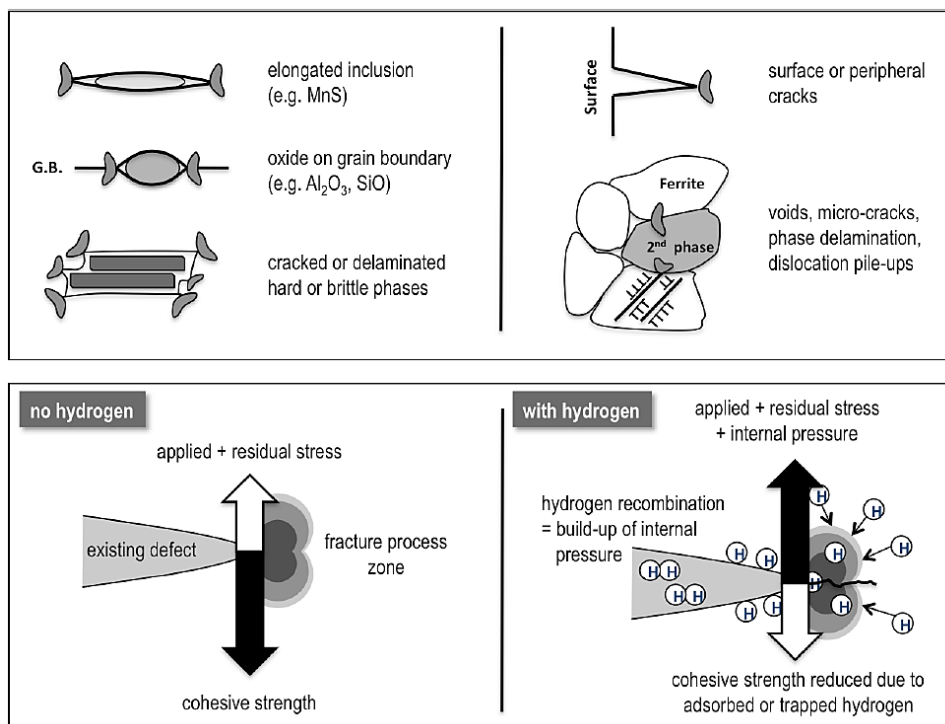


Figure 4.35 Typical defect and embrittlement mechanism

This is the classical pressure theory, but several mechanisms have been exposed to explain the hydrogen embrittlement phenomenon. Firstly it should be said that the damages produced are divided into reversible and irreversible; the firsts are generated by atoms migration and accumulation that lead to delayed fracture; this embrittlement is reversible, in fact, with hydrogen removal treatment damages can be restored. The seconds, instead, derive from atoms combination and formation of hydrogen molecules at defect sites, resulting in induced cracking.

Some of the main mechanisms are:

- HIPT, hydrogen-induced phase transformation: specific metals combine with H to form brittle hydrides, which can arise spontaneously (with high H-concentration) or induced by stress. H-concentration is distributed due to the effect of stress gradient field that could diffuse or accumulate H; in this case, if the concentration reaches a critical level fracture can occur. In high strength steels (such as martensitic) there are residual stress from phase transformation that make more sensitive these steels to H-concentration and embrittlement. In addition, the great level of stress applied to these components could increase the phenomenon. Cracks result along a specific cleavage plane within the hydrides, and addition of this occurrence could take to crack propagation.
- HEDE, hydrogen-enhanced decohesion: hydrogen reduces the cohesive metallic interatomic interactions so that atomic separation is prone to occur under low tensile stress. The higher H-concentration the higher decline in interatomic forces. Fractures in HEDE mechanism take place in an intergranular way, in which hydrogen segregates at grain boundaries and reduces the cohesive interactions between the metal atoms.
- HELP, hydrogen-enhanced localized plasticity mechanism: dislocation proliferation and motion is promoted by hydrogen, and their accumulation causes microvoids premature failures, which occur as dimple fractures. An important aspect is the interaction between the hydrogen atmosphere and dislocations: it reduces their short-range interaction, enabling their easier migration.
- HESIV, hydrogen-enhanced strain-induced vacancies: this mechanism is similar to HELP, with the difference of vacancies instead of dislocations.

In some trials it has been found that HEDE and HELP mechanisms sometimes occur in combination, and the prevalence of one or the other is established by the local H-concentration.

Hydrogen embrittlement can be reduced with some methods: steel cleanliness and avoidance of inclusion, surface treatments in order to minimize microcracks, optimization of the microstructure and introduction of precipitates as traps for hydrogen. Niobium acts in these two latter strategies.

The trapping provided by defects or particles depends on some factors, for example their size, shape, occurrence and status. On the basis of the traps there is the division into reversible and irreversible ones: to distinguish them it's possible to set a threshold value for activation binding energy of about 60 kJ/mol. Grain boundaries, dislocation and coherent precipitates compose the first class, while the second one contains, for example, inclusions, voids and incoherent precipitates. Irreversible traps are stronger than the reversible, but these ones can also play an important role since they may affect the kinetics of hydrogen, reducing the necessary time to reach a critical local concentration. In order to give a numerical comparison for the reversible traps, niobium carbides have an activation energy of more than 40 kJ/mol, while the other defects like dislocations and grain boundaries have an average value of about 22 kJ/mol. In addition it could be said that for coherent precipitates, the trapping position is expected to be at the stress field in the matrix surrounding the particles, while, for the incoherent precipitates, it is located at the matrix-particle interface.

Concerning the irreversible traps, they are more dangerous, because their binding energy is higher, so hydrogen can't leave anymore. Inclusions like Al_2O_3 and MnS have and higher

energy (respectively 72 and 79 kJ/mol) compared to incoherent NbC (average of 65 kJ/mol) and this is detrimental: niobium carbide, in fact, are finer and dispersed in the matrix, so they are ideal candidate for improve resistance, since they avoid agglomeration zone of hydrogen. It is reported that NbC are stronger than the carbides arising from the other two microalloying elements Ti and V.

On the contrary, inclusions could promote accumulation, because they are larger, more elongated and dispersed less uniformly; so they attract more hydrogen facilitating cracks nucleation and propagation.

[54]It has been discovered that niobium has other beneficial consequences: its presence promotes the formation of low angle grain boundaries (LAGB) at the expense of the high angle boundaries (HAGB). This has been found positive for the resistance to embrittlement in the steel with niobium; it is believed that this enhancement results from lower density of HAGB, which have high lattice distortion and high stored energy that provide an easier path to crack nucleation and propagation.

In addition, it has been observed that in the coincidence site lattice (CLS) boundary maps, niobium decreases the amount of $\Sigma 3$ boundary. Similarly to the HAGB, they reduce the hydrogen embrittlement resistance of the steel, and formation of NbC reduces their proportion. Higher boundaries, such as $\Sigma 5$, $\Sigma 11$ and $\Sigma 13$ have low angle misorientation and low energy, so are more resistant to intergranular cracking. The kernel average misorientation (KAM) analysis, which belongs to EBSD, is accompanied to the reconstructed CLS map, because it gives information about misorientation angles (beside dislocation density and stress status).

The following figure 4.36 resume graphically the advantage of niobium addition.

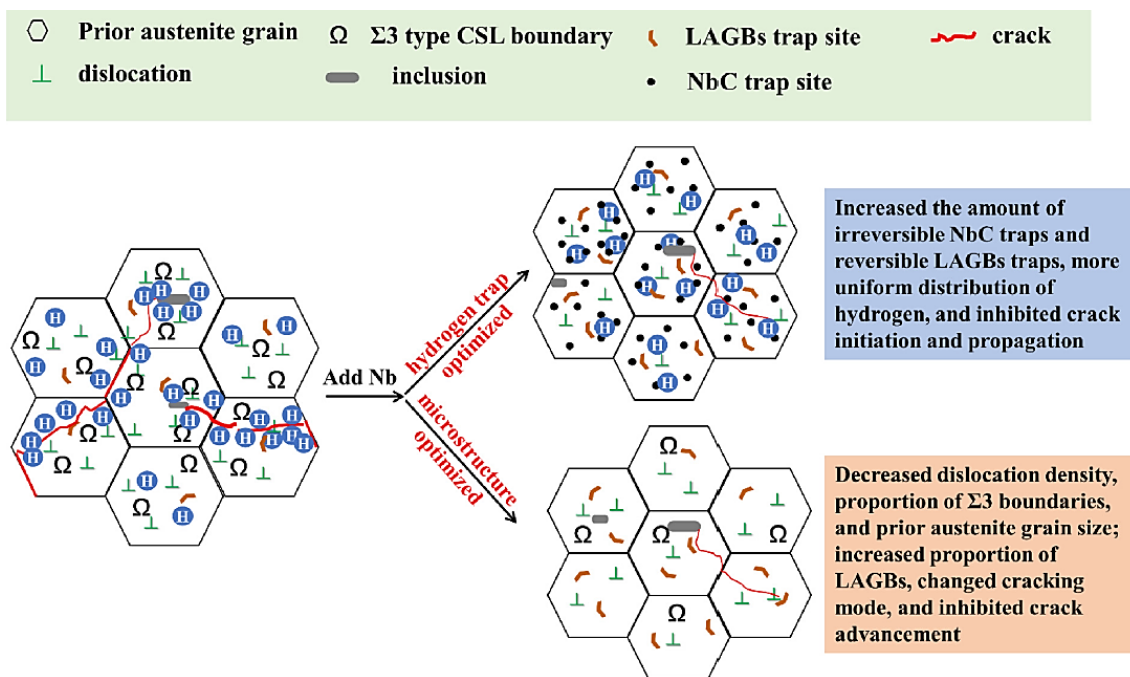


Figure 4.36 Nb effect on HE: better uniformity it's clearly visible, as well as the difficulty of crack formation

Occurrence of hydrogen embrittlement is more probable in the high strength steel, due to their great strength that leads also to less resistance to embrittlement. Therefore numerous studies were conducted on the HE effect on these steels and the strategies to reduce it. One of these, which illustrate distinctly the Nb benefits, was carried out by Zhang et al. [54], who investigated the effect of spherical dispersed NbC on hydrogen embrittlement in a martensitic steel.

The research involve three trials with different amount of niobium, in order to appreciate its contribute; the basic steel has the following composition: 0,235%C - 1,20% Mn - 0,31% Si - 0,166% Cr - 0,041% Al and other small fractions. Trials are divided into N1, N2 and N3 based in the percentage of niobium: the first is Nb-free, while the others have respectively 0,021% and 0,055%. The three plates were subjected to the same treatment that consists in an ordinary process, with soaking at 1230°C for 1 hour, hot rolling and reheating at 930°C for 3 minutes followed by water quench to fix the steel condition. Hydrogen was introduced by an electrochemically charging with a solution of H₂SO₄ and thiourea at 0,5 mA/cm for 1 hour. With this operation it's possible to determinate the hydrogen diffusivity D_{AP} and diffusion hydrogen concentration C_0 . The permeation curves reveal that larger amount of NbC leads to smaller D_{AP} and larger C_0 , that means more difficulty in diffusivity (and also in aggregation along defects site), and higher concentration before crack, because H is more distributed.

The steel exhibit a lath martensite microstructure and in the uncharged condition the tensile strength is more than 1600 MPa; the effect of niobium is also visible here, through the well-known strengthening mechanisms. In N2 and N3 steels numerous niobium carbides are observed (obviously their volume fraction increase with Nb); they have a spherical shape and size ranging between 4 and 30 nm, with an average diameter of 10 nm.

With hydrogen charging, mechanical properties decrease, but the most noteworthy reduction regards elongation: due to the embrittlement, in fact, the value drops by 8,4% to 2,3% of the Nb-free specimen. Niobium is very beneficial in elongation recovery: for N2 the value before crack is 3,8% and for N3 it is 5,7%. So the steel could be subjected at more than double deformation compared to N1. Consequently also the tensile stress is increased with larger amount of niobium.

Fractography characterization shows that for the specimens without hydrogen, the fracture appears as ductile with dimple morphology. Behaviour changes for charged condition, that is represented in figure 4.37.

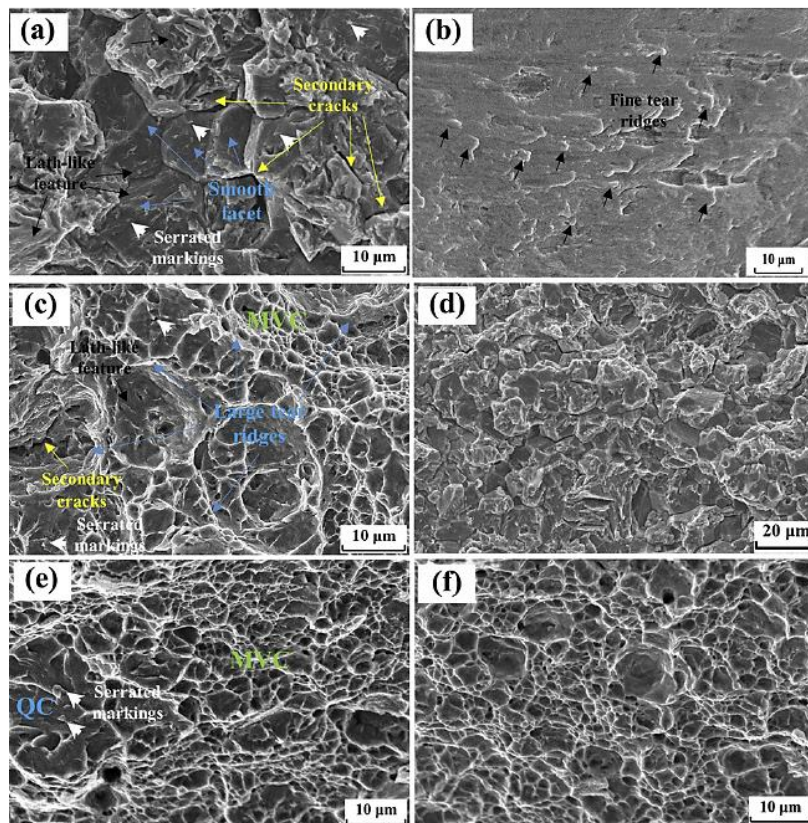


Figure 4.37 Micrographs for martensitic steel with 0,24% C after charging with (a)(b) 0% ,(c)(d) 0,02% and (e)(f) 0,05% Nb

N1 steel exhibit the worst condition: fracture is mainly brittle, with intergranular (a) and quasi-cleavage (b) zones; secondary cracks promote propagation along the grain boundaries. Niobium addition encourage growth of ductile fracture zones: intergranular and quasi-cleavage areas (d) are reduced and within them, microstructure is refined, in fact the damage line are shorter and distributed. Nevertheless, large part of the fracture is constituted by ductile microvoids (c) and some large tearing ridges appeared, which means that region was subjected to a more significant plastic deformation, i.e. more elongation before fracture (mainly ductile).

The best status is achieved by N3 steel, where the intergranular and quasi-cleavage zones are further prevented, and the ductile microvoids is the primary mode (e, f).

The coexistence of intergranular and quasi-cleavage areas may indicate a possible combination of HEDE and HELP mechanisms; the latter is proven by KAM analysis (figure 4.38 a), that shows a high dislocation density in correspondence of the crack (so its propagation is assisted by dislocation multiplication). HEDE mechanism, instead, is suggested by the presence of branch crack along grain boundaries (figure 4.38 b), which derives from local hydrogen concentration that reduces cohesive energy.

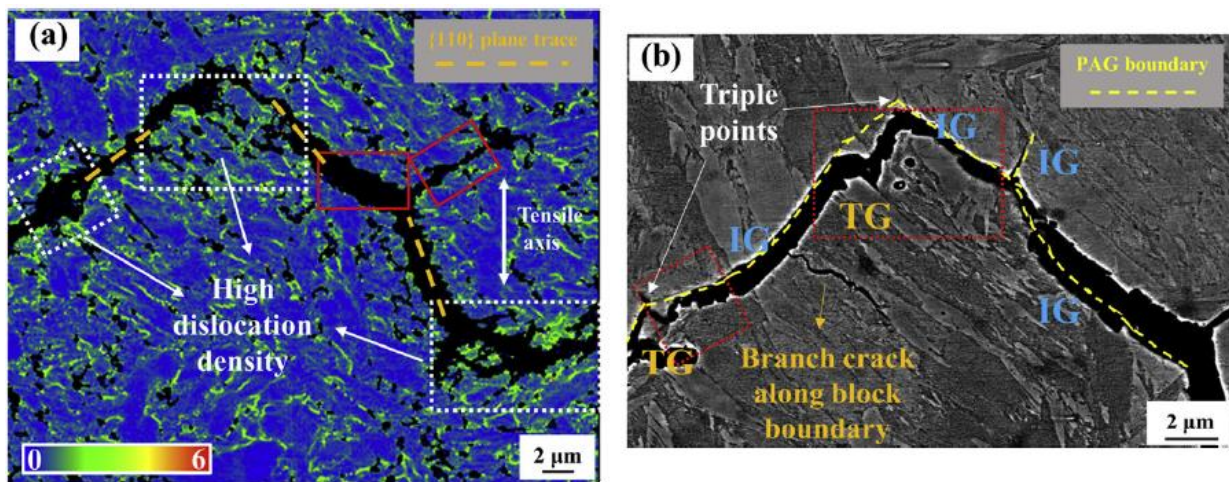


Figure 4.38 (a) KAM map enlargement on a fracture and (b) examples of branch cracks. The steel is N1

Investigation on the grain boundary distribution shows that with addition of niobium increases by about 10% the fraction of LAGB ($< 5^\circ$), which are considered beneficial for hydrogen embrittlement, as said before. Consequently, portion of HAGB decreases. Microstructural refinement thanks to niobium results in larger total surface area of the grain boundaries, so the absolute value of low angles is higher and contribute more to resistance.

Lastly it was evaluated the reconstruction CLS boundary maps: the fraction of $\Sigma 3$ boundaries is the widest for all the specimens, but those with niobium exhibit lower proportion (almost 40% less); this condition help the material resistance to embrittlement.

Summarizing, niobium precipitates increase the HE resistance through several ways: they act as hydrogen traps that homogenize its distribution (hindering HEDE), they reduce the $\Sigma 3$ boundaries and the average misorientation angle in KAM analysis, their presence increases the LAGB fraction, and they directly pin hydrogen-dislocation atmosphere obstructing their movement and multiplication (inhibiting HELP).

Several studies were also carried out to research the effect of another element in addition to niobium. Among these, it will be reported in this section two works on combination with molybdenum and vanadium.

The first was performed by Jo et al. [55] on the ultra-high-strength steel “32MnB5”, that is used in the reinforcing structural parts. The base steel is chemically composed by: 0,32%C - 1,20% Mn - 0,25% Si - 0,12% Cr - 0,04% Al - 0,03% Ti. For the first variation it was added 0,05% Nb and for the second another further addition of 0,2% Mo. Respectively these two samples will be called N and NM.

Specimens followed a typical hot rolling scheduling (even with simulation of coiling condition at 550° for 1 hour); then they were cold rolled, annealed at 900°C for 6 minutes, and directly quenched. Also in this case the specimens were electrochemically charged, with a solution of NaOH.

Grain refinement by Nb and Nb + Mo is clearly evident from the micrographs: the prior austenite grain of the base steel is about 9 μm, while for the N and NM steels is 4,65 μm and 4,22 μm. Precipitates were found in all trials: in the base sample, in fact, Ti presence enables precipitation of coarsen cuboidal titanium carbo-nitrides. For the other cases, fine spherical niobium carbides and (niobium + molybdenum) complex carbide were found in N and NM trials. Statistical analysis reveals that the particles size range is slightly smaller for the (Nb + Mo) addition. For completeness it should be reported that the complex NbMo precipitates are detected as Nb-rich core with Mo nucleation on the surface; they also contain some amount of chromium, boron and titanium.

With regard to mechanical characteristics, it’s obvious that increasing the hydrogen-charging, their values drop, but the important aspect is the elongation; if the hydrogen amount is increased, then elongation at which fracture occurs is widely reduced. The remarkable effect of Nb and (Nb + Mo) is noticeable here: the elongation loss, in fact, is reduced with these two elements. It is clearly visible in the graph in figure 4.39; Nb has the largest influence, and Mo helps its effect.

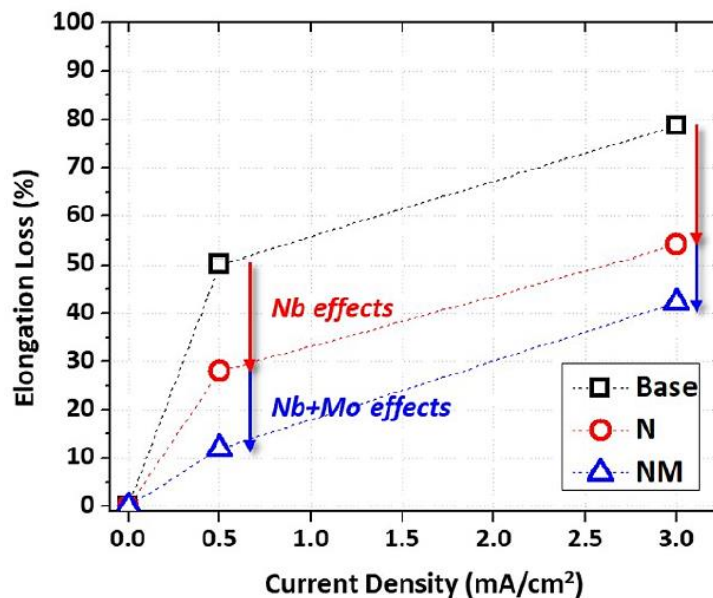


Figure 4.39 Advantages on elongation loss from the value of the uncharged specimens

The diffusion time of hydrogen is higher in N and NM steels due to the larger number of precipitates that act as H-traps (mechanism of coherent and incoherent particles trapping is the same already mentioned). As in the previous study, grain refinement gives further contribute to low diffusivity, since the diffusible hydrogen per unit of grain boundary area is decreased and more distributed; in fact hydrogen diffusivity it’s almost 35% less for N steel and 50% for NM, compared to the base steel.

Examinations of the fracture surface denote that for the Nb-free samples the damage occurs within a great portion in an intergranular and cleavage way, and in the remaining part, it is composed of ductile dimples along with a few quasi-cleavage facets. In addition, from an aesthetical point of view, dark-gray and light-gray distinguish respectively the two typologies.

In N and NM trials the light-gray area, that represent the ductile fracture, gets more and more space; in particular in steel with both niobium and molybdenum, the intergranular fracture is almost totally disappeared (in steel with only niobium, anyway, it represents a small portion of 7,5% located in the central region), and in it's place there are some quasi-cleavage facets and dimples. These are deeper that in the ductile area. The colouring of areas remains light-gray for the ductile zone, while the "brittle" zone is marked by dark-gray, which is, however, more clear than the authentic brittle area of the Nb-free specimen. This means that brittle behaviour is mitigated compared to the other conditions.

The effects of vanadium as the element of co-addition with niobium were investigated by another group of researchers [56]. The steel in question is a spring steel, and it consists of 0,58%C - 0,76% Mn - 1,6% Si - 0,34% Cr - 0,01% P - 0,05% S. The Nb-steel has 0,022% Nb and the Nb-V steel has also 0,12% V. Materials used for the experiments were subjected to process of forging, hot rolling normalizing and quenching. Hydrogen was charged again with electrolytic solution of NaOH. As expected, the diffusion coefficient was smaller for the microalloyed steels than that in the conventional one. Niobium has the greatest effect and vanadium doesn't bring heavy contributions because its precipitates are larger and, so, they are less efficient H-traps.

A severe Ultimate strength reduction (and the connected elongation) translates into a brittle fracture: steel, in fact, is not able to provide an adequate plastic deformation. The configuration with both niobium and vanadium supplies smaller percentage of strength reduction, and this is beneficial to fracture resistance.

In figure 4.40 there are a presentation of how the fracture surfaces look like: again, in the base steel (b) it manifests itself as an intergranular way along the grain boundaries and cleavage. In the microalloyed conditions it change into transgranular and quasi-cleavage.

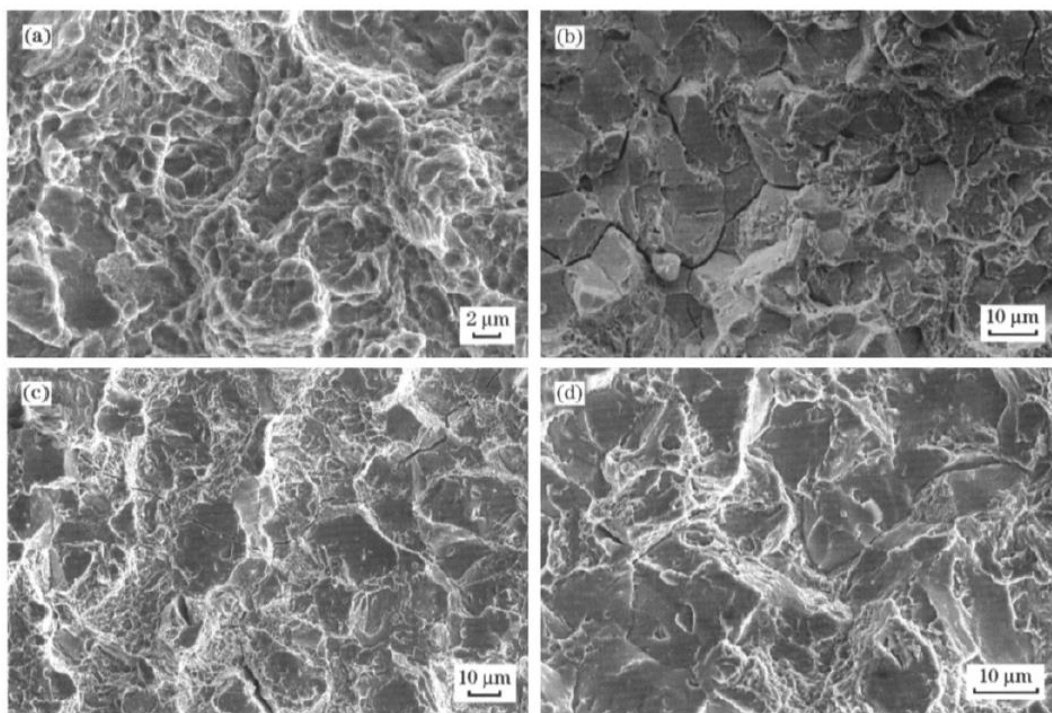


Figure 4.40 Micrographs of condition: (a) uncharged, (b) charged, (c) with Nb and (d) with Nb and V

4.6 Corrosion resistance

In order to obtain a durable lifecycle for a steel product, resistance to atmospheric agents should be adequate; several applications, including automotive construction, require this property. It depends on some factors, such as chemical composition, second phase nature and non-metallic inclusions. In particular this latter aspect is important, and niobium (or other microalloying elements) through precipitation could improve the steel condition.

An investigation [57] was conducted to see the effect of combined inclusions and precipitates on the initiation and propagation of pits. Pitting, in fact, occurs preferentially at material defects. The specimen was a weathering steel with the following composition: 0,06%C - 0,64% Mn - 0,2% Si - 0,88% Cr - 0,017% P - 0,28% Cu - 0,2% Ni - 0,079% Sb - 0,029% Si - 0,025% Nb - 0,033% Ti.

Precipitates due to their heterogeneous nature could represent sites for corrosion, but this happens especially with large particles, since nanoscale ones has been evaluated negligible in pitting corrosion. The present work, nevertheless, focuses on the effect of interaction between precipitates and inclusions; in the considered steel, the first was mainly (Ti, Nb)N, and the second were alumina and other oxides (although also MnS is widely recognised ad initiation site). Figure 4.41 shows some example of precipitate-inclusion interaction. From the EDS analysis reported in (b), it's possible to see that inclusion are composed of CaS and MgO; it should be said that their dimension are smaller than the usual inclusions encountered in steels and, on the other hand, precipitates are larger than usual. However they are reported here because they are the only ones to have effect on corrosion and could embed inclusions (as said, the nanometrics don't have relevant effect).

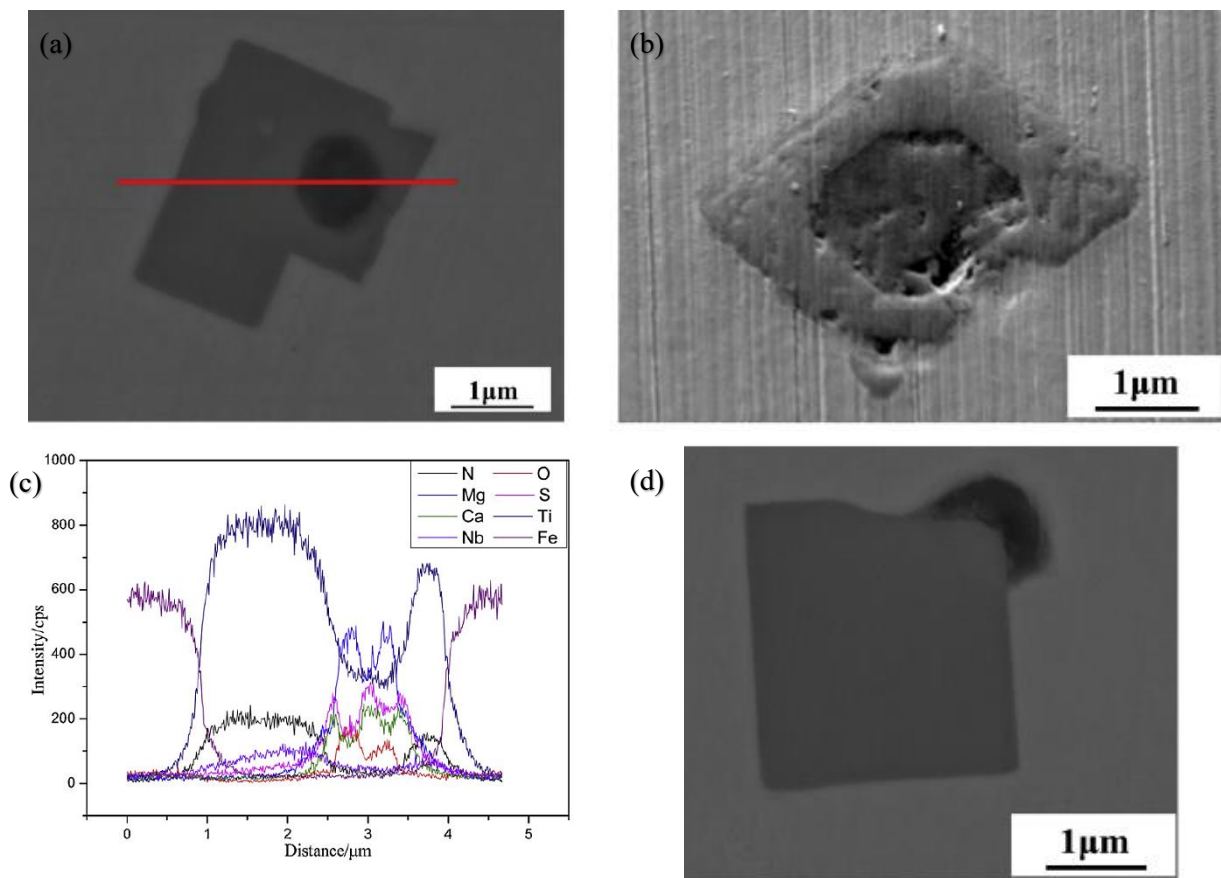


Figure 4.41 (a) (Ti,Nb)N cuboidal precipitate and (c) relative EDS map; examples of inclusion encapsulated in the precipitate (b) and outside of it (d)

Electrochemical analysis were executed to detect the electrical properties in the surroundings of precipitates and inclusions. These analyses revealed that precipitates have the highest Volta potential and inclusions have the lowest one, in comparison to the matrix. Therefore, inclusions dissolve preferentially and start pitting process due to electrochemical corrosion occurrence of anodic and cathodic reaction (anode is the element with lower potential). Relevant importance has the position of the inclusion: as visible in figure 4.42, pitting behaviour is affected by this.

In the experiment it was used a solution of NaHSO_3 , in order to accelerate the corrosion process and see the effect in short times; obviously as the immersion period was extended, pits and derived products increased.

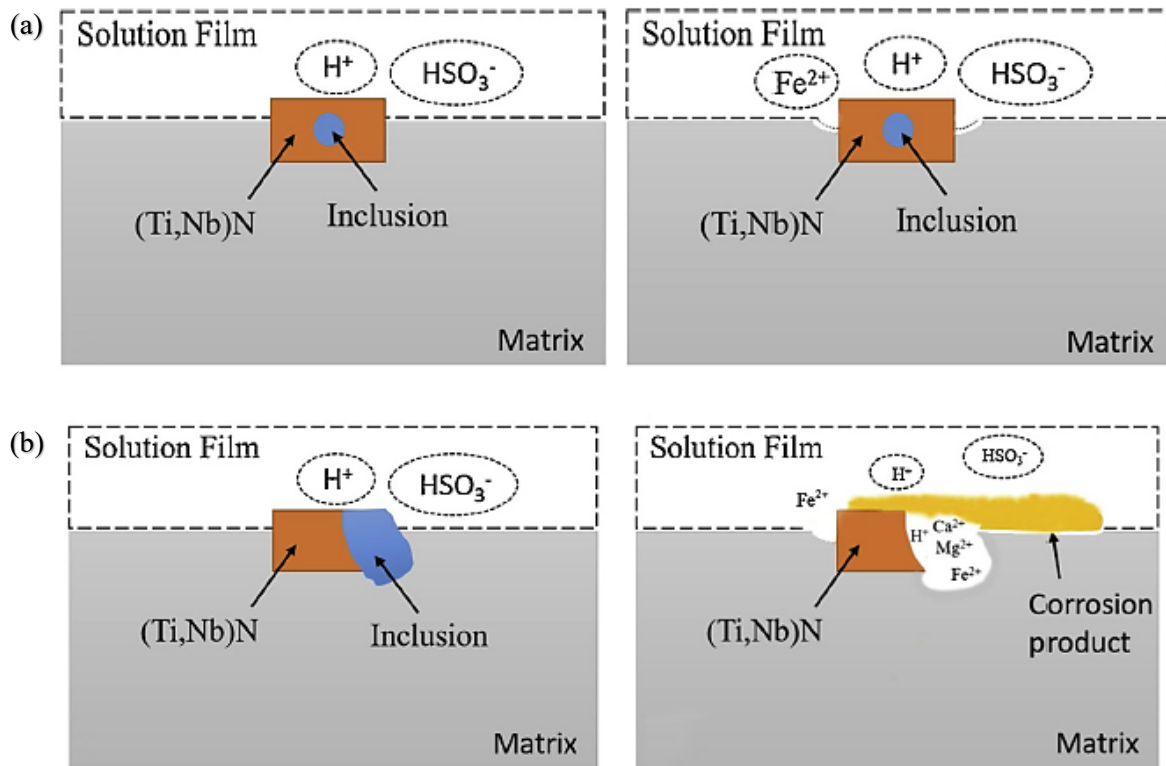


Figure 4.42 (a) Inclusion embedded and (b) in contact with the matrix

It's easily perceivable that the better condition occurs when inclusion is completely encapsulated by the precipitate phase (a). In this situation an anodic (matrix) dissolution takes place, but its depth is reduced because the process is very slow, and, in addition, no corrosion product were observed. Instead, when the inclusion is in direct contact with the matrix, it dissolves in the solution forming a deep pit. The hydrolysis of the metal ions in the pit acidifies it and so, the surrounding matrix is in a state of dissolution. The resulting corroded zone is bigger than the previous condition.

Dissolution of the matrix could be intensified by the reduction reaction between the matrix and the precipitates above mentioned; this, in particular, is more pronounced when the particle size is remarkable, since the contact area is larger. Therefore, control of composition and inclusions in the steel is important here too.

Nevertheless, even the microstructure has effects on the corrosion resistance, as studied by Rodionova et al. [58] in cold-rolled microalloyed steels for automotive building. These are low carbon (0,06% - 0,07%) steels of two strength class of 340 and 420. Niobium content is 0,046% for the first typology and 0,081% for the second (higher Nb percentage strengthen the material for the established mechanisms).

Specimens were subjected to a continuous annealing process, and to an accelerated method to evaluate the atmospheric corrosion resistance; it consist in immersion cycles (10 minutes) in

a NaCl solution followed by air drying (50 minutes). 30 cycles are considered effective for reliable results. Samples followed hot rolling, cold rolling and annealing, and some variations has been made with regard to the process parameters, in order to evaluate their influences. Microstructures are various: polygonal ferrite and block ferrite (elongated and having cementite particles nucleated on small inclusions), in which there are nanosize niobium carbide, for class 340; the same polygonal and block ferrite compose the 420 class, but it's grain size is smaller due to more incomplete recrystallization. In addition it were observed regions of degenerated pearlite, and the niobium precipitates were both nanosize (2-10 nm) and sub-micron (40-80 nm) probably due to greater Nb amount.

Corrosion resistance has been observed to increase with a reduction in grain size; this is attributed to a stable passive film, which develop in metal with grain refined (high-angle boundaries and high dislocation density favour the formation of the surface film). The effect of corrosion rate is tangible: it is measured as weight increase (g/m^2) after 30 immersion cycles, and its value drops from about 9 to 2 respectively for the largest and the smallest grain dimensions. It is possible to express this quantity also per unit of time ($\text{g/m}^2\cdot\text{h}$), which corresponds to corrosion rate (mm/year); obviously, even for this expression the corrosion reduction is around 77%. Incompleteness of recrystallization for the higher-strength class encourage passivation and increase in dislocation number, which is beneficial.

Degenerate pearlite is considered a positive factor for resistance: it has greater dislocation density and its structure is more uniform than that with lamellar pearlite; this translates into shorter ferrite-pearlite grain boundaries that are galvanic cells for corrosion.

It has been found a little negative contribution regarding precipitates density: for larger content, in fact, there is a small deterioration in resistance, which may be connected to the mechanism described in the previous example because, as seen, a little corrosion at precipitates-matrix interface could take place. Nevertheless, this effect is limited (a few percentage units) and the benefits of strengthening, grain refinement and inclusions embedding overcome disadvantages.

Another section in automotive field where is important an adequate corrosion resistance is the exhaust system; since the condition in which these components work are complex, materials have stringent requirement to satisfy. Besides the heat resistance due to the high temperature work (higher than 600°C), steels must have an excellent corrosion resistance, for example in the muffler, where the condensate of exhaust gas could cause pitting.

Li et al. [59] studied the effect of niobium on the performance of a stainless steel for exhaust systems. The steel investigated is a 409 ferritic stainless steel, which is prominent in the modern usage thanks to their properties of low thermal expansion coefficient and high thermal conductivity (in addition to their good performance in relation to the cost-effectiveness). In the investigation three variants have been taken into consideration, in order to see the effect of only Ti or Ti-Nb addition; the specimens composition is reported in table 5. Niobium amount in this case is widely greater than in microalloyed steels examined until now.

Steel grade	C	Si	Mn	P	S	Cr	Ti	Nb	N
409Ti	0.011	0.38	0.19	0.013	0.002	11.17	0.21	/	0.01
409Ti-0.15%Nb	0.005	0.33	0.23	0.012	0.001	11.15	0.11	0.15	0.01
409Ti-0.30%Nb	0.01	0.32	0.21	0.015	0.001	11.24	0.21	0.30	0.01

Table 5 Chemical composition of the steels

The corrosion condition were simulated through a cycle of 6 days in which samples are maintained in a mixture of acids at 80°C until the solution is evaporated (subsequently it is refilled); then, the last day, they dried at 250°C. After this process it was evaluated the resulting corrosion depth, through the empirical formula: $d = (M_1 - M_2)/2 \cdot S \cdot d$, where M_1 and M_2 are the weights before and after cycles, S is the surface and d is the density.

Results are displayed in the diagram in figure 4.43: the measures were made for 3, 4 and 5 cycles that correspond to the points highlighted, but it's possible to extend over time the curve, since the linearity of the trend and the assumption of a constant corrosion rate. The values in the graph should be considered in a qualitative way, because they are “disproportionate” due to the severe simulation of corrosion condition. However, contribute on resistance brought by niobium is quantified in about 40% more.

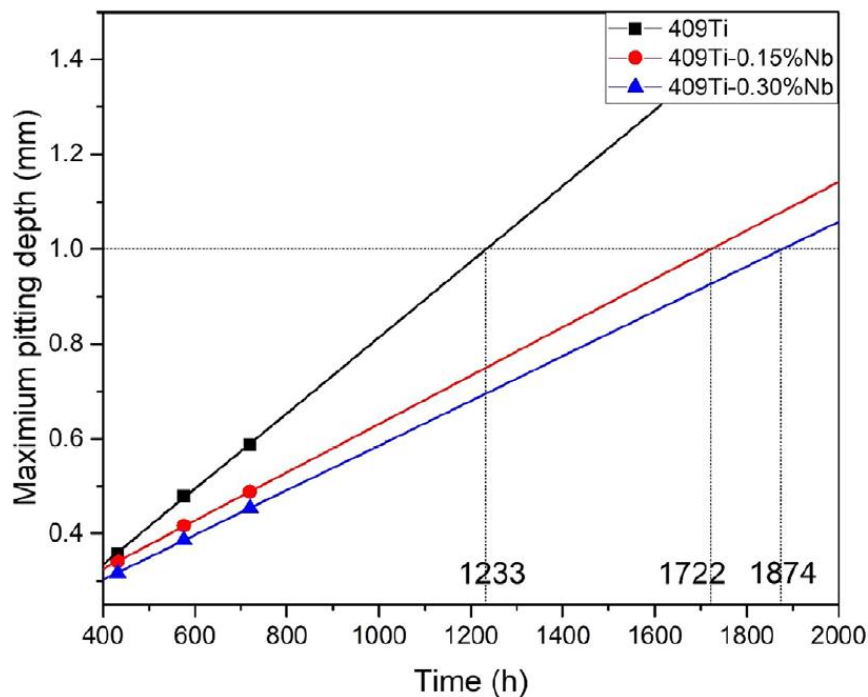


Figure 4.43 Time prediction for pits depth

Specimens with both Ti and Nb show better resistance, and the lifetime of the component can be significantly increased: 409 Ti-Nb, in fact, owns about 15% higher fatigue limit in comparison to 409 Ti (and further improvement is obtained with higher niobium amount). Fatigue cracks could be triggered by microvoids from corrosion, thus its resistance is attributed to the control of inclusions (which in this case are complex and irregular-shaped (Nb,Ti)(C,N) and other elements) by niobium: their shape is more regular (so there are less concentration of stress) and their size is heavily reduced. This is beneficial since the contact zone between inclusion and matrix, as seen previously, is a nucleation zone for pitting. Additionally, for large particles, the passive film on the surface is more easily susceptible of discontinuities, which lead to more probability of corrosion.

Beside the control of shape and size of precipitates, niobium has another great function for corrosion resistance: reaction with carbon (in order to form NbC) preventing the formation of chromium carbides ($Cr_{23}C_6$). This steel typology, in fact, has a high fraction of chromium, that is the source of oxidation resistance, but on the other hand represents also the possibility of sensitization. This process is related to the combination at high temperature of Cr with the free C (which is not completely removable), that leads to formation of chromium carbide and depletion of chromium in certain areas as it's represented in figure 4.44. Therefore, these zones with depleted Cr are susceptible to corrosion attack, since near the carbides the chromium

content may be too low. In addition, if the carbides form a continuous network on the grain boundary (visible in the figure), then there is the risk of failure due to a separation between boundaries. Niobium presence enables a “capture” of the free carbon that is no longer available for combination with chromium that can play its role.

Sensitization occurs also in welding of stainless steels, so niobium is useful even in this case, by ensuring prevention to chromium oxidation and continuous corrosion resistance. This is useful in the cycles of heating and cooling of the exhaust system: repeated cycles could cause cracks due to thermal expansion, and cracking of the outer oxide layer of the part may cause corrosion. If grain boundaries are separated due to the carbide networks, then the process is accentuated. Niobium enhances adherence and protect steel from oxidation [60].

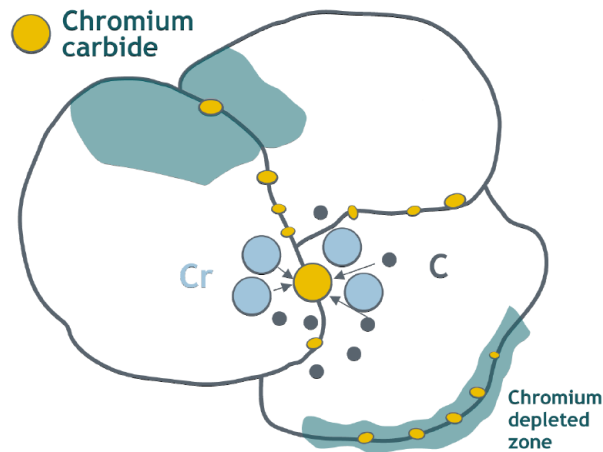


Figure 4.44 Attraction of C by Cr and consequent depletion in some areas

Going back to the study on the 409 stainless steel, tensile tests was conducted at high temperature (to which it could be subjected an exhaust system); it revealed that strength decreases with increase in temperature, but the niobium steels exhibit higher values. This is related to the classical strengthening effects of niobium, especially precipitation and also solid solution since a relevant Nb fraction has remained. Microstructure stabilization is helpful in deformation resistance at high temperature (creep resistance), which allows an extended lifetime.

5. NIOBIUM IN AUTOMOTIVE STEELS

The progress in car development along the last decades opened up the possibility of utilization of a broad variety of high strength steels, in replacement of “simple” mild steels. This improvement enables to exploit the different features of the various steel types according to the function that they have to perform. In the contemporary vehicles mild steels represent the minority, in fact the largest range includes steels from nearly zero to up 0,35% C for the strongest ones; this range mainly represents metals shown in the second chapter.

In this section, therefore, are presented the common typologies used in automotive, including the effect of niobium in them. Professor H. Mohrbacher and other authors have produced many articles about these themes; some of them are general [61-64] and their contents will be integrated in the following pages, along the various section. Others, instead, are focused on specific steel, so they will be mentioned whenever a dedicated category will be treated.

5.1 Dual phase

Dual phase (DP) are a typology of multi-phase steels, so named due to the simultaneously presence of more than one phase. DP are characterized by a soft phase in which is dispersed a harder one. Typically the first is ferrite and the second is martensite, but the latter can be eventually bainite (in any case the softer pearlite it's avoided). Coexistence of two phases allows to have excellent combination of strength and elongation: this is the reason for their significant use in car body (the fraction can reaches the order of 20% of the weight).

DP cover a large portion of the strength-elongation steel diagram, having higher strength values than the HSLA, almost as those of the martensitic, but maintaining good elongation (they have high n -value and consequently show fine behaviour to drawing). Their denominations follow the strength values, and the typical range extends between 450 and 950 MPa, but higher classes are achievable.

Mechanical properties of dual phase depend on the volume fraction of martensite: basically its larger amount brings more strength (and less ductility). Nevertheless this is not the only factor, in fact distribution and interaction between hard and soft phase has a preeminent role: especially aggregation and coarsening of martensite islands could leads to issues of local embrittlement. Other microstructural parameters, such as size or hardness ratio, influence the deformation behaviour, without neglecting thermomechanical treatment to which they are subjected.

These steels are produced by a process of hot rolling, cold rolling and thermal treatment that consists of intercritical annealing and quench. Consideration made in the following part are generally referred to the condition at the end of the thermal process.

Terada et al. [65] studied two types of dual phase steels fabricated by different heat treatment in order to understand the mechanical interaction between ferrite and martensite. A correlation image technique helps the measurement of the local deformation.

The specimen has this chemical composition: 0,087%C - 1,77% Mn - 0,79% Si - 0,02% Cr - 0,009% P - 0,01% Mo - 0,003% N. Two schedules were performed: in the first, trial was intercritically annealed (760°C - 840°C) for 30 minutes and water quenched to fabricate martensite, while in the second, steel was austenitized at 950°C for 30 minutes, intercritically annealed (720°C - 820°C for 30 minutes) and then water quenched.

Microstructure obtained in the first case consists of a network structure of martensite dispersed in the ferrite matrix; for the other schedule, the hard phase is isolated. In figure 5.1 it's possible to observe these two condition, in which the annealing temperature was 760°C for (a) and 740°C for (b). Ferrite grains are black and the martensite ones are white.

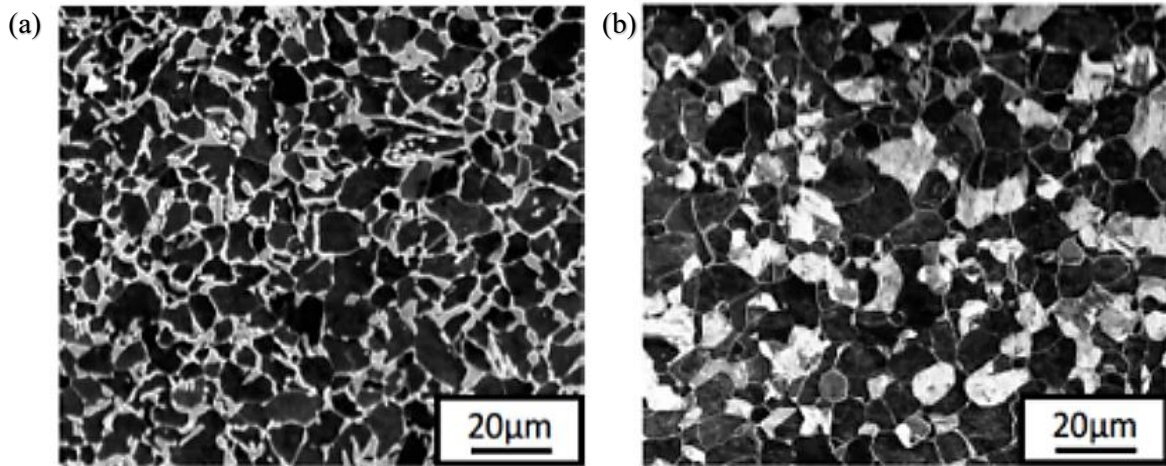


Figure 5.1 SEM microstructure for the first schedule (a) and for the second (b)

The difference is clearly visible: fraction of martensite is the same (28%) but its distribution differs. Grain size is fairly larger for the austenitizing + annealing condition (in particular the martensite grains due their aggregation) and with higher temperatures, martensite ones increased widely (from 28% to 64%) at the expense of ferrite; this is due to the rise in volume of the hard phase.

Microstructural status affects the results of the tensile test: the networked martensite shows better strength-ductility balance than the isolated martensite. This last one, in fact, in a tensile strength vs elongation graph, occupies a zone of slightly higher strength (it reaches about 1200 MPa against 1150 MPa of the network condition) but lower elongation. This is reflected in deformation analysis displayed in figure 5.2, in which the map indicating the Von Mises equivalent stress is superimposed on the micrographs (the analysis consists in a tensile test supported by digital image correlation in order to investigate the deformation behaviour).

Specimens in figure have 28% martensite and were subjected to a strain of 6,4%; as it can be observed, in the networked structure the strain distribution is more homogeneous and the maximum values are higher (that means more elongation). The strain-localized regions (yellow and red) propagate across the martensite within the ferrite grains, due its softer phase and its capability to deform.

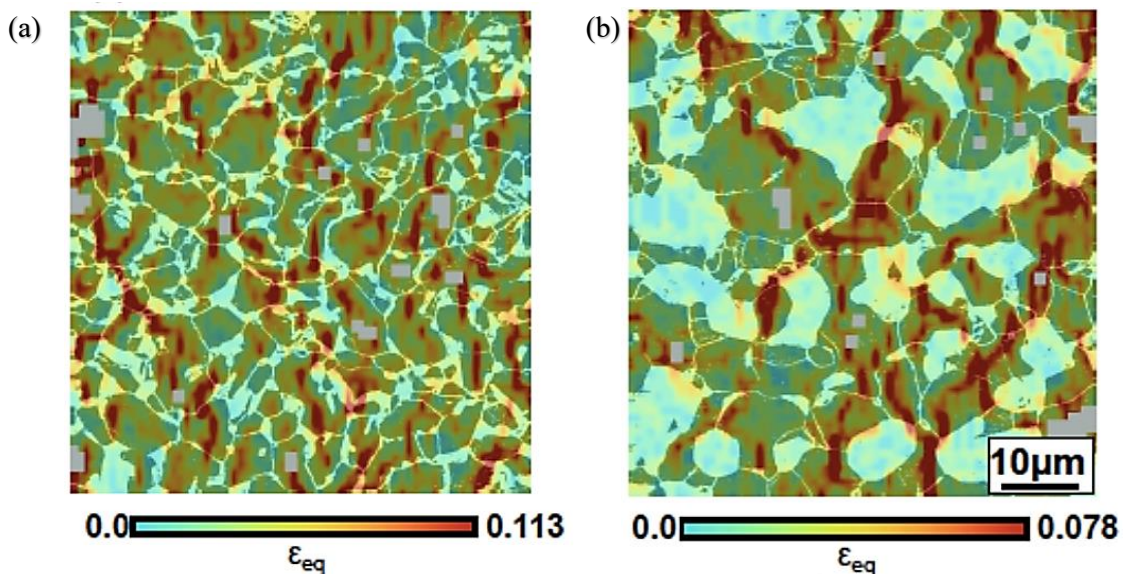


Figure 5.2 Local strain distribution for (a) networked martensite and (b) isolated

Strain values for (b) are lower than the case (a): this reflects a smaller possibility of elongation. Thus, it can be concluded that a networked structure allows better and more uniform strain field than a microstructure with isolated (and coarsen) martensite grains. This results in better behaviour during deformation. When a more brittle phase is partitioned, in fact, the possibility of unexpected failure increases, for example during die bending or stretch flanging. Harmful dislocation build-up can occur in ferrite grain when it encounters a hard phase grain, and this leads to delamination at the ferrite-martensite boundary or to cracking of the martensite if it is structured in islands. These micro-damages can grow and propagate, having injurious effects.

Riskiness of the phenomenon can be reduced with microstructural optimization, as just seen in the example; niobium is a valid countermeasure for this harmfulness. A simple addition to the base DP steel results in microstructure refinement with smaller martensite island and more regular dispersion in the matrix [66]. Appropriate processing conditions make improvement further efficient.

Microstructural refinement brings some advantages: besides strengthening effect, the most remarkable effect is toughness enhancement: figure 5.3 demonstrate this in bending operation for a DP 780 steel grade.

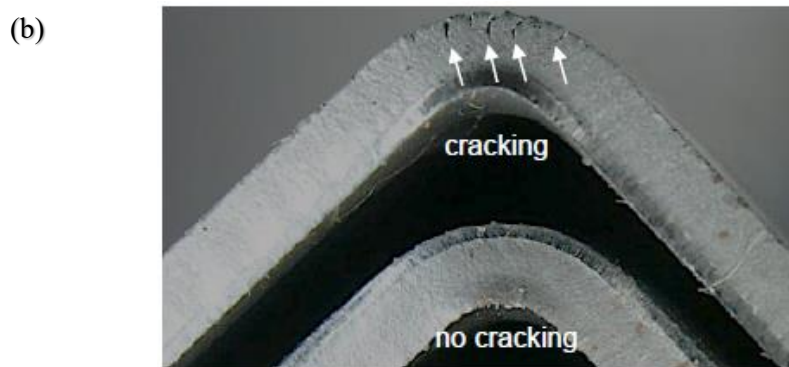
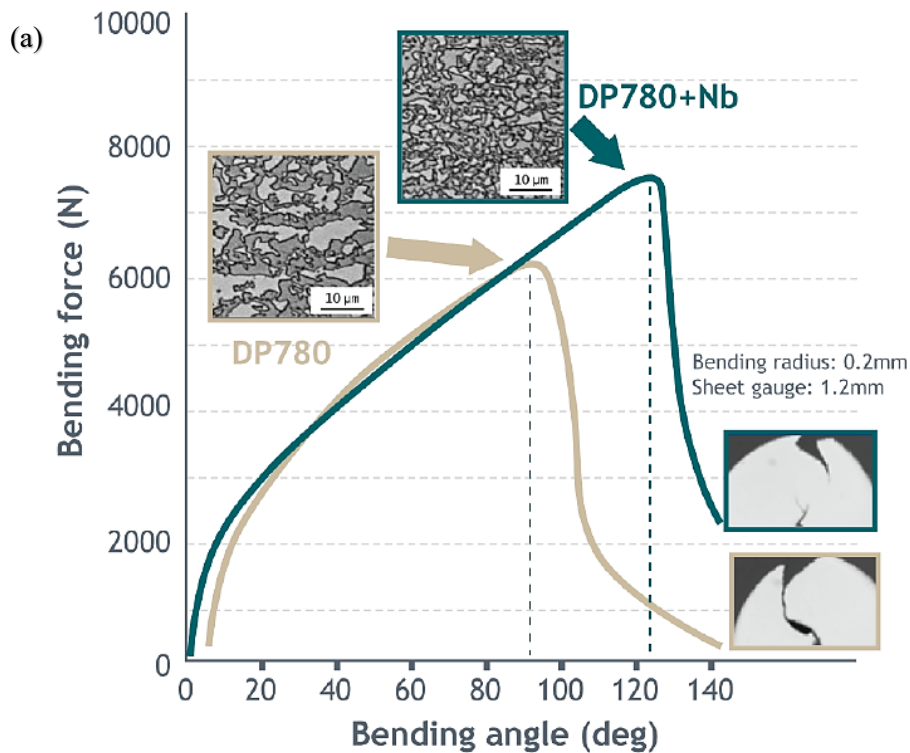


Figure 5.3 (a) Nb effect on bending (b) and fracture avoidance

Phase homogenization by niobium is evident, and this enables increased bending angles (achievable with higher forces). As it can be seen in 5.3 (b), for the standard sample the production of a V-shape profile is critical (several failures mean productivity loss), while for the niobium-version, margin is enlarged; minimum bending radius, in fact, drops by about 30%. Consequently also flanging and hole expansion ratio are enhanced.

Strengthening by niobium could translate into the possibility of achieve the same desired mechanical properties with smaller amount of martensite: this allows a reduction in carbon content that is beneficial for hole expansion ratio and weldability.

Dual phase steel, in general, are subjected to hot dip galvanizing cycles; an important phase is the intercritical annealing [67]. Austenite formation in this stage is significant because it will influence the subsequent phase distribution; it is the first step during annealing and depends to the condition of previous cold rolling. The higher temperature and carbon content, the greater amount of austenite formed in the phase transformation, which happens preferentially along grain boundaries or carbide particles (in fact pancaked austenite enhances ferrite nucleation due to the larger grain boundary).

Partitioning of carbon is fundamental for structural condition and location of the hard phase: refinement by niobium results in shorter diffusion distance (thanks to smaller grains) and thus, more efficient partitioning of carbon; martensite islands are more easily avoided.

Preliminary rolling and coiling condition determine the amount of niobium remained in solution and that is available for further precipitation. A low coiling temperature of 500-550°C (after hot rolling) increase the precipitation potential during the intercritical heat treatment: this is visible in figure 5.4 (b) where it's analysed a DP 800 steel with 0,1% C and 0,03% Nb.

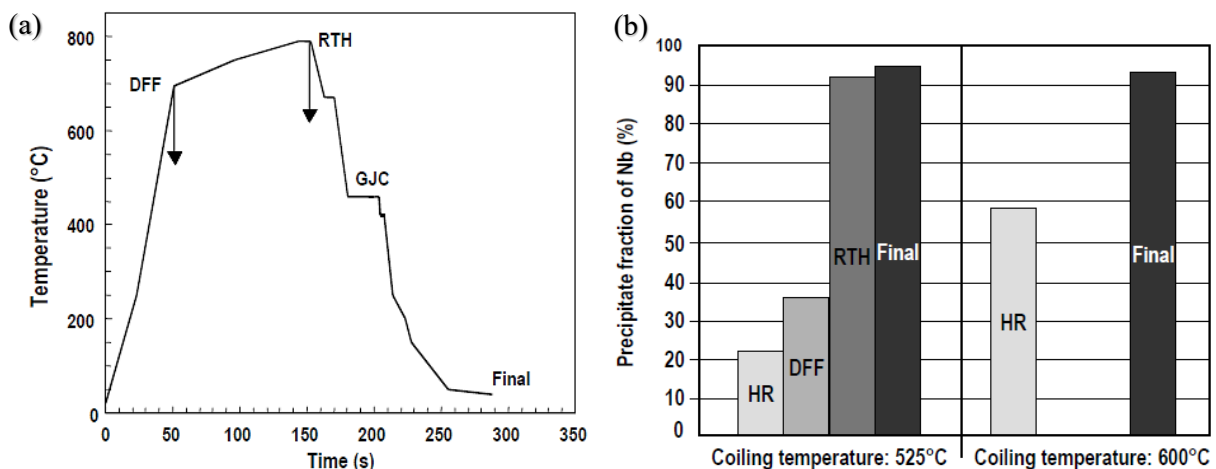


Figure 5.4 (a) Annealing cycle and **(b)** precipitation progress from hot rolling HR to final. The graphs acronyms are: DFF=direct flame furnace, RTH: radiant tube heater (soaking section), GJC: gas jet cooling

It this phase pre-existing precipitates enlarge their dimensions and are less effective, but particles formed during this stage are very fines and their amount is considerable.

Even in dual phase, niobium delays recrystallization and experience proves that T_{NR} is typically increased by around 20-50°C; therefore, pancaked structure is achievable more easily and this means more nucleation sites (grain boundaries) for austenite, so the process is accelerated with niobium in DP steels (alongside the shifting of phase transformation to long times in CCT diagrams that help the formation of harder phases).

Enhanced ferrite formation (thanks to better carbon partitioning) enriches the remaining austenite in carbon, so it's possible to obtain a larger amount of martensite, depending on the requirements. Even if its amount is lower, martensite is optimized and stronger, and this is reflected in mechanical properties: Nb addition improve yield and tensile strength, as it can be seen in figure 5.5.

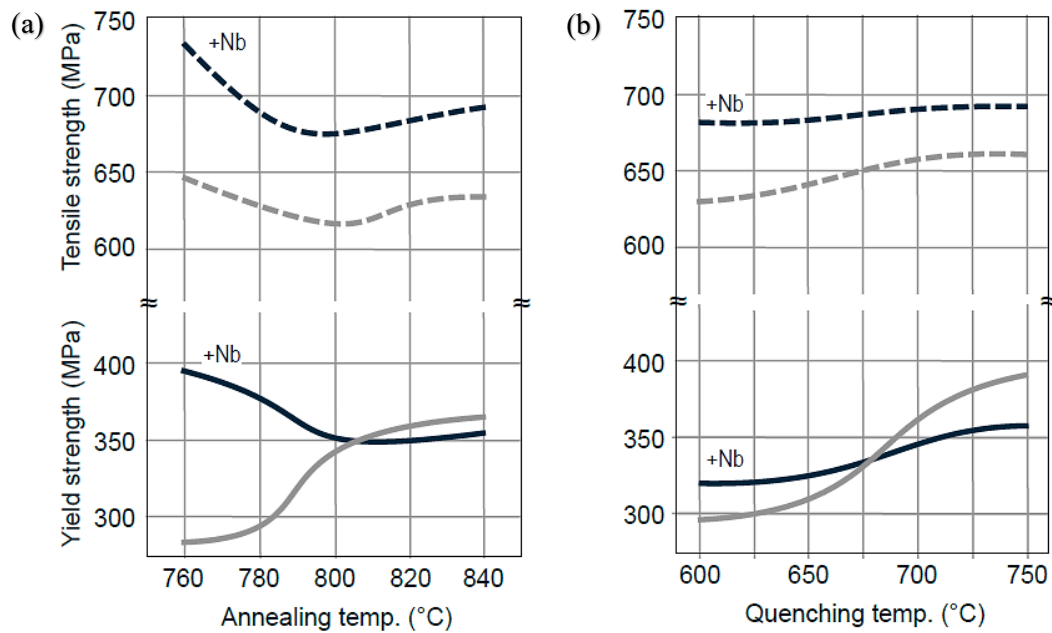


Figure 5.5 Experimental results for yield and tensile strength at annealing and quenching temperature variation. For (a) values are obtained after a subsequent quench at 750°C, while for (b) the preceding annealing is conducted at 840°C and steel is slow cooled from this value to the starting temperatures of quenching

Strengthening effect of niobium is evident, in particular for variation in annealing temperature; reduction of yield strength at high annealing temperature is due to the overcoming of the recrystallization delay, which weakens Nb actions. Instead, by varying quenching temperature the increase is less pronounced because the transformation kinetics is very quick for finer grains: the yield stress for Nb steel doesn't change significantly compared to the base steel; here, in fact, microstructure is already refined and the transformation rate is further intensified.

Refined microstructure of the final product is also beneficial in mechanical properties scattering: niobium in fact reduce this phenomenon, for example between the transverses and parallel rolling direction. Isotropy sometimes is a requisite for customers, and noticeable mismatch may leads to part rejection.

After annealing, steels can be subjected to a galvanizing operation: in this process it's important the coating adhesion of the zinc layer. Oxidation of some elements could leads to adhesion problems; nevertheless, niobium is beneficial also in this area. In fact comparison of a reference steel with a variant (with reduced C and an addition of 0,01% Nb) shows better behaviour in the coating-surface interface, being this latter more uniform and unified.

During zinc bath (conducted by holding the component at around 450°C), there is the risk of partial bainite formation due to the relatively low carbon content in certain areas or grains. Bainite, compared to martensite, reduces tensile strength and n -value, which is an important characteristic of DP. Thus, generally bainite should be avoided and alloying elements can achieve its delay. In order of effectiveness some example are molybdenum, chromium, manganese, nickel and silicon, which slow the transformation kinetic. Niobium, as said, has also a powerful similar effect, but its low addition and low availability after precipitation limits its contribute.

In addition Mo is the is the most uncritical alloying element with respect to surface oxidation; so, it is preferred to, for example, chromium and silicon due to their affinity with oxygen, although combination of Cr with Nb is beneficial in strengthening in DP medium classes.

A study carried out by Mohrbacher et al. [68] centralizes and resumes the microstructural evolution and progress of niobium precipitation during an industrial process for a high-ductility DP980 steel. Specimen composition and treatments are schematized in table 6.

Alloy (mass %)	C	Mn	Si	Cr	Nb	Ti	B
DP980 HD:	≈0.2	2.2-2.6	0.5-1.0	<0.7	0.03	<0.02	<0.003
Processing stage	Slab soaking	Finish rolling	Coiling	Batch annealing	Continuous annealing		
Temperature:	1240°C	>900°C	≈600°C	580°C/10h	850°C		

Table 16 Steel composition and process

For completeness it must be said that between batch and continuous annealing there is a cold rolling operation (70% reduction); it is made after batch annealing to avoid overloading in the mill. A final zinc bath is performed after continuous annealing: it acts as the first part of quenching.

Investigation was done for three conditions: as hot rolled, after batch annealing before cold rolling and in the finished product. Their characterization consists in:

- As hot rolled: ferrite and pearlite compose a banded microstructure and the status between head-center and tail-head position. In this one, there are some areas of degenerated pearlite and lath martensite, sign of faster cooling; in fact also hardness is greatly higher in this position (300 HV vs about 230 HV)
- After batch annealing: microstructure is similar to the previous condition, with pearlite decomposed into spheroidal cementite. Hardness values are slightly reduced (≈210 HV) and less scattered.
- Final product: the obtained microstructure is very fine and homogeneous. Some martensite islands are detected, but the majority is dispersed martensite (high-C twinned and low-C lath). A little fraction of retained austenite was identified by EBSD analysis. Hardness is increased to an average value of 300 HV. Percentage of martensite and ferrite is fairly similar, 45-48%; this high value of hard phase allows the great strength of this class.

Tracing of precipitates was a substantial part of the work: it was made by TEM for the three stages. Examination shows that NbC density increases subsequently over the proceeding process, as represented in figure 5.6. Particles occurrence in (c) looks like it would be less than in (b), but it is due to their smaller size, in fact, in the next magnification (d) the large density is visible.

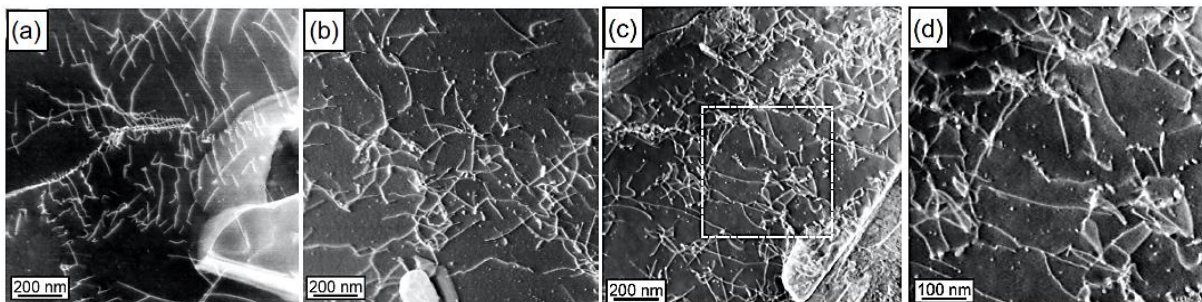


Figure 5.6 Precipitation evolution for (a) as rolled, (b) after annealing, (c) final condition and (d) magnification of dashed area in (c)

Particles have mainly a spherical shape and their average size is 10, 12 and 7 nm respectively for the three status. The size increase for the second condition is due to a small coarsening during annealing: in this phase fine particles are not yet precipitated and those formed previously enlarge slightly their dimension. Until this moment, in fact the precipitation percentage is 60-70% and the last fraction is developed in the final processes that lead to finer carbides. After coiling, instead, percentage is only 10%, in fact the particles count is small compared to the other condition (188 per μm^3 vs 1072 and 2480 per μm^3). These consideration are matched in the precipitation kinetics diagram similar to that one in figure 4.17; here coiling intersects the curve for 10% precipitation, batch annealing window is located between 50% and 90%, and the final continuous annealing is located above all curves, so precipitation is complete.

Precipitation kinetics is governed by the solubility products, exposed in previous chapter, and also by presence of Mn, Cr and Si that affect C and N activity (even if their effects is quite well balanced).

Precipitation strengthening is evaluated by the Orowan mechanism that quantified it in 180 MPa; nevertheless, correction with the more complete Ashby formula, leads to drastic reduction in strength increase of about 80 MPa (due to the high number of dislocation that could annihilate each other).

Microstructural refinement is the other central mechanism in this investigation, and it is estimated in the order 70 and 150 MPa for yield and tensile strength. Although no importance has been given to the scheduling of hot rolling below T_{NR} , ferrite grain presents itself rather fine. Besides pinning force exerted by precipitates and drag by solute elements, other metallurgical processes that give a contribute take part. For example the spheroidization of the original pearlite during batch annealing, or the fast heating rate that delays recrystallization in favour or enhanced austenite formation: it nucleates at the interface between ferrite and spheroidized Fe_3C resulting in a “necklace” of austenite grains around ferrite grains. High defects density in ferrite represents other nuclei for austenite within grains, so further refinement is obtained thanks to many nucleation sites.

It can be concluded that the addition of 0,03% Nb is very effective for this DP steel, since it homogenizes soft and hard phases, and it gives a strengthening contribute of about 180 MPa.

5.2 Transformation induced plasticity

TRIP steels are multiphase typically containing ferrite, bainite (some fraction of martensite is also possible) and retained austenite. Peculiarity of these metals is the transformation of the retained austenite in martensite during deformation (for example during forming), as displayed in figure 5.7.

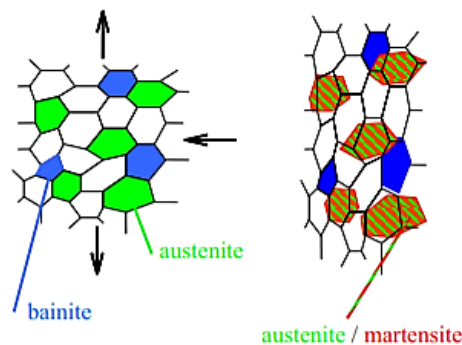


Figure 5.7 Mechanism of TRIP

This induced transformation enhances formability, in fact they have elongation values slightly higher than DP, while strength is similar. In addition, retarded transformation of these steels increases strain-hardening coefficient, delays necking instability during forming, and makes them suitable for crash part in a vehicle, because during impact the mechanism is triggered and mechanical properties are improved (in this case austenite must be very stabilized because the higher stability, the later transformation, which in these situations must take place only during a crash).

As in dual phase, microstructural control is important, but, moreover, it's fundamental the stability of austenite against strain induced martensitic transformation. This is made by accumulating sufficient carbon to reduce temperature at which austenite transforms to martensite below room temperature.

Similarly to DP, TRIP are subjected to an intercritical annealing cycle, followed by rapid cooling and isothermal holding to develop bainite. Formation of pearlite that results in carbon loss should be avoided. Bainite is obtained through holding at sufficient low temperature (about 400°C) and alloying elements help its achievement by modifying the CCT curves (for example Mn, Si or Al, but it's presence must be kept under control because they can lead to other problems). In this stage bainite rejects carbon to austenite, which reaches 1,4-1,8% C; carbon enrichment starts already in the intercritical annealing phase, but it is usually insufficient to ensure austenite stabilization at room temperature, so formation of bainite is necessary. Higher value of carbon supersaturated leads to more stability, more volume of retained austenite and lower martensite start temperature. Volume has to be controlled, in order to obtain the required combination of mechanical properties. Carbon percentage in TRIP is quite higher than in DP, but it is limited at level of 0,2-0,5% (although in automotive this value generally not exceed 0,3%) to avoid future problem for example in welding.

Microstructural optimization is, again, a key factor for optimizing the final properties; as expected, niobium manifest its effect in this field, mainly through grain refinement and precipitation, and combination with TMCP enhances results. Figure 5.8 shows a refined microstructure where phases (white grains are retained austenite) are more homogeneous and their grains are finer.

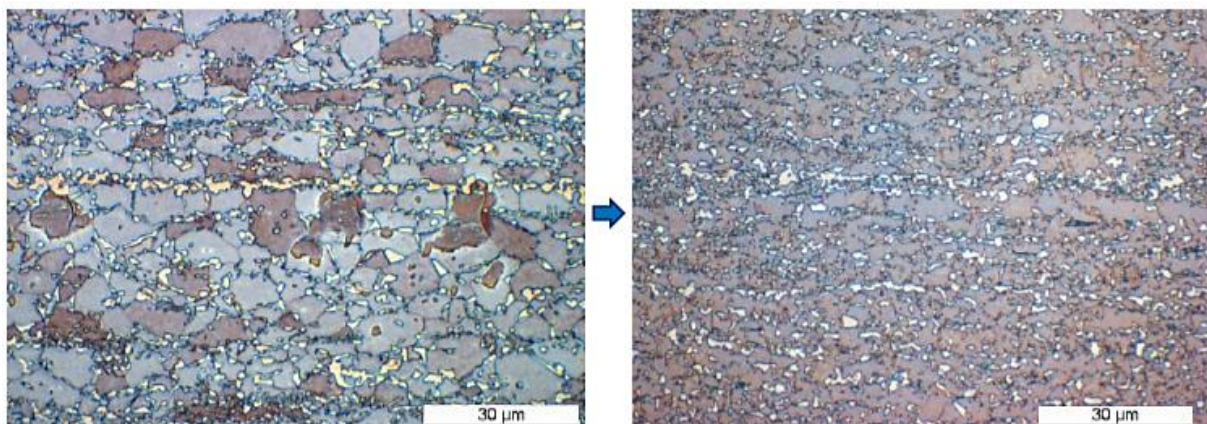


Figure 5.8 Refinement by Nb in a TRIP 700

Coiling temperature is a remarkable aspect for processing and precipitation: low value ($\approx 500^\circ\text{C}$) was found to determine a marked decrease of martensite start temperature, but this level is too low to ensure a complete precipitation of Nb that stay in solution. On the other hand at 700°C particles coarsening occurs, so coiling temperature in the range $600\text{-}650^\circ\text{C}$ is optimal for fine precipitates that pin grain coarsening and strengthen material.

Smaller grains can accumulate more easily the carbon necessary to stabilize austenite at ambient temperature; this is due the shorter distance for carbon partitioning.

Niobium is considered an inhibitor for bainite: the retarded bainite formation is attributed to an enhanced ferrite formation during cooling thanks to, again, the finer microstructure. Dispersion of small carbonitrides, additionally, result in deactivation of nucleation site for bainite, and niobium in solid solution slows down the transformation kinetics. Therefore, as result of these mechanisms, there are more carbon available for retained austenite, whose stability and volume is increased.

Importance of stabilization by niobium is also detected in the galvannealing operation: here there is risk of retained austenite decomposition for higher temperatures. In Nb-TRIP steel has been observed that this phenomenon is reduced.

Concerning the mechanical characteristic, the effect of niobium on strength is not so powerful in TRIP compared to classical microalloyed steel, especially in the as-annealing condition: in fact, ferrite is enhanced and it can bring some contribution, but bainite is weakened due to C depletion, so strengthening is not so intense. However slight increase in yield and tensile strength is detected with niobium in an Al-steel, as is can be seen in figure 5.9 (a). Here, strength is in function of the holding time for bainite formation, but this is rather marginal (apart from the first moment).

On the other hand, the peculiarity of TRIP in strengthening occurs after plasticity deformation, where the improvement is perceivable. This phenomenon is better understandable in figure 5.9 (b).

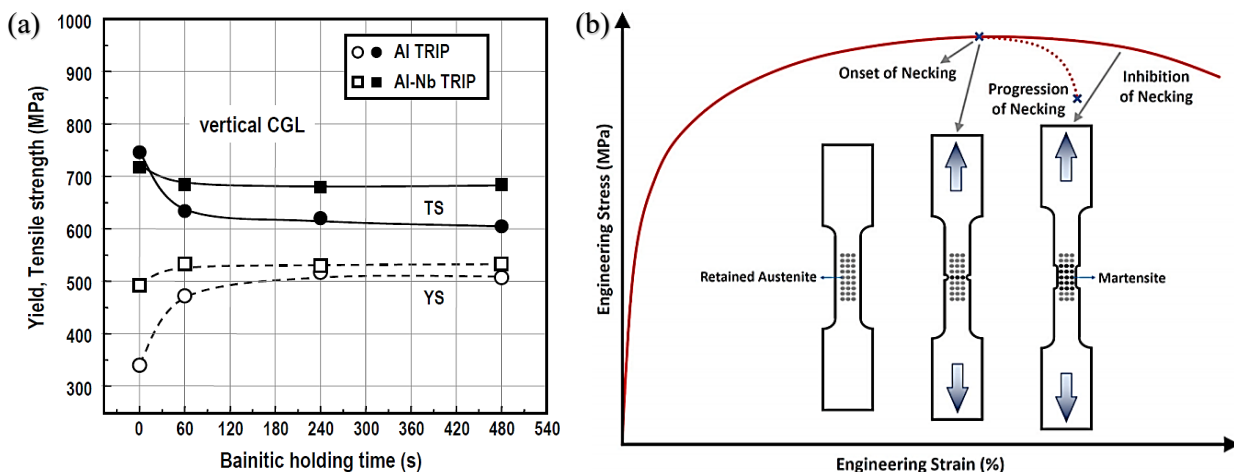


Figure 5.9 (a) Influence of bainitic holding time at 400°C and (b) consequences of transformation induced plasticity

Practical investigation of niobium impact on a TRIP sheet steel was conducted by Hausmann et al. [69]. Base steel has the following composition: 0,17%C - 2,6% (Mn + Cr + Mo) - 0,78% Si - 0,005% N. Four variant were adopted: 0% - 0,025% - 0,045% and 0,09% Nb.

After hot rolling, coiling (650°C) and cold rolling, specimens were fully austenitized (to see the primary austenite grains) at 900°C for 60 s. Then, treatment follow two ways: holding for 30, 120 or 600 s at temperature ranging from 350°C to 475°C, or holding for 1200 s at 400°C. This considerable number of treatments adjustment was made in order to have a detailed correlation between microstructure and mechanical properties. Nevertheless, here it will be exposed mainly the effect of niobium, without going into details of the thermal variation (since these aspects have already been presented in other previous examples).

Micrographs show that with niobium austenite grains decrease more than 50%, and bainite appears more globular compared to the lath-like one of the reference material. Moreover, considerably less cementite was found in bainite, indication that carbon (of which cementite is

rich) has been rejected to retained austenite. In addition retained austenite changes its morphology from lath to blocky-like.

Niobium was observed precipitates into two NbC population: fine and coarsen. The second increases further its size when Nb amount is larger, weakening the effect of grain refinement; therefore, excessive Nb addition may not bring advantages, and the optimum percentage of niobium for precipitation was evaluated 0,025%. This value is the best choice also for the maximum amount of retained austenite achieved (more than 10%), because further Nb addition doesn't increase its quantity. On the contrary, there is less bainite in the three Nb-variant, which confirms that it delays bainite formation for the benefit of retained austenite.

A tensile test was conducted to analyse the stability of the austenite against the strain induced martensitic transformation: this valuation was done by measuring the amount of retained austenite as a function of tensile strain. Its fraction decreases with increasing plastic deformation, and the result exhibits that all steel versions have almost the same trend, but the niobium versions maintain greater austenite percentage.

Yield and tensile strength as function of bainitic holding time have the same behaviour of those in figure 5.8 (a), and are stabilized after about 200 s. Their values are respectively 800 MPa and 1000 MPa. Elongation capability follows similar trend, with a stabilization at 200 s; samples with niobium have an extra of about 2% elongation, but there are no significant differences between the various Nb amounts.

This stable behaviour after a certain bainitic holding time can be attributed to the stabilization of retained austenite due to carbon enrichment as the bainitic transformation proceeds. With lower bainitic transformation temperature, instead, TRIP effects (increase of strength and elongation after strain) could decrease: this is due to the formation of lath-like bainite (or even tempered martensite if temperature is very low) in replacement of the globular one.

In conclusion it can be said that the addition of 0,025% Nb represents the sufficient amount and the best way to exploit its advantages in this type of TRIP steel.

5.3 Martensitic and press hardening

[53,70,71] These type of steels are the strongest ones, since their tensile strength can reach values in the order of 2000 MPa; consequently elongation remain quite low, approximately less than 10%. They are mostly composed by lath martensite (small amounts of ferrite or bainite may be present) that is achievable with relatively high carbon content, up to 0,4% (although upper percentage could be employed for high-carbon martensitic steels).

Their application in passenger cars includes components used in zones where collapse is not tolerated, for example bumper beams or floor area, which have to redistribute impact loads without crashing.

Martensitic steels are divided into two “macro-categories”: the first includes steels that are cold rolled, thermally treated for the martensitic transformation and then are slightly bended or formed; the second, instead, comprises steels in which the hardening treatment is made in hot dies (press hardening). The first type requires a minimum level of ductility because they are formed at room temperature, unlike the second type in which forming occurs at high temperature.

Strength of martensite (once the totality of the structure has been reached) is linearly proportional to carbon content. For low value of this latter parameter, the crystal structure of the lath martensite is bcc and the solute carbon atoms segregate to dislocations during the quenching process; when C increases (over 0,2%) structure becomes slightly tetragonal and

carbon (once defect sites are saturated) remains in octahedral interstitial sites and hardening is more pronounced. Over 0,5% C, microstructure becomes more complicated with formation of plate martensite and retained austenite.

Martensitic formation depends on fast cooling rate sufficient to prevent other softer phases transformation. Some alloying elements assist formation and hardenability: beside C, some of them are Mn, Cr, Mo and especially B. It, in fact, delays pearlite and bainite formation in CCT diagrams, and it's very effective for hardenability by segregating to the austenite grain boundaries before quenching. It's important that boron nitrides are suppressed, and to achieve this, titanium is added, with the aims of formation of the stable TiN.

With an addition of 0,002% B it's obtained the minimum cooling rate for fully martensite formation; over this value there is the possibility of constitution of complex $Fe_{23}(C,B)_6$ particles on the austenite grain boundaries. These are brittle intermetallic particles and consume boron, so its availability for hardening effect is loss and further cooling speed reduction is suppressed. Additionally, these complex precipitates deteriorate toughness and DBTT. Combination with molybdenum can give another contribute at decrease in critical cooling rate.

Furthermore, boron effect on hardenability is perceivable in hardenable diameter: experiment on a water quenches steel (0,5% Mn, austenite grain size ASTM 4) shows that B addition increase remarkable the hardenable diameter of the tested specimens; for example, for 0,3% C, it changes from 15 to 20 mm.

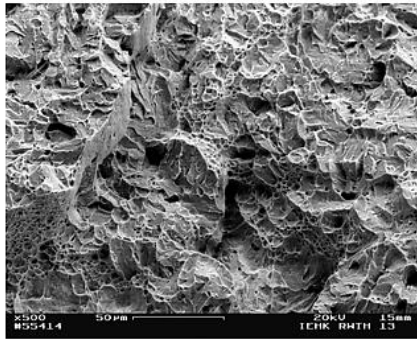
The criticality of this steels typology is the relatively low toughness at low temperature, which can leads to brittle behaviour (the issue of hydrogen embrittlement for this steels has been already treated in section 4.5). In automotive, since the atmospheric condition could be severe, this must be avoid because the safety component can't fail in a catastrophic way. Increasing hardness (for example through carbon) worsens impact energy absorbed, so it is necessary to use methods to balance characteristics and optimize steel behaviour.

Niobium beneficial consequences in these steels is not so much important in strengthening, but in toughness and fractures containment. In fact, besides steel cleanness from impurities (N and P that segregate at grain boundaries facilitating cracks, and S that forms elongated MnS that act as preferred crack paths), microstructural refinement is an effective mechanism to reduce brittleness. This is evident in figure 5.10, where Nb is added to a classical high strength steel.

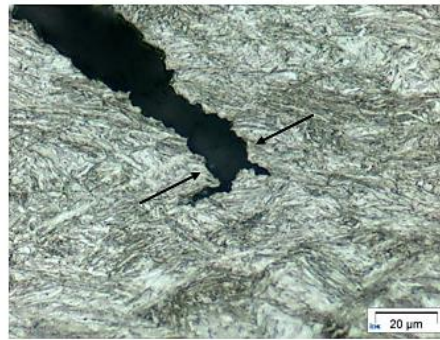
With the development of advanced high strength steels, new methods and use of advanced materials, the properties were enhanced and applications in vehicles were enabled. An important feature that must have automotive high strength steel is bendability; in this, niobium acts with the usual mechanisms, and thanks to grain refinement, its addition can remarkably increase bending angle. A test developed by carmakers for bending angle evaluation is VDA 238-100, which consists in a quasi-static bending test in a three-point configuration. On this basis, critical bending angle range is 55-60°. Addition of 0,05% Nb improve greatly the condition of a simple 22MnB5 industrially produced: in the standard configuration, in fact, its bending angle value was in the critical range, but with 0,05% Nb it reaches level of about 100°.

Hydrogen influence is deleterious due to the risk of embrittlement and delayed fracture, and obviously, it decreases the bending angle achievable. Beside the positive effect of niobium already mentioned, an higher deformation rate could be beneficial, since the H-diffusivity is slowed down and accumulation is reduced.

Standard 22MnB5

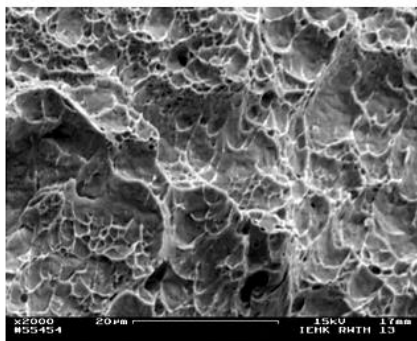


Brittle appearance



Single crack

Modified 22MnB5+Nb



Ductile appearance



Stable microcracks (voids)

Figure 5.10 Enhancement performed by niobium on fracture

Fracture appearance for brittle behaviour can manifest mainly in two ways: intergranular and transgranular; this type occurs through the prior grains. Lath martensite is composed by laths packets, often divided into blocks; lath boundaries are low-angle boundaries and they cannot provide great resistance to crack propagation because they don't impose significant crystallographic discontinuities. Instead, packet and block boundaries are high-angles ones, and they are more effective in arresting fracture; they determines the effective grain size, so their number increase is beneficial because there are more resistance areas. Number increase means smaller size, and, since they constitute the grain, if they are smaller then also grain size could result reduced.

Smaller grain size is beneficial for the intergranular fracture mode, in which crack propagates itself along grain boundaries; so, as said previously, fracture extends more difficultly because it has to follow a longer path. In figure 5.11 it can be seen the effect of microstructural refinement on a 22MnB5 steel. The average grain size drops from 11,3 μm to 5,4 μm , while mechanical properties are increased with niobium, and in particular the ultimate elongation, that gains about 15% (from 9 to about 10,4%).

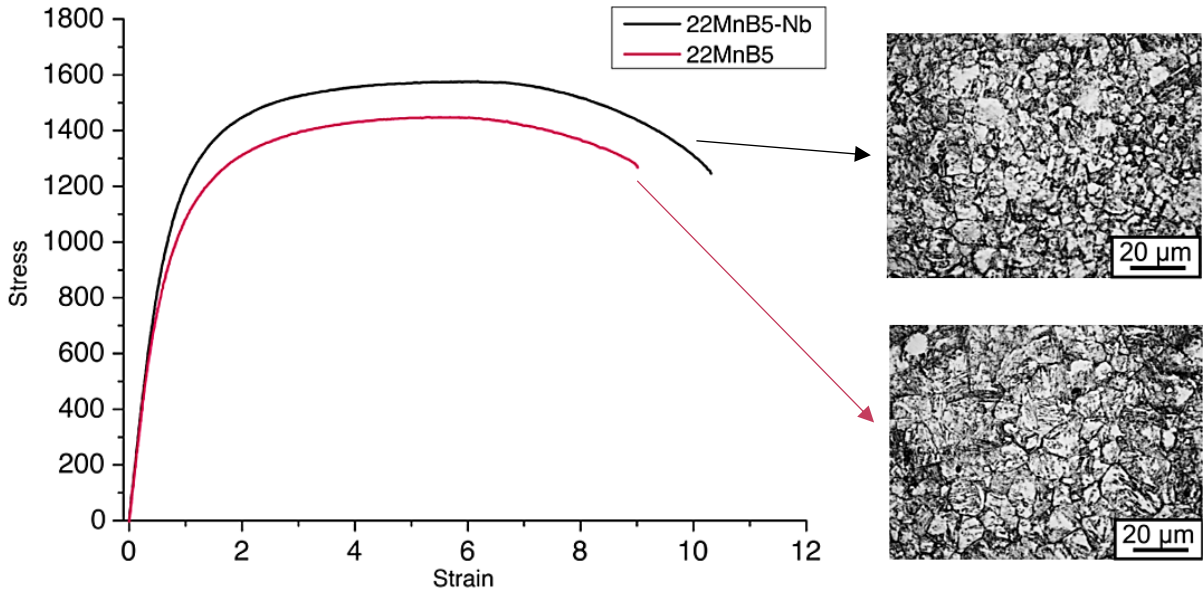


Figure 5.11 Microstructural contribution to mechanical properties

Necessity of smaller grains increase with higher steel grade: as it can be noted in figure 5.12, materials with higher strength level (due to more carbon) possess a brittle behaviour larger than lower grades. So, further toughness contribution has to be given, and niobium is the most efficient metallurgical approach in translating the critical line that separates ductile to brittle condition.

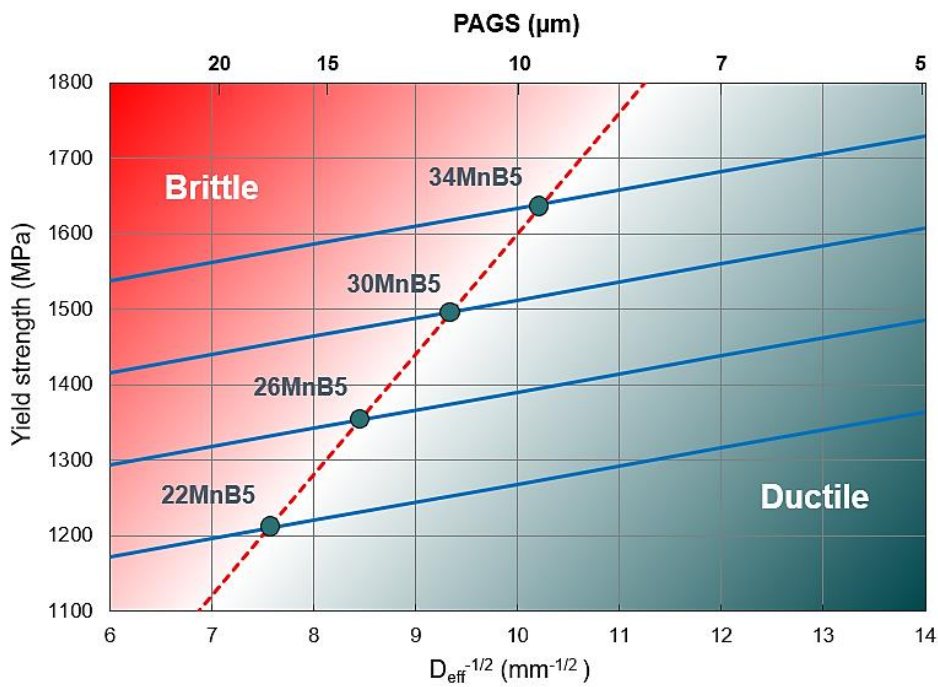


Figure 5.12 Critical grain size for some martensitic steels

Another method for restoring ductility is a tempering/reheat quenching treatment instead of direct quenching (that is cheaper but leads to weaker elongation); nevertheless this procedure has limits: too low temperature could have no effect, and too high ones could deteriorate

strength (main feature of martensitic steels). Niobium may represent a solution, since during reheating it can precipitates and prevents grain coarsening, which affect mechanical properties.

This effect is supported and encouraged by Mo: experimental studies reported in [70] shows that its precipitation in combination with niobium mitigates the strength loss due to tempering treatment. This is visible in gain of hardness for specimens with various Mo fractions; steel in question is a 0,2% C - 1,4% Cr - 1% Mn, and %Mo added are 0,2 - 0,5 and 0,7%. Further 0,3% Nb is included at 0,7% Mo to see the effect of co-addition.

Graphical results proves that for the samples with molybdenum hardness is considerably increased in comparison to the base steel, and niobium further supports this phenomenon. To give some numerical data, with an annealing temperature of 600°C (for 1 h) the hardness of reference steel is 22-23 Rockwell C, while for the three Mo variants it is respectively around 28, 30 and 34 Rockwell C. Last trial with niobium and molybdenum shows a value of about 37 Rockwell C.

It should be said that molybdenum addition in this steels is restricted to parts with huge thickness, and the relative application are under development; commercial uses, in fact, is not diffuse today, but the studies are aimed at future application.

Press hardening (or hot stamping) steels are a type of martensitic steels that follows the processes displayed in figure 5.13: components are preliminarily rolled, coiled and blanked. Then, steel blanks are heated (eventually preformed previously) and transferred into a stamping die for the hot forming operation and the final rapid cooling to obtain the hardened material. It occurs when the die is in full contact with the deformed sheet through conduction, since the heat transfer quenches the hot austenite into martensite.

From 2000 these steels use in automobiles has increase and now covers a large percentage of the body in white. Their main application in passengers car are roof or door reinforcements, front or rear bumper, front rails and A- or B- pillars.

Addition of niobium manifest itself during heating, when the amount that is in solution after rolling can precipitate. Its effects improve toughness of the final product that is more resistant to crash and has a lower ductile to brittle transition temperature.

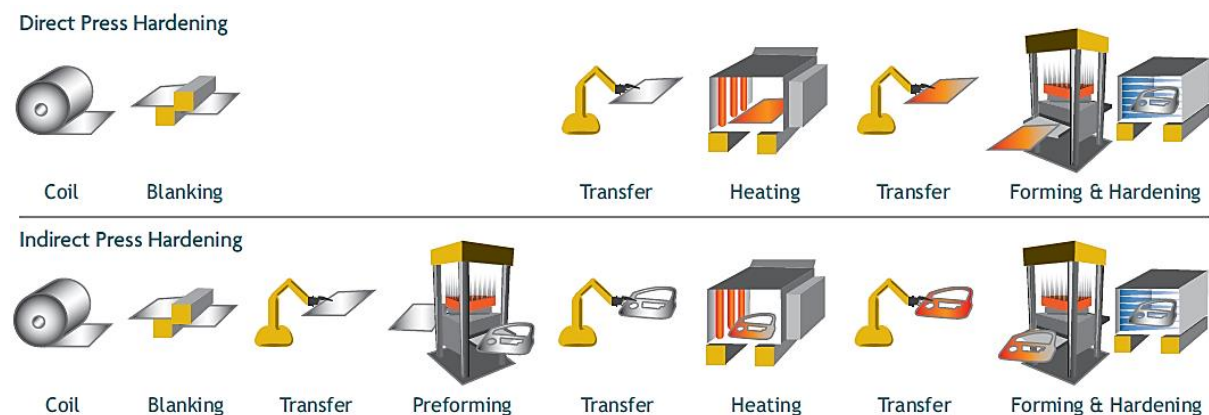


Figure 5.13 Steps for direct and indirect PH

5.4 Interstitial free

Unlike the previous sections in which are described some high strength steels, in this one will be presented the interstitial free (IF) steels, a typology whose main feature is the excellent elongation and, so, formability. IF belong to the ultra low carbon (ULC) family, which is a steel class in which the carbon and nitrogen content is generally less than 80 ppm, although the use of modern vacuum degassing system allows to obtain level of < 30 ppm [72].

Low amounts of interstitial C and N involve low strength but high elongation; for this reason they are adopted for automotive components that may have different curvatures and thus require precision in formability rather than high strength. Some examples are rear floor pan, hood panels, spare wheel well, front and rear door inner, which may have complex shapes.

Carbon and nitrogen are typically stabilized by small addition of titanium and niobium; they “capture” interstitials to form precipitates. The lower free-C and N, the better formability, as shown in figure 5.14 (a), where it’s represented the effect of Nb addition.

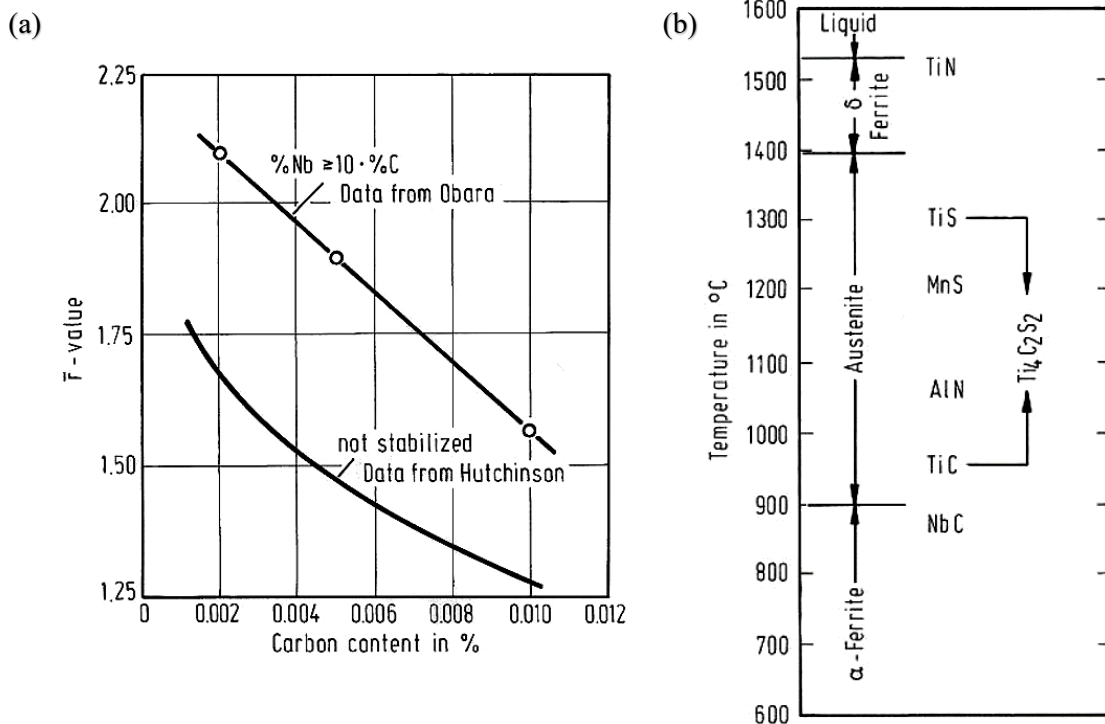


Figure 5.14 (a) Enhancement of r-value with Nb stabilization and (b) sequence of precipitation in IF steels

Titanium shows high reactivity with N, S, C and also P; for vacuum treated Ti-IF steel, the progress of precipitation is represented in figure 5.14 (b). The first specie that is formed at high temperatures is the well-known TiN; then, depending on the level of Ti, S and Mn, TiS precipitation can occur, and it is preferred to MnS (due to the disadvantages that it can brings). TiS sulphide could combines with TiC, absorbing its carbon, forming complex titanium carbosulphides; this reaction is accepted because it stabilize both C and S without two separates precipitation. Full stabilization of carbon by Ti requires also to fix N and S, and the amount of titanium is based, at least, on a stoichiometric approach, which is:

$$\text{Ti} = 4 \cdot \text{C} + 3,42 \cdot \text{N} + 1,5 \cdot \text{S}$$

where the numerical coefficient are calculated from the atomic weight ratios of the elements. An excess of titanium can lead to surface streaking the final coated product, which is aesthetically undesirable.

For niobium stabilized IF steel, instead, Nb mainly fixes carbon, because sulphur is naturally fixed by manganese, and nitrogen amount is reduced by precipitation of AlN (aluminium, in fact, is present in the steels since they are Al-killed). Therefore niobium addition can be just stoichiometric, that means 7,74·% C. Excessive Nb amount have the several benefits already explained in this discussion.

As a comparison, a full stabilization requires less niobium than titanium: for a steel with 0,003% C - 0,0053% N - 0,008% S, it's necessary at least 0,036% Ti, while only 0,023% Nb. Reduction by one third results in appreciable economic convenience for large production plant.

A common practice is the dual stabilization with titanium that fixes nitrogen and niobium that fixes carbon; in this case it's used the stoichiometric values for both the atoms respect to N and C respectively, so they are 7,74·% C for niobium, and 3,42·% N for titanium. Ti-Nb IF steels are less susceptible to cold work embrittlement (which will be better explained subsequently) and also exhibit better spot-weld characteristics.

Development of a refined microstructure is beneficial also in this steels, since r-value and ductility are positively influenced by it. Hence, classical effects of niobium have to be accompanied by a thermomechanical controlled process. Here, the rolling forces are lower than those in HSLA (due to lower strength level), but an increase in rolling load can be detected, indicating that no recrystallization occurs below certain temperatures; this is observed in particular in Nb IF steel. Niobium that remains in solution at the end of hot rolling (for example due to over-stoichiometric addition) retards the austenite to ferrite transformation; this leads to finer ferrite grains and strength increase of about 20 MPa compared to Ti-IF steel. Grain refinement can also promote the avoidance of "earing" after deep drawing and the "orange peel" appearance at the painted surface of the heavily drawn parts.

Slightly higher coiling temperature, in the range 600-700°C, are applied for IF, because it allows the formation of precipitates larger than the "normal": them, in fact, enhance the development of a <111> texture, which is beneficial for formability. Temperatures over 725°C, however, should be avoided due to the risk of formation of an aggressive scale on the as-hot rolled strip, expensive to remove during pickling.

IF steels are used for automotive parts that are exposed, so they are usually coated to protect the substrate from corrosion through a process of galvannealing. Niobium addition is, again, a better solution thanks to a more uniform coating reaction: Nb slows down the Fe-Zn coating reaction, allowing its regulation. Fast reaction (most likely in Ti-IF) could produce a so-called outburst uncontrolled reaction, and the formation of an undesired brittle phase.

This steel typology is usually produced with certain niobium levels, so strengthening is achieved by solid solution of some alloying elements: for example manganese and silicon, which give a contribution of 4 and 10 MPa respectively, for each 0,1% fraction added. Anyway, the most effective strengthening element is phosphorus that provides 100 MPa per 0,1%. Additionally, this increase is more pronounced for Nb-IF steels than for the Ti-IF ones, as it can be seen in figure 5.15 (a). This is related to the propensity of titanium to form FeTiP, which deplete the matrix of P available.

Moreover phosphorus could segregate to grain boundaries causing their decohesion and the secondary cold work embrittlement (SCWE). This phenomenon occurs especially at low temperature, and, in fact it determines also a ductile to brittle transition temperature, that is displayed graphically in figure 5.15 (b).

Addition of boron is a good method to reduce that issue: it fills the sites at grain boundaries leaving P in solid solution for strengthening. Effect of B on the ductile to brittle temperature related to SCWT is quantified in a very strong reduction as visible in figure 5.14 (b). Furthermore, high level of niobium promotes a better trend because this element has lower affinity for carbon than titanium, so there is more carbon available, which could compete for grain boundaries occupation (although its level it is low since the nature of IF steels).

Therefore, the effect of boron is amplified by niobium. In turns, boron provides further grain refinement in Ti-Nb IF steels thanks to mechanism of solute drag on grain boundaries.

An innovative approach consists in dual addition of Ti and over-stoichiometric Nb: grain refinement attributed to niobium strengthens the material, favours formability through nucleation sites for <111> texture, avoids softening in the heat affected zone due coarsen grains and reduces the SCWE temperature. This latter effect is dominated also by segregation to grain boundary, and since there is enough niobium amount, addition of boron can be avoided.

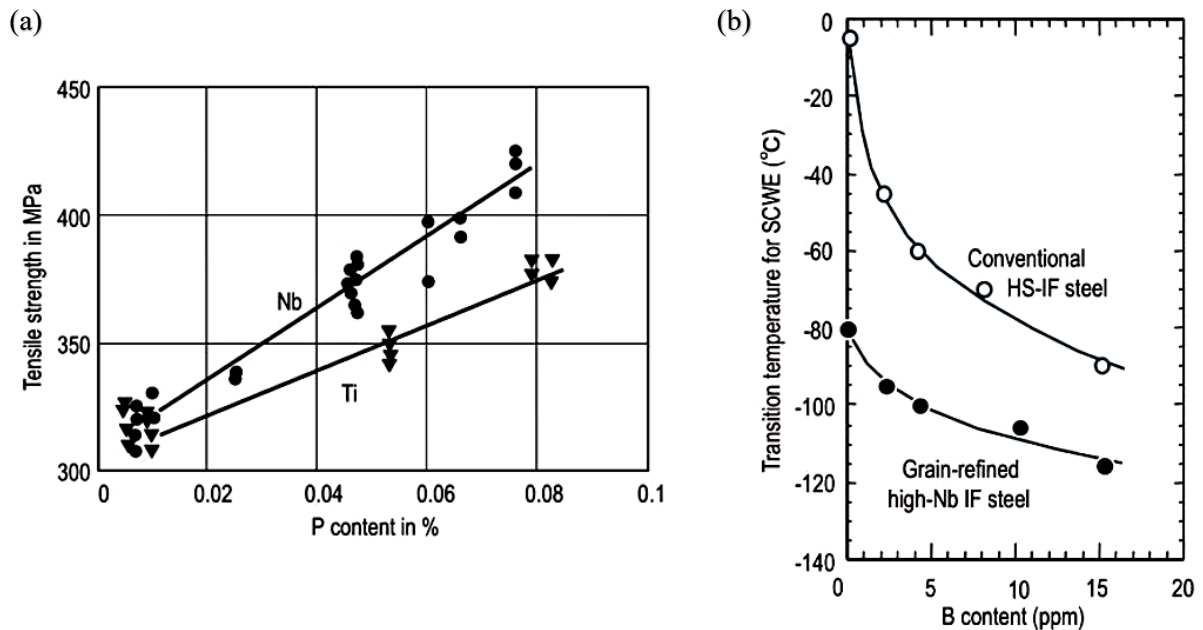


Figure 5.15 (a) Strengthening by P and (b) effect of B and Nb on SCWE

The effect of microstructural refinement on a dual stabilized Ti-Nb IF steel was investigated by Ghosh et al. [73]. They aimed to examine the possibilities of a good combination of yield strength, ductility and corrosion resistance through thermomechanical controlled processes.

The steel is chemically composed by: 0,0026%C - 0,14% Mn - 0,007% Si - 0,008% S - 0,052% Al - 0,031% P - 0,0021% N - 0,012% Nb - 0,042% Ti.

Three schedules were conceptualized to study the effect of the hot rolling temperature range on mechanical properties: pure austenitic, austenite to ferrite transformation and pure ferritic range. A_{r3} and A_{r1} for this steel are 860°C and 701°C, while T_{NR} (calculated through the Boratto equation mentioned in chapter 4.3) is 970°C. Taking into account these critical temperatures, the controlled rolling was carried out 1050, 800 and 650°C. Specimens were soaked for 1 h at 1200°C, then rolled at the three conditions with a reduction of 50% or 80%; in addition, the samples in the ferritic region was also annealed for 100 s at 850°C in order to partially recover the heavily deformed structure.

The microstructure, composed by large and inhomogeneous grains in the as-cast condition, starts to refine already in the pure austenitic condition: being above T_{NR} there is recrystallization, but excessive grain coarsening is avoided thanks to the titanium nitrides. As in the other schedules, grains size is smaller for the 80% reduction, and the dislocation density is higher, compared to littler deformation.

In the transformation region, ferrite grains begin to be elongated, and in the pure ferritic range this situation is mostly visible, together with formation of deformation bands. At low deformation temperature is also increased the grain boundaries misorientation.

The annealing operation after rolling in the ferritic region leads to the expected recrystallization; since its time was not too much long, complete recrystallization didn't occur and mechanical properties weren't deteriorated greatly, as it can be seen in figure 5.17 that resumes the stress-strain curves for all the conditions.

In figure 5.16 is reported the EBSD analysis of the specimens after annealing; the misorientation angle is comparative higher for the 80% rolled sample (c) in comparison to the 50% one (a). In fact for the most deformed condition, the high angle boundary is attributed to the finer grain size that are somehow recrystallized, but with compact dimensions. This is visible in the magnifications (d) and (e), which have wider colour variation than the magnification (b) related to the sample with 50% deformation. Those are representative, because mostly of the respective areas examined reflect the enlargements. The majority of the grains show low angles boundaries, but for the sample with greater deformation fraction of low angles is decreased and that of the high angle is increased.

In both cases there is a sort of bimodal structure with fine and large grains, where the finer ones are developed along the grain boundaries of the pre-existing larger ferrite grains. In the most deformed sample, anyway, the grain average is smaller and there is also the presence of ultrafine grains (even 1-3 μm), which derive from recrystallization of the elongated structure into subgrains. High dislocations density allows this mechanism due to the higher possibility of recombination.

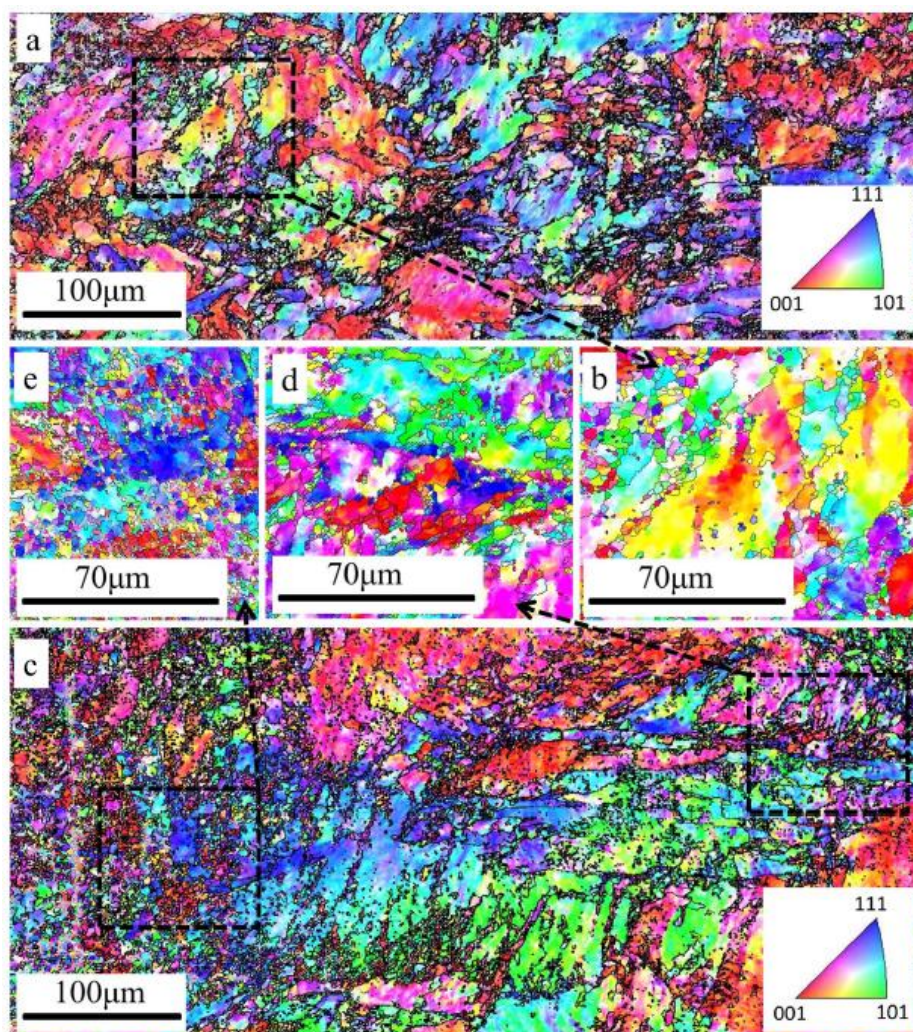


Figure 5.16 EBSD analysis of ferritic region for: (a) 50% rolled + annealed and (b) its magnification, (c) 80% rolled + annealed and (d-e) relative magnifications

Precipitation doesn't show unusual behaviour with formation of niobium and titanium precipitates (with an average size of 10 and 20 nm respectively). However it's remarkable to mention the presence of titanium sulphides at high temperatures, and, moreover, the formation of the Fe(Ti + Nb)P for the schedule in the ferritic region. Similarly to the previously mentioned FeTiP, these large particles are deleterious for formability because they deplete steel of titanium and phosphorus, and weak the <111> texture. However, above 800°C these are dissolved and formability is restored (so annealing is beneficial).

Mechanical properties reflects the nature of interstitial free with high elongation and low strength; nevertheless, an adequate process can enhance the characteristics. They are resumed in figure 5.17 (the homogeneous annealed specimen represents the condition after soaking with no deformation): trend follows the expectation with an obvious growth for the steel with 80% of deformation. Strength increases with lower rolling temperature, simultaneously with a lowering of *n*-value. Annealing enhances this parameter: for example its value for the ferritic rolled sample changes from 0,122 to 0,168. The coefficient of anisotropy has a similar behaviour; in particular, annealing allows the dissolution of the Fe(Ti + Nb)P particles enhancing the <111> texture that is directly related to anisotropy.

Hardness investigation confirms the strength behaviour with an increase for lower deformation temperature, and a decline for annealing.

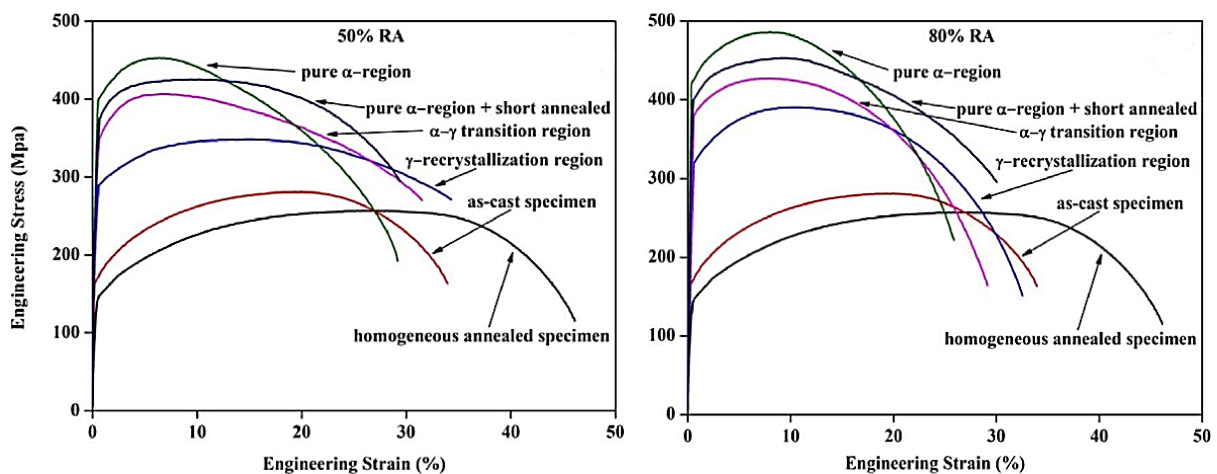


Figure 5.17 Stress-strain curves for 50% and 80% reduction

Finally, a corrosion analysis was conducted on the samples rolled in the ferritic region and annealed. The results (of the potentiodynamic polarization test) show that the worst attitude is that of steels with larger grains, primarily the post soaked (homogeneous annealing) example; finer microstructure promotes the formation of a surface film on the surface of fine grained material, which has more boundary area and so passivation is easier. It is also believed that high angles grain boundaries give a positive contribution for a thicker passivation layer.

Electrochemical potential difference between the matrix, grain boundaries and precipitates influences the corrosion of IF steels; controlled rolling allows to obtain refined microstructure with a certain number of defects (particles, grain boundaries, dislocations) that reduce the potential difference with the matrix due to the reduction of the corrosive ions per galvanic cell.

Including all the effect and consequences seen in this paragraph, it can be concluded that ferritic rolling integrated with a subsequent short annealing it's an effective way to produce this type of steels, in order to have both good formability and mechanical properties.

5.5 Bake hardening

Bake hardening (BH) steels are a variant of interstitial free steels in which carbon is not completely stabilized but a certain little amount is left in solution. This typology was introduced to remedy the characteristic of the IF that have a weak dent resistance, due to the low strength level. For exposed panels in a passenger car, this property is fundamental from an aesthetic point of view, together with a great corrosion resistance. For these reason were developed the BH steels for exposed applications in automotive [74,75].

Bake hardening effect consists in a strain aging mechanism that usually occurs during painting, a process that is conducted for 20 minutes at a temperature of approximately 170°C. The phenomenon is related to the presence of free carbon that prevents movement of dislocations: the Cottrell atmosphere of C are formed around the dislocation cores, pinning them and resulting in an increase of yield strength. Bake hardenability is usually defined by the difference between flow stress at 2% elongation and the lower yield strength after the painting treatment. Figure 5.18 clarifies this concept.

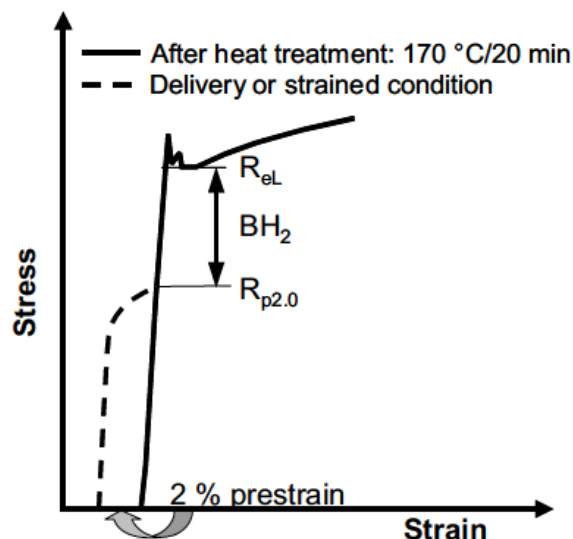


Figure 5.17 Bake hardenability by tensile test

This value is called BH_2 and normally it is required a minimum of 30 MPa. Carbon level control is important in order to obtain sufficient hardening effect, but it shall not exceed because it could lead to the appearance of stretcher-strains in the pressing process.

Carbon and nitrogen are similar to conventional IF steels, but the microalloying strategy is different. In order to have an appreciate bake hardening effect, a certain level of free carbon is necessary and there are mainly two possibilities: having an under-stoichiometric addition of Ti and Nb, or employing an high annealing temperature to dissolve carbides that release carbon. A mixture of the two mechanisms is also a potential way.

Solute carbon in BH should be in the range of 5-10 ppm; this is a small window, in fact the difficulty for the steelmaker is to accurately adjust the amount of free carbon in this range. Bake hardenability increases with growing solute carbon content, but there are limitation: below that level, BH_2 doesn't deliver sufficient strengthening, while above, ageing phenomenon at ambient temperature may cause stretcher-strain defects during press forming. In addition, high annealing temperatures rise BH because the carbide dissolution is more complete and more C is released, and fast cooling amplifies this effect because it prevents the NbC re-precipitation.

Similarly to IF steels, also in this case niobium or niobium-titanium variant are better than the titanium configuration, because Ti combines with C, N and S, therefore the solute carbon amount is more difficult to control. In Ti-steels, for example, the Ti/C ratio has to be higher than Nb/C ratio for an optimum BH effect.

In the other two conditions, instead, Nb stabilizes C and Ti or Al (if titanium is not present) stabilize N, and the “attention” can be focused on niobium addition and process parameters. An appreciable response of 30-50 MPa can be achieved with annealing temperature range of 820-850°C for a nearly-stoichiometric Nb addition. Nevertheless, sometimes for special applications, temperature has to be reduced due to risk of heat buckles; thus, under-stoichiometric value could be adopted, because the precipitates fraction is already smaller and it’s not required excessive dissolution. This situation is visible in figure 5.19.

A BH2 level over 50 MPa should be avoided due to ageing resistance at room temperature that leads to stretcher defect cannot be guaranteed; however, if a substantial dent resistance requires a higher BH value, then a small amount of molybdenum can represents a solution, since molybdenum reduces carbon mobility at room temperature (although at the temperatures used for painting, the beneficial effect disappears).

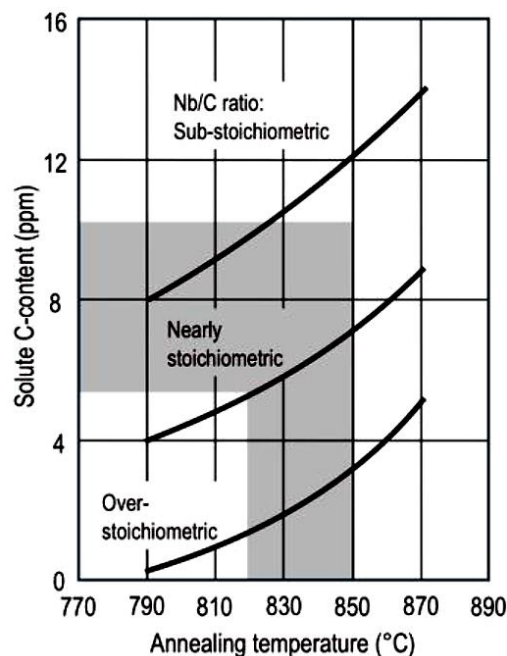


Figure 5.19 Annealing condition for a correct solute C-content

As said, bake hardening steels can be in version niobium- or titanium- or a mixture; vanadium could represent an alternative, but it isn’t a strong carbon stabilizer, so its use is not very common in this steel category.

In this section it’s presented the influence on precipitation of Ti and Nb in BH steels (which is similar to IF, since BH are a subgroup of IF). In titanium steels, TiN are the first particles formed during cooling slightly over 1400°C, and they dissolve only partially at reheating temperatures before rolling. Then, below a temperature of about 1250°C, there are the precipitation of the MnS, which are followed by the $Ti_4C_2S_2$ formation that starts at 1100°C; this requires a partial dissolution of MnS particles. Manganese, in fact, has a powerful influence on sulphur and with high amount, titanium sulphides could be suppressed (for example for Mn percentage above 1,4%). Titanium carbides, instead, precipitate if the Ti content is at least 0,04%.

For Nb microalloyed BH steels, above the slab reheating temperatures all the precipitates are dissolved; the first formation is that of MnS that fix sulphur, then aluminium stabilizes nitrogen by AlN, starting from a temperature of about 1050°C. Lastly, around 900°C, precipitation of NbC can occur. It is influenced by coiling temperature and the Nb/C ratio, so a control of the rolling parameter is required for the desired results. It is reported that an addition of boron can increase NbC stability, and moreover improve the resistance at secondary-work embrittlement that can affect also these steels.

In Nb-Ti BH steels, there are a double stabilization as described previously. The amount of titanium determines the occurrence of precipitates, because if its addition is low, then other elements (Mn or Al) can replace it.

The ease of carbon control, anyway, is better in pure Nb BH, because in Ti-only BH or in Nb-Ti BH with an high content of titanium, precipitation is more complicated due the formation of various particles type that deplete the steel from titanium available for C stabilization. Therefore, Ti-only approach is not recommended for BH steels.

The effects of niobium and process parameters (coiling and annealing) on bake hardening response, were investigated by Storozheva et al. [76]. They studied these effects in a 0,0025%C - 0,125% Mn - 0,003% Si - 0,007% S - 0,038% Al - 0,007% P - 0,002% N - 0,012% Ti steel for future production of automotive sheet. Niobium was added in the range 0,01-0,022% in order to examine five Nb/C; this means that the ratio varied from 0,5 to 1,3 (compared to the stoichiometric one). In addition it was evaluated also Nb/C_{eff} that is related to the effective carbon content in case of formation of Ti₄C₂S₂; in this case, values are higher since the precipitates deplete the available carbon.

Samples were soaked, hot rolled, coiled at 650 or 770°C and cold rolled to the final thickness of 0,8 mm. Lastly, annealing was conducted in a range of 790 – 890°C for 60 s.

Mainly three parameters affect the resultant bake hardening effect: first of all the carbon content that is in solid solution after rolling and annealing, which is represented in figure 5.20. It decrease with higher Nb/C ratio due to the intensification of niobium carbide; higher annealing temperatures promote greater carbon content due to the easier dissolution, as said before. In addition low coiling temperature decreases C in solution (the curves that follows the circle points in the figure). This aspect could be related to the finer grains produced during coiling: in fact, carbon segregation during cooling from annealing is intensified in fine grains.

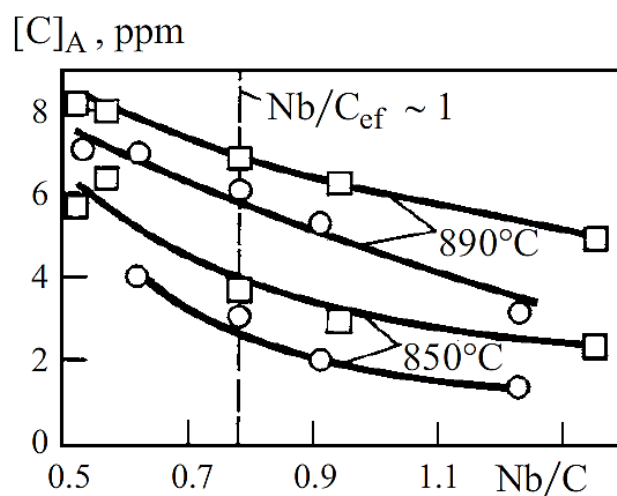


Figure 5.20 Dissolved carbon after annealing as function of Nb/C

The maximum values of yield strength are obtained with an annealing temperature around 850°C, because in this range the balancing between precipitates dissolution and the subsequent formation of coherent segregation (which hinder dislocations) during aging process is optimized.

Very high annealing temperature, nevertheless, could represent a negative factor: it allows a greater dissolution, but it could lead to loss of strength when steel is subjected to long overaging. In fact, the peak of strength during aging is given by coherent segregations, but for longer times, these lose coherence and the yield strength begins to decrease.

BH₂ effect depends on carbon content, which, in turn, depends on the Nb/C ratio and the annealing temperature, as it could be seen in figure 5.21. Here is represented also the influence of high and low coiling temperature (respectively square and circle points). It's noticeable that with over-stoichiometric ratio, the increase in strength due to bake hardening is really restricted.

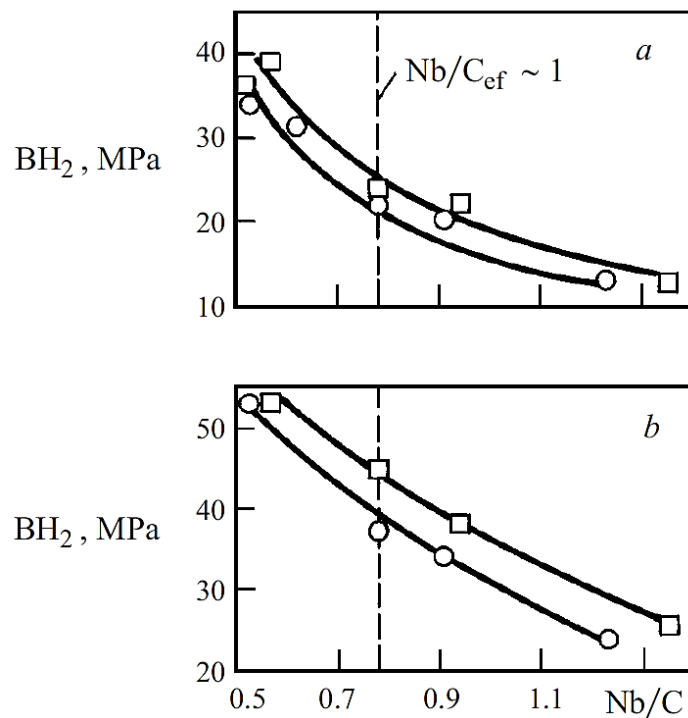


Figure 5.21 Bake hardening effect in samples annealed at (a) 850°C and (b) 890°C

CONCLUSION

This thesis was aimed to investigating the role of niobium in the automotive steels. In order to achieve a useful weight reduction from an environmental point of view, essential in the last years, niobium can represents a good strategy.

This element was discovered in 1801 and nowadays its production is predominantly performed by CBMM, a Brazilian society that over the year has implemented increasing extraction technology, and makes it possible a continuous development in its research and applications.

During the research it has been found that a small addition of Nb has great effect on steel, for example an amount of 0,01% Nb in hot rolling could increase the mechanical properties even by 25%. Mechanisms by which it acts are mainly three:

- Grain refinement: this is the most important effect because it allows an enhancement of both strength and elongation. It works through the solute drag of the atoms in solid solution and the pinning force exerted by precipitates. Thanks to grain refinement it's possible to obtain a pancaked structure during hot rolling, in which grain are elongated; since the recrystallization process is delayed, fragmentation of this elongated grains leads to new smaller ferritic grains. This process is easier with niobium, because it increases the T_{NR} and decreases A_{r3} , and this means that the window for pancaking is enlarged.

Finer microstructure strengthens materials thorough the Hall-Petch mechanism, and simultaneously makes fracture propagation more difficult, since the cracks has to follow a longer pathway.

- Precipitation: analysis of solubility products and application of an optimized controlled process result in an efficient precipitation, which causes grain refinement and give a strengthening contribute. It depends on size and shape of the particles, in fact their consequences have been presented in some scientific reached reported in the discussion. Precipitation occurs during the various phases of steel production, and its "outputs" are affected by situation in which they are formed: for example the shape of early precipitates could different from the others due to the interaction with Ti particles that are more stable at high temperatures. On the other hands, instead, NbC (the main niobium precipitates) formed in the ferritic region or during coiling are finer and their possibility of coarsening is reduced for the shorter time at lower diffusivity condition. Combination with other element (microalloying or others) has been investigated, together with comparison of the several standings.
- Prevention of hydrogen embrittlement: this phenomenon appears especially in the high-strength steels, which are subjected to a more brittle behaviour. Hydrogen accumulation is cause of delayed fractures that are deleterious for a correct fatigue resistance. Niobium is beneficial for this aspect because it acts as a hydrogen trap, so a more uniform and distributed dispersion it's achievable. In this way, H accumulation is avoided and ductility is increased.

It has also been found that niobium induces other microstructural implications (such as more low angles grain boundaries) that help embrittlement resistance.

Subsequently, it was carried out an examination on the principal typologies of steels used in automobile construction; niobium effects on the various categories are more or less the same, but in each type single feature is more or less pronounced in comparison to another one. For example in the multi-phase steels, niobium exerts a microstructural and phase control, with a contribute of homogenization. In very high-strength martensitic steel microstructural

refinement is, again, the best Nb effect, because in these steels there is no request of strengthening, but elongation. Smaller grains arising from niobium allow to gain some fraction of achievable strain, so ductility is increased. In ultra low carbon steel, instead, the fundamental feature is the formability; thus, the importance of niobium lies in control of the interstitial atoms (mainly C and N) in order to satisfy the requirement of ductility and strength (if necessary)

Therefore, it can be concluded that in a perspective of growing improvements that distinguishes the contemporary age, niobium play a prominent role in a lot of applications, in particular in the automotive field, where a very large fraction of the steel is microalloyed with niobium.

REFERENCES

1. D'aiuto F., *Effect of niobium in the 3RD gen steel*, presentation for international meeting Metals for road mobility, 2019
2. <https://en.institut-seltene-erden.de/>
3. <https://www.britannica.com/>
4. Meyer L., *History of niobium as a microalloying element*, introduction to the session 'Application of Niobium as a Microalloying Element' at the International Conference Niobium, 2001
5. <https://cbmm.com/>
6. <https://niobium.tech/en>
7. De Souza O.; Filho P.; De Fuccio R., *Mining, ore preparation and ferroniobium production at CBMM*, 1981
8. E.B. Cruz; D.P. Fridman; M.C. Carboni; R.C. Guimarães; M.A. Stuart Nogueira, *Dissolution of FeNb in liquid steel*, Fundamentals and Applications of Mo and Nb Alloying in High Performance Steels – Volume 2, 2015
9. <https://roskill.com/market-report/niobium/>
10. <https://miningmarketwatch.net/nby.htm>
11. <https://seekingalpha.com/instablog/2366771-rockstone/4918404-commerce-resources-records-highest-niobium-mineralized-sample-to-date-miranna>
12. <https://stockhead.com.au/resources/vanadiums-price-is-at-13-year-high-where-is-it-going-next>
13. <https://roskill.com/market-report/vanadium/>
14. <https://www.metallirari.com/vanadio-forte-2019/>
15. <https://roskill.com/market-report/titanium-metal/>
16. <https://www.metalbulletin.com/>
17. Krauss G., *Steels : Processing, Structure, and Performance*, A S M international, 2015
18. Campbell F.C., *Elements of Metallurgy and Engineering Alloys*, A S M international, 2008
19. Villalobos J.C.; Del-Pozo A.; Campillo B.; Mayen J.; Serna S., *Microalloyed Steels through History until 2018: Review of Chemical Composition, Processing and Hydrogen Service*, 2018
20. Vervynckt S.; Verbeken K.; Lopez B.; Jonas J., *Modern HSLA steels and role of non-recrystallisation temperature*, International Materials Reviews, 2012
21. Rowe J.D., *Advanced Materials in Automotive Engineering*, Elsevier Science & Technology, 2012
22. Billur E., *Challenges in Forming Advanced High Strength Steels*, paper for conference: New Developments in Sheet Metal Forming, 2010
23. Hilditch T.B.; De Souza T.; Hodgson P.D., *Properties and automotive applications of advanced high-strength steels (AHSS)*, 2015
24. Paul S.K., *A critical review on hole expansion ratio*, Materialia, 2020
25. Mohrbacher H., *Metallurgical Effects of Niobium and Molybdenum on Heat-Affected Zone Toughness in Low-Carbon Steel*, applied science, 2019

26. Kirkwood P.R., *The Weldability of Modern Niobium Microalloyed Structural Steels*, Proceedings of the Value-Added Niobium Microalloyed Construction Steels Symposium, 2012
27. Mohrbacher H., *Application of high strength steels in lightweight commercial vehicles*, Advances in Manufacturing, 2015
28. Kalpakjian S.; Schmid S.R., *Tecnologia Meccanica*, quinta edizione, Pearson prentice Hall, 2008
29. Leng Y., *Materials Characterization: introduction to Microscopic and Spectroscopic Methods*, John Wiley & Sons, Incorporated, 2013
30. Courtas S.; Grégoire M.; Federspiel X.; Bicaïs-Lepinay N.; Wyon C., *Electron BackScattered Diffraction (EBSD) use and applications in newest technologies development*, Microelectronics Reliability 46, 2006
31. Kelly T. F.; Miller M. K., *Atom probe tomography*, Rev. Sci. Instrum. 78, 2007
32. Sauvage X.; Lefebvre W.; Genevois C.; Ohsaki S.; Hono K., *Complementary use of TEM and APT for the investigation of steels nanostructured by severe plastic deformation*, Scripta Materialia 60, 2009
33. Gault B.; Loi S.T.; Araullo-Peters V.J.; Stephenson L.T.; Moody M.P.; Shrestha S.L.; Marceau R.K.W.; Yao L.; Cairney J.M.; Ringer S.P., *Dynamic reconstruction for atom probe tomography*, Ultramicroscopy, 2011
34. Kirkwood P.R., *Thermomechanical Controlled Processing (TMCP) Delivering the Advantages of Niobium Technology*, technical document available on www.niobium.tech, 2020
35. Gomez M.; Medina S.F., *Role of Microalloying Elements on the Microstructure of Hot Rolled Steels*, International Journal of Materials Research, Vol. 102, 2011
36. Chen X.; You M.; Guo A.; Zhan W.; Li H.; Xu Y.; Zhai Q., *The influence of niobium on the microstructure and properties of CrMo steel*, HSLA Steels 2015, Microalloying 2015 and Offshore Engineering Steels, 2015
37. Shanmugam S.; Misra R.D.K.; Mannering T.; Panda D.; Jansto S.G., *Impact toughness and microstructure relationship in niobium- and vanadium-microalloyed steels processed with varied cooling rates to similar yield strength*, Materials Science and Engineering A 437, 2006
38. CBMM, *How much niobium can I use?*, paper available on www.niobium.tech, 2018
39. Mohrbacher H., *Precipitation of niobium in carbon steel: Fundamentals and application strategies*, presentation available on www.niobelcon.com, 2019
40. Klinkenberg C.; Bleck W., *Niobium Carbide Precipitation in Microalloyed Steel*, Steel Research, 2004
41. Webel J.; Herges A.; Britz D.; Detemple E.; Flaxa V.; Mohrbacher H.; Mücklich F., *Tracing Microalloy Precipitation in Nb-Ti HSLA Steel during Austenite Conditioning*, metals, 2020
42. Dutta B.; Sellars C. M., *Effect of composition and process variables on Nb (C, N) precipitation in niobium microalloyed austenite*, Materials Science and Technology, 1987
43. Patel J.; Klinkenberg C., *Hot Rolled HSLA Strip Steels for Automotive and Construction Applications*, 2003
44. Bernhard E., *Cold rolled HSLA sheet and strip products*, International Symposium Niobium, 2001

45. Sanz L.; Pereda B.; López B., *Effect of thermomechanical treatment and coiling temperature on the strengthening mechanisms of low carbon steels microalloyed with Nb*, Materials Science & Engineering A 685, 2017
46. Jung J.G.; Bae J.H.; Lee Y.K., *Quantitative Evaluation of Dynamic Precipitation Kinetics in a Complex Nb-Ti-V Microalloyed Steel Using Electrical Resistivity Measurements*, Met. Mater. Int., Vol. 19, No. 5, 2013
47. Costa e Silva A., *Challenges and opportunities in thermodynamic and kinetic modelling microalloyed HSLA steels using computational thermodynamics*, Computer Coupling of Phase Diagrams and Thermochemistry 68, 2020
48. Kostryzhev A.G.; AlShahrani A.; Zhu C.; Cairney J.M.; Ringer S.P.; Killmore C.R.; Pereloma E.V., *Effect of niobium clustering and precipitation on strength of an NbTi-microalloyed ferritic steel*, Materials Science & Engineering A 607, 2014
49. Mohrbacher H., *Principal effects of Mo in HSLA steels and cross effects with microalloying elements*, International Seminar in Applications of Mo in Steels, 2010
50. Pan H.; Ding H.; Cai M.; Kibaroglu D.; Ma Y.; Song W., *Precipitation behavior and austenite stability of Nb or Nb-Mo micro-alloyed warm-rolled medium-Mn steels*, Materials Science & Engineering A 766, 2019
51. Subramanian S.; Youm Y.; Nie W.; Miao C.; Shang C.; Zhang X.; Collins L., *EBSD characterization of HAZ from single and multi-pass welding of niobium microalloyed linepipe steels*, Proceedings of the international seminar on welding of high strength pipeline steels, 2013
52. Li X.; Ma X.; Zhang J.; Akiyama E.; Wang Y.; Song X., *Review of Hydrogen Embrittlement in Metals: Hydrogen Diffusion, Hydrogen Characterization, Hydrogen Embrittlement Mechanism and Prevention*, Springer Nature, 2020
53. Mohrbacher H., *Metallurgical optimization of martensitic steel sheet for automotive applications*, NiobelCon, 2010
54. Zhang S.; Wan J.; Zhao Q.; Liu J.; Huang F.; Huang Y.; Li X., *Dual role of nanosized NbC precipitates in hydrogen embrittlement susceptibility of lath martensitic steel*, Corrosion Science 164, 2020
55. Jo M.C.; Yoo J.; Kim S.; Kim S.; Oh J.; Bian J.; Sohn S.S.; Lee S., *Effects of Nb and Mo alloying on resistance to hydrogen embrittlement in 1.9 GPa-grade hot-stamping steels*, Materials Science & Engineering A 789, 2020
56. Zhang C.; Liu Y.; Jiang C.; Xiao J., *Effects of Niobium and Vanadium on Hydrogen-Induced Delayed Fracture in High Strength Spring Steel*, journal of iron and steel research, international, 2011
57. Xue W.; Li Z.; Xiao K.; Yu W.; Song J.; Chen J.; Dong C.; Li X., *Initial microzonal corrosion mechanism of inclusions associated with the precipitated (Ti, Nb)N phase of Sb-containing weathering steel*, Corrosion Science 163, 2020
58. Rodionova I.G.; Amezhnov A.V.; D'yakonov D.L.; Shaposhnikov N.G.; Baklanova O.N.; Gladchenkova Y.S., *Study of the effect of microstructure characteristic on corrosion resistance of cold-rolled micro-alloyed sheet steels (HSLA) of strength classes 340-420 for automobile building*, Metallurgist, Vol. 63, 2020
59. Li M.; Zhang W.; Wang X.; Chen E.; Chen C.; Zhang H.; Shang C., *Effect of Nb on the Performance of 409 Stainless Steel for Automotive Exhaust Systems*, steel research international, 2018

60. CBMM, *Niobium in automotive exhaust systems*, paper available on www.niobium.tech, 2018
61. Mohrbacher H., *The effects of niobium microalloying in second generation advanced steels*, International steel technologies symposium, 2008
62. Mohrbacher H., *Direct and Indirect Benefits of Niobium Microalloying to Automotive Sheet Steel*, Conference Proceedings of The 1st International Conference on Automobile Steel, 2016
63. Pichler A.; Hebesberger T.; Traint S.; Tragl E.; Kurz T.; Kremaszky C.; Tsipouridis P.; Werner E., *Advanced high strength thin sheet grades: improvement of properties by microalloying assisted microstructure control*, International Symposium on Niobium Microalloyed Sheet Steel for Automotive Application, 2006
64. Zhao J.; Jiang Z., *Thermomechanical processing of advanced high strength steels*, Progress in Materials Science 94, 2018
65. Terada D.; Ikeda G.; Park M.; Shibata A.; Tsuji N., *Reason for high strength and good ductility in dual phase steels composed of soft ferrite and hard martensite*, IOP Conf. Series: Materials Science and Engineering 219, 2017
66. Mohrbacher H., *Advanced metallurgical concepts for DP steels with improved formability and damage resistance*, Proceedings of the international symposium on new developments in advanced high-strength sheet steels, 2013
67. Mohrbacher H., *Low Carbon Microalloyed Cold Rolled Hot Dip Galvanized Dual Phase Steel for Larger Cross-Sectional Areas with Improved Properties*, Galvatech conference, 2011
68. Mohrbacher H.; Yang J.; Chen Y.; Rehrl J.; Hebesberger T., *Metallurgical effects of niobium in dual phase steel*, metals, 2020
69. Hausmann K.; Krizan D.; Spiradek-Hahn K.; Pichler A.; Werner E., *The influence of Nb on transformation behavior and mechanical properties of TRIP-assisted bainitic-ferritic sheet steels*, Materials Science & Engineering A 588, 2013
70. Mohrbacher H.; Morris J.W.; Krauss G., *Fundamentals and practical approaches of optimizing martensitic steels for use under severe operating conditions*, International Symposium on Wear Resistant Alloys for the Mining and Processing Industry, 2018
71. CBMM, *Niobium in press hardening steels*, presentation available on www.niobium.tech, 2018
72. Mohrbacher H., *Niobium Based Metallurgical Concepts and Strategies for the Production of IF-HS and IF-BH Steel Grades*. International Conference on Interstitial Free Steels: Manufacturing Applications IFSTEEL-2010, 2010.
73. Ghosh S.; Singh A.K.; Mula S.; Chanda P.; Mahashabde V. V.; Roy T.K., *Mechanical properties, formability and corrosion resistance of thermomechanically controlled processed Ti-Nb stabilized IF steel*, Materials Science & Engineering A 684, 2017
74. Escher C.; Brandenburg V.; Heckelmann I., *Bake hardening and ageing properties of hot-dip galvanized ULC steel grades*, The Minerals, Metals & Materials Society, 2006
75. Speer J. G.; Hashimoto S.; Matlock D. K., *Microalloyed bake-hardening steels*, The Minerals, Metals & Materials Society, 2006
76. Storozheva L. M.; Escher K.; Bode R.; Hulka K.; Burko D. A., *Effect of niobium and coiling and annealing temperature on the microstructure, mechanical properties and bake hardening of ultralow-carbon steel for the automotive industry*, Metal Science and Heat Treatment Vol. 44, 2002

ACKNOWLEDGEMENT

I would like to thank all the people involved in the realization of this thesis. First of all a heartfelt thank you goes to Fabio D'Aiuto, contact person of CBMM; his support and knowledge supply have been essential for the realization of the work.

A special thank is reserved for my family, especially for my parents who have contributed financially and, above all, emotionally, supporting me at all times.

Last but not least, I am grateful to all my friends, colleagues and travelling companions for the great moments we spent together during all these years.

Without the contribution of each and everyone of you I would not have achieved these accomplishments.